**Universidad
Rey Juan Carlos**

Departamento de Ciencias de la Naturaleza
y Física Aplicada

Dynamics and Topology in
Complex Networks

Juan Antonio Almendral Sánchez

June, 2006

Miguel Ángel Fernández Sanjuán, Catedrático de Física Aplicada del Departamento de Ciencias de la Naturaleza y Física Aplicada de la Universidad Rey Juan Carlos

CERTIFICA:

Que la presente memoria de Tesis, titulada *"Dynamics and topology in complex networks"*, ha sido realizada bajo mi dirección por Juan Antonio Almendral Sánchez para optar al grado de Doctor por la Universidad Rey Juan Carlos.

Y para que conste que la citada Tesis reúne todos los requisitos necesarios para su defensa y aprobación, firmo el presente certificado en Móstoles a quince de junio de dos mil seis.

Móstoles, 15 de junio de 2006

Fdo. Miguel Angel Fernández Sanjuán
Catedrático de Física Aplicada
Universidad Rey Juan Carlos

A mi padre

Agradecimientos

Por último, no puedo olvidarme de mis *padres*, en particular de mi padre que no vivió lo suficiente para ver este momento. Sin su apoyo incondicional, incluso cuando no entendían completamente mis decisiones, esta tesis no existiría.

Móstoles, junio 2006
Juan

Contents

4   Classical approach to dynamical systems   77

5   Dynamics in complex networks   97

6   Conclusions   111

Chapter 1

Introduction

What is the relation between neurons in the brain, components in an electric circuit, web pages in Internet or genes in our DNA? It looks like we can hardly find a link. They are natural and man–made systems constituted by many units whose individual behavior may be understood or not. However, despite the enormous differences among them, it turns out that all these systems can be analyzed from the point of view of the so–called complex networks theory.

In this approach, the properties that we find in a system cannot be derived from its features at a lower level of description. For instance, however much we understand the dynamics of a neuron or the mechanisms involved in the neurobiochemistry of the brain, they are not enough to understand the emergent properties that our brain exhibits, such as memory or language.

This is in complete disagreement with the reductionism viewpoint which affirms that we just need to analyze exhaustively every single component of a system to globally understand it. This belief assumes that, once we have "broken" a system into well studied pieces, it can be reassembled to derive all its relevant properties [1]. This is likely the thought that lead Carl Anderson to declare, after his discovery of the positron in 1932, *The rest is chemistry!*

Reductionism considers that all variables are important to describe Nature and, consequently, the knowledge we derive from a system cannot be exploited in others. On the contrary, complex networks theory considers that there are irrelevant variables, which can be neglected, and behaviors shared by different systems. The success of this methodology in the past years makes complex networks theory an essential ingredient to study complex systems.

1.1 Complex systems

The science of complex systems is regarded as one of the most important scientific challenges for the next years since *its manifest destiny is prospecting, mapping, colonizing and developing the "interdisciplinary" territory* between the traditional sciences [2]. This broad scope is probably the reason why it is not easy to find an all–encompassing definition of complex systems.

Nevertheless, we can start identifying some misleading prejudices which should be discarded.

Simple systems have a simple behavior. There is a large number of examples show-
ing how simple models exhibit complex behaviors. For example, it is well
known that the nonlinear dynamics of a forced pendulum or a double pendu-
lum (even if it is not externally forced) are chaotic [3].

A complex behavior is due to complex causes. This idea, related to the previous one,
leads us to believe that only a complex model can explain the true nature of
reality. However, not only the understanding of reality is much better with
a simple model, but even its precise description can be often achieved with a
simple model.

A property rather common in complex systems is that they show *fine–tuned
processes in time and fine–tuned structures in space, apparently, out of nothing
but "randomness"* [4]. This is due to the fact that complex systems always lie
between order and disorder. For instance, the spatial distribution of the flour beetle
Tribolium is neither random nor geometrical [5]. Actually, this balance between
order and disorder is what an observer intuitively identifies as "complexity".

If complex systems are found at the edge of chaos [6] is because their evolution
is not commanded by an external organizing principle, but they self–organize (e.g.
flour beetle). Interestingly, this situation is also typical in critical phenomena or
phase transitions [7], whose study in the context of the Statistical Physics caused
the development of two key concepts: Universality and scaling.

Universality. An important feature in complex systems is that the global behav-
ior cannot be derived from its parts. For example, the global dynamics of a
population is not the mere aggregation of individuals. There is not an av-
erage individual whose behavior can be considered "typical" to analyze the
population as a sum of these "standard people". Furthermore, the psycholog-
ical features of each person, despite their importance to characterize him as
individual, are useless to describe the whole population.

Universality explains why we can find the same global behavior in apparently
different systems. When a system presents universality means that it follows
universal laws that are independent of the constituents. Consequently, the ex-
istence of universality implies that some subtle, and usually simple, mechanism
is at work.

Given the impossibility of reducing some systems to their components, it is
convenient to differentiate between complicated and complex systems. A com-
plicated system has a large number of components governed by well defined
rules to accomplish a function in a limited range of responses to environmental
changes (e.g., an aircraft). On the contrary, *the connectivity of the components
in a complex system is plastic and roles may be fluid in order to self–adapt to*

changes (e.g., a flock of geese) [8]. Then, while in a complicated system the reductionism is still valid, in a complex system fails.

Scaling. The presence of scaling laws in a self–organized system implies that its functionality is not affected by changes in its size. In other words, a system with scaling properties does not have an optimal size since it keeps working as new elements are added. For instance, no human being has ever been taller than 3 meters because we have a well defined scale. A person one order of magnitude taller is beyond the physiological possibilities of human body. Such a giant would die overwhelmed by his own weight as a whale beached at the seaside. However, a city with some thousands of inhabitants can grow up to 10 millions since it self–organizes to cope with the increase of population [9]. Then, since a city can be fully functional for very different sizes, we say that it scales.

1.2 Networks

Complex systems are often constituted by many elements interacting among them. Hence, before considering the nature of the elements, the first step is just to describe the set of interactions by means of a network. From this viewpoint, each element is represented by a *site* (physics), *node* (computer science), *actor* (sociology) or *vertex* (graph theory) and the interaction between two elements corresponds to a *bond* (physics), *link* (computer science), *tie* (sociology) or *edge* (graph theory). Graphically, nodes are depicted as dots and links as segments connecting two of these dots.

Given the simplicity of this methodology, networks appear everywhere [10]. For instance, the physical connections between computers on the Internet can be regarded as a network. And this approach is enough to derive several results about its connectivity and to uncover the nodes that can be overloaded by the requests of their neighbor computers [11]—two nodes joined by one link are called *neighbors* in the jargon of networks.

Since the number of computers on the Internet is large and changing, we can focus on the level of routers—special computers that control the transfer of data. Then, routers are nodes in our network and their physical connections are links. Furthermore, since routers are united in domains, it is also possible to consider a network in which each domain is a node and links stand for connections between domains (see Fig. 1.1).

Many other examples can be analyzed as networks. The following are only a few of them:

Ecological and food webs. Species in an ecosystem can be seen as nodes in a network and the existence of a prey–predator relationship between them is rendered as a link [12].

Word web of human languages. Words can be also considered as nodes and the semantic or syntactic connections in a given language as links [13].
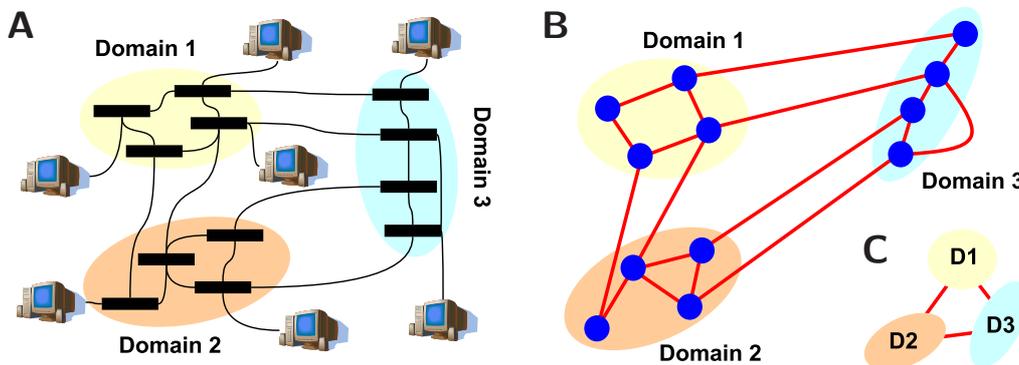
Figure 1.1. Schematic representation of the physical connections on the Internet. To transfer a file between two users, the packets encoding the file travel from the source host to the destination host via routers. (A) This figure depicts how hosts connect to routers (black boxes) and routers among them. (B) The corresponding network at the level of routers is drawn and, (C) the network at the level of domains.

Social networks. We can describe the relationships in a social group as links in a network whose nodes are people [14].

Neural networks. If we represent the 282–neuron neural network of the nematode *C. elegans* as a network, nodes are neurons and links are their synaptic connections [15].

Metabolic networks. Metabolites are regarded as nodes and the chemical reactions between them define the links [16].

It is important to remark, however, that the definitions of node and link are not always easily applied to a real system. For example, can we say that "put up" are two words? Orthographically, there is a blank thus they are two words. However, semantically, "put up" refers to a concept that cannot be reduced to the meanings of each word and, in this sense, it is one word. Similar ambiguities to identify nodes or links cause that, sometimes, the description of a system as a network is not straightforward.

1.2.1   Types of networks

A set of nodes joined by edges is only the simplest network. We may find a complex system whose constituents can be classified into several non–overlapping groups. Then, the elements in each group may be represented with their own vertex. Likewise, we may have several types of edges to distinguish different relationships.

For instance, in a social network we can differentiate nodes by nationality, sex, age, or many others. And edges can represent friendship, animosity, or geographical proximity. Figure 1.2 is an example of social network whose links are romantic/sexual relations between students in an anonymous high school and nodes differentiate men and women [17].
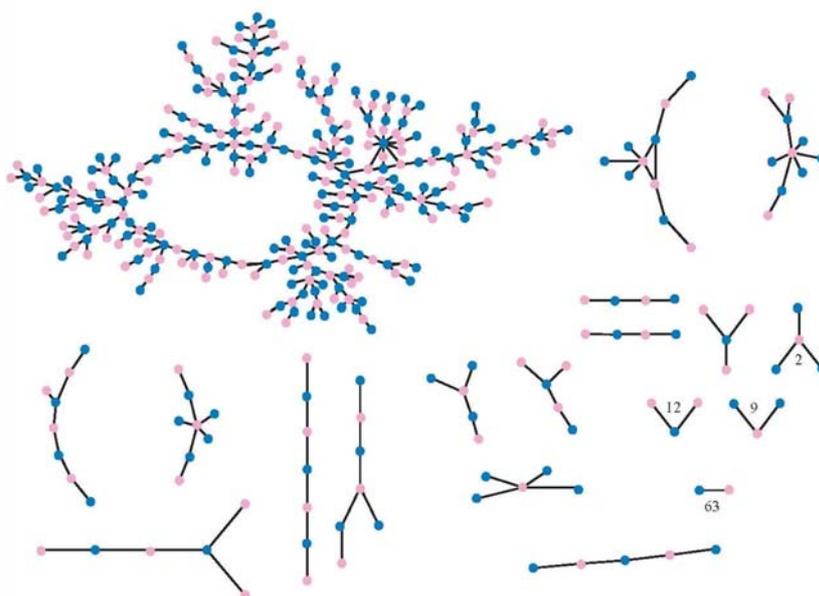
Figure 1.2. The structure of romantic and sexual relations at a high school. Each circle is a student (men in blue and women in pink) and lines connecting them represent romantic/sexual relations occurring within the six months preceding the interview that allowed gathering the data. The numbers close to some figures count how many times that pattern was observed. After [17].

Directed and undirected networks

We have been implicitly assuming that the relationship between nodes is symmetric. This is indeed true if a link represents, say, geographical proximity—if A is close to B, then B is close to A. However, in many cases the connection between nodes is asymmetric since the edge runs only in one direction. When this happens, we say that the link is *directed*—directed edges are also known as *arcs*.

For instance, trophic relationships in a food web are good examples. Figure 1.3 is a simplified representation of the Arctic food web in which the asymmetry of the relationships are evident. The polar bear preys on three types of seals but seals do not prey on polar bears. This is graphically shown as three arrows from the polar bear to the seals.

Networks composed of directed edges are referred to as *directed networks* or sometimes *digraphs*. Likewise, those networks without directed edges are called *undirected networks*. Notice that an undirected network can be represented by a directed one having two edges between each pair of connected vertices, one in each direction—graphically, we can draw A—B as A⇄B.

Weighted networks

Edges can also carry weights to measure the capacity or the intensity of the relationship between two vertices [18]. Examples are the existence of strong and weak ties
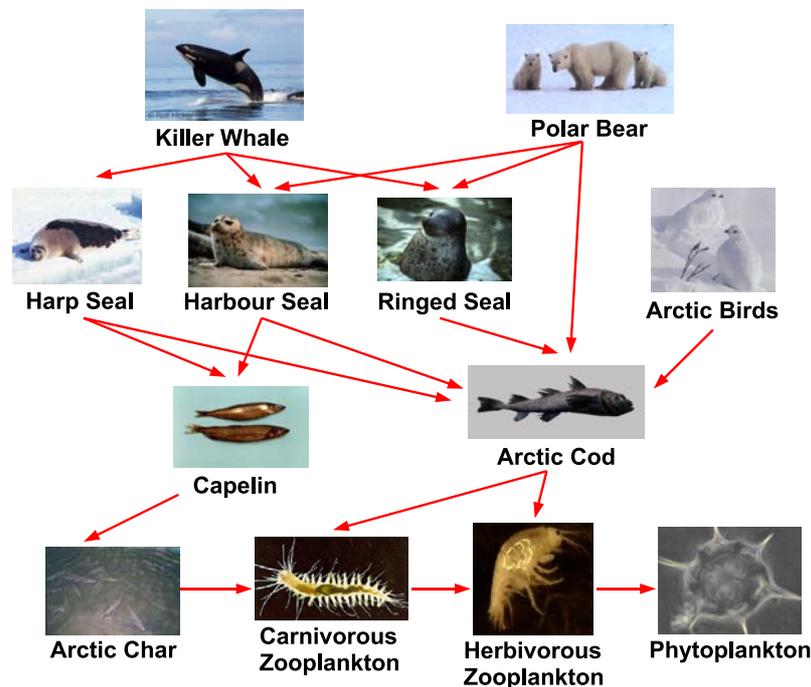
Figure 1.3. The Arctic food web as an example of a directed network. This is a simplified representation since only the important trophic relationships appear and the nodes corresponding to arctic birds, zooplankton and phytoplankton comprise several species. The links are represented graphically as arrows to show the asymmetry due to the fact that there is a predator–prey relationship.

in social networks [19], uneven fluxes in metabolic reaction pathways [20], unequal traffic on the Internet [21], or different predator–prey interactions in food webs [22]. All these networks are better described as *weighted networks*—networks in which each edge has associated a value measuring the strength of the relationship (see Fig. 1.4C).

Bipartite networks

One of the simplest examples of network with different vertices is the so–called *bipartite network*, which has two types of nodes and links joining only nodes of unlike type (see Fig. 1.4D). The network depicted in Fig. 1.2, corresponding to a high school, is almost bipartite since there are two kinds of nodes (men and women) and all edges but one connect a man with a woman.

Actually, many social networks are bipartite—in the jargon of sociology are known as *affiliation networks*. Since a person can be member of several groups (e.g., a football club), it is natural to consider two types of vertices—one for people and the other for groups—with links between them representing group membership (see Fig. 1.4D). Some examples are networks of chief executive officers [23], boards of directors [24], scientific collaborations [25], or sexual contact networks [26].

Bipartite networks are often studied by projecting them onto one set of vertices or the other—they are called *one–mode projections*. Figure 1.4D shows a bipartite network and its two one–mode projections. In particular, if we suppose that blue nodes are directors of companies and green nodes are boards, how do we calculate the neighbors of, say, director 3 in the corresponding one–mode projection? Since this director is member of boards A and B, he becomes neighbor of $1 - 2 - 4$ because 2 is also in B and $1 - 4$ are in A. The projection onto boards is similar. For example, board A is integrated by director $1 - 3 - 4$, thus its neighbors are B and C since director 3 is also in B, 4 is in C and 1 is only in A.
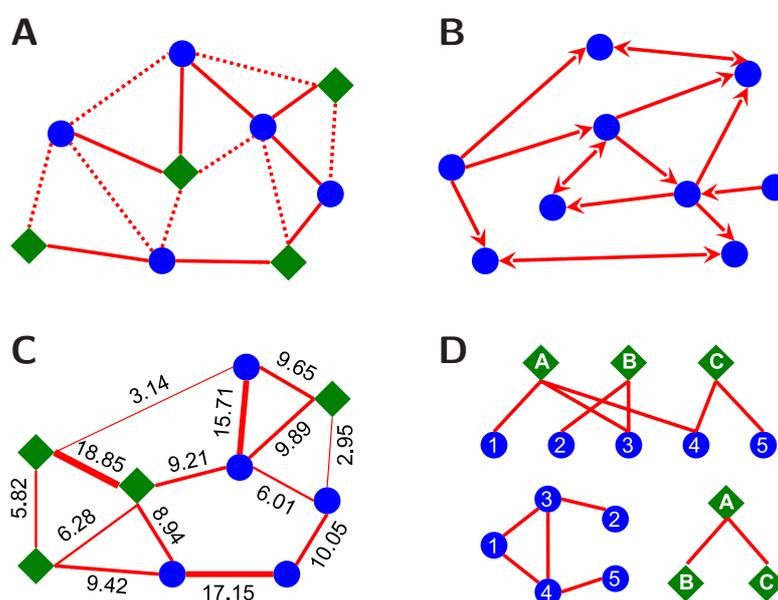
Figure 1.4. Graphical representation of the main types of networks. (A) Here a general network is depicted with two types of vertices (blue circles and green diamonds) and two types of edges (dashed and dotted lines). (B) This figure shows a directed network as a set of vertices linked with arrows to emphasize the directionality of the edges. Notice that the bidirectional arrows between some pairs of nodes in fact represent two directed edges. (C) In this weighted network each edge has associated a value measuring the strength of the relationship. Although the edges in this case are undirected, it is also possible to define weights in a directed network. (D) Bipartite networks (top diagram) are characterized by having two types of nodes and links connecting always vertices of unlike type. They can be projected onto one set of nodes or the other to obtain an undirected network (bottom diagram).

Adjacency and weights matrices

All the former networks can be described using a matricial formalism and, usually, it is a fruitful approach to study their properties. Given a network with N nodes,

we can define the so–called *weights matrix* $\mathcal{W}$ whose entry w_{ij} $(i, j = 1, ..., N)$ is the weight of the link from node i to node j.

If there is no weights in the network, we define instead the *adjacency (or connectivity) matrix* $\mathcal{A}$. The elements of $\mathcal{A}$ are fixed as follows: $a_{ij} = 1$ $(i, j = 1, ..., N)$, if the link from i to j exists, and $a_{ij} = 0$ otherwise (see Fig. 1.5).

A
$$\begin{pmatrix} 0 & 1 & 0 & 1 \\ 1 & 0 & 1 & 1 \\ 0 & 1 & 0 & 0 \\ 1 & 1 & 0 & 0 \end{pmatrix}$$

B
$$\begin{pmatrix} 0 & 1 & 0 & 1 \\ 1 & 0 & 0 & 0 \\ 0 & 1 & 0 & 1 \\ 0 & 1 & 0 & 0 \end{pmatrix}$$
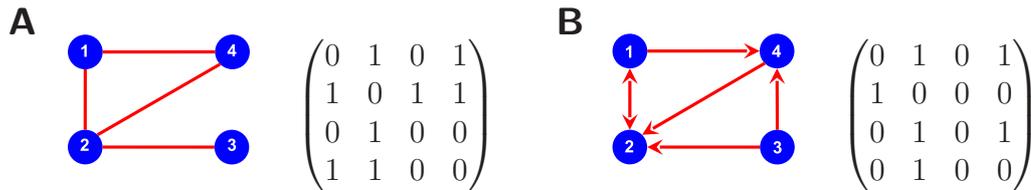
Figure 1.5. The adjacency matrix. An undirected network is shown on (A) and a directed network on (B). Notice that the diagonals of the matrices only contain zeros and that the undirected network has associated a symmetric matrix.

We can obtain the *Laplacian matrix* $\mathcal{L}$ (also known as *Kirchhoff matrix*) from the adjacency matrix $\mathcal{A}$. The Laplacian matrix is simply $\mathcal{L} = \mathcal{K} - \mathcal{A}$, where $\mathcal{K}$ is a diagonal matrix with elements

$$k_{ii} = \sum_{j=1}^{N} a_{ij}.$$

Note that all rows of $\mathcal{L}$ sum, by definition, zero.

From the *spectra* of $\mathcal{L}$—the set of its eigenvalues—we can derive useful information about the corresponding network [27, 28]. This is due to the fact that spectral properties are related to the topological features of the network.

1.2.2   Basic concepts about networks

Once we have defined the best network to describe a real system, we can start studying its features. Many quantities have been proposed in the past few years to analyze a network, but three of them are of major importance to understand the recent development of complex network theory [29].

Average path length

A *path* in a network is defined as a sequence of vertices in which each successive vertex, after the first, is adjacent to its predecessor in the sequence. Then, a path between a given pair of vertices is said to be a *shortest path* if its weight is minimal—the *weight of a path* is just the sum of the weights that we find along the path. In unweighted graphs, since all edges have weight one, the weight of a path is just the number of edges.

We define the *distance* d_{ij} between vertices i and j as the weight of the shortest path that connects these two vertices. Then, the *diameter* of a network with N

nodes is the maximal distance between any pair of vertices and the *average path length* ℓ is the average distance between all pairs of vertices (see Fig. 1.6A),

$$\ell = \langle d_{ij} \rangle = \frac{1}{N(N-1)} \sum_{i \neq j} d_{ij} \,.$$

Notice that the former definitions are only valid if the path between two nodes exists. However, this is false in general. For instance, we may find in a directed network that there is a path from node A to B but not from B to A. Likewise, in an undirected network, nodes are not usually in a unique *component*—the set of nodes that can be connected through a path—but in several isolated components.

Nevertheless, there are two possibilities to tackle this problem. In the case of undirected networks, it is usual to calculate the average path length only within the *giant connected component*—the component with more nodes. An alternative approach to avoid working only with the largest component is to define the average path length as the "harmonic mean" distance between all pairs,

$$\ell = \frac{1}{\langle d_{ij}^{-1} \rangle} = \left(\frac{1}{N(N-1)} \sum_{i \neq j} \frac{1}{d_{ij}} \right)^{-1},$$

where $d_{ij} = \infty$ if there is no path between nodes i and j. Some authors call *efficiency* of a network to $\mathcal{E} = \langle d_{ij}^{-1} \rangle$ (see Fig. 1.6B).

A

B
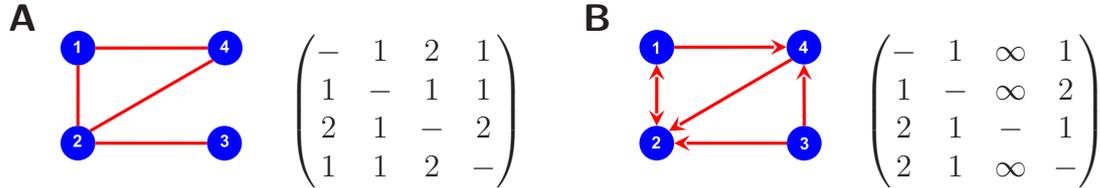
Figure 1.6. The average path length. (A) Here it is depicted an undirected network and the corresponding distance matrix $\mathcal{D}$, whose entry d_{ij} is the distance from node i to j. The average path length may be obtained from $\mathcal{D}$ as $\ell = \langle d_{ij} \rangle = 1.3$ or $1/\mathcal{E} = 1/\langle d_{ij}^{-1} \rangle = 1.2$. (B) A directed network and its distance matrix $\mathcal{D}$ are shown. Since some pairs of nodes cannot be connected and the distance between them is infinite, we can only use the efficiency to measure the average path length, $1/\mathcal{E} = 1.6$.

Despite the concept of efficiency can be applied to any network, it has been adopted only occasionally [30] since, usually, the numerical difference between both methods is little but the analytical treatment is more difficult using the "harmonic mean". This is due to the fact that many directed networks can be analyzed as undirected and because, as we will see later, the giant connected component of a real network often spans the majority of its nodes.

Degree distribution

This concept is the simplest and most studied one–node feature that we can find in a network. Since it is still an open question how to define this quantity in a weighted

network, we focus here on directed and undirected networks. The *degree* of a vertex i, k_i, is defined as the number of edges that are connected to i. In terms of the adjacency matrix is just

$$k_i = \sum_{j=1}^{N} a_{ij} ,$$

where N is the number of nodes in the network.

We can then calculate the *degree distribution* $P(k)$, which gives us the probability of finding a vertex with degree k, as $P(k) = M(k)/N$, where $M(k)$ is the number of vertices whose degree is k (see Fig. 1.7A). Obviously, we can also calculate the *average degree* or *coordination number*,

$$\langle k \rangle = \frac{1}{N} \sum_{i} k_i = \sum_{k} k P(k) = \frac{2L}{N} ,$$

where L is the total number of edges in the graph.
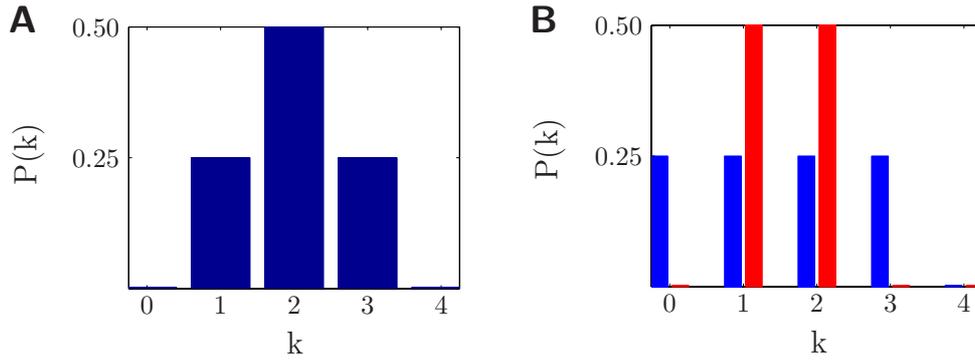
Figure 1.7. The degree distribution. (A) Here the degree distribution of the undirected network in Fig. 1.6A is plotted. Since the degrees are $k_{i=1...4} = \{2, 3, 1, 2\}$, the average degree is $\langle k \rangle = 2.0$. (B) The in–degree (blue) and the out–degree (red) distributions of the directed network in Fig. 1.6B are shown. The in–degrees are $k^{\text{in}}_{i=1...4} = \{1, 3, 0, 2\}$ and the out–degrees are $k^{\text{out}}_{i=1...4} = \{2, 1, 2, 1\}$, thus $\langle k^{\text{in}} \rangle = 1.5$ and $\langle k^{\text{out}} \rangle = 1.5$

If the network is directed, the degree of a node is twofold. We have the so–called *out–degree* of the node (i.e., the number of outgoing links),

$$k_i^{\text{out}} = \sum_{j=1}^{N} a_{ij} ,$$

and the *in–degree* (i.e., the number of ingoing links),

$$k_i^{\text{in}} = \sum_{j=1}^{N} a_{ji} .$$

Consequently, we need two distributions, $P(k^{\text{out}})$ and $P(k^{\text{in}})$, to describe the network (see Fig. 1.7B).

Clustering coefficient

Watts and Strogatz (WS) define in [31] the *local clustering* of a vertex i, C_i, as the ratio between the number E of edges connecting the k_i nearest neighbors of i and the total number $k_i(k_i - 1)/2$ of possible edges between these nearest neighbors,

$$C_i = \frac{2E}{k_i(k_i - 1)}.$$

C_i is only defined for those vertices i with degree greater than 1 and it is always a number between 0 and 1. While $C_i = 1$ means that all neighbors of node i link each other (node 4 in Fig. 1.8C), $C_i = 0$ implies that there are no links between them (node 4 in Fig. 1.8B).
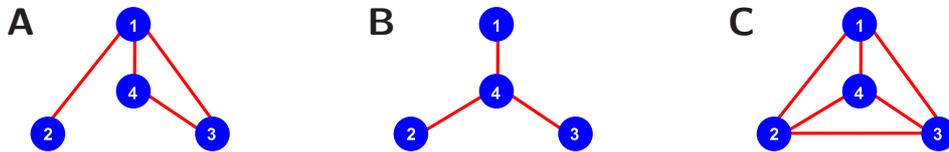
Figure 1.8. The clustering coefficient. The local clustering C_i and the clustering coefficient $\overline{C}$ are here calculated for three simple examples. (A) $C_{i=1\ldots4} = \{1/3, \text{NA}, 1, 1\}$ and $\overline{C} = 7/9$. (B) $C_{i=1\ldots4} = \{\text{NA}, \text{NA}, \text{NA}, 0\}$ and $\overline{C} = 0$. (C) $C_{i=1\ldots4} = \{1, 1, 1, 1\}$ and $\overline{C} = 1$.

Since the definition of local clustering given by WS holds only for undirected networks, several authors have proposed other alternative measures to include directed and weighted networks [32, 33]. Although these measures are not equivalent in general, they all define the local clustering of a vertex i in a directed network as

$$C_i^{(d)} = \frac{A}{k_i(k_i - 1)},$$

where A is the number of arcs (directed edges) linking the k_i nearest neighbors of i. Note that $C_i^{(d)}$, applied to an undirected network, coincides with C_i since an edge can be seen as two arcs, one for each direction.

The *clustering coefficient* of a network, $\overline{C}$, is just the average value of C_i. Since the local clustering is within the interval $[0, 1]$, the clustering coefficient is also a number between 0 and 1. Notice that $\overline{C} = 1$ is only possible in a *full connected network*—a network in which each node is linked to every other node (see Fig. 1.8C).

The clustering coefficient has its roots in Sociology where it is named *fraction of transitive triples* or, simply, *transitivity*. In a social group, it is typical that two individuals with a common friend (a *connected triple* in the jargon of Sociology) are also friends and, consequently, they form a triangle—this set of three nodes completely connected is called a *transitive triple* in Sociology. Then, transitivity measures the ratio of triangles in a network of acquaintances as

$$T = 3 \times \frac{\text{number of transitive triples}}{\text{number of connected triples}}.$$

The transitivity T and the clustering coefficient $\overline{C}$ are different mathematically since the latter weights the contributions of low–degree vertices more heavily [34]. For instance, T and $\overline{C}$ coincide in networks B and C of Fig. 1.8, as expected since they are two extreme cases, but network A has $T = 3/4$ and $\overline{C} = 7/9$. In this case, the difference is small but it can be striking in other social networks, as in the network of film actors where $T = 0.20$ and $\overline{C} = 0.79$.

Both measures are used in the literature since, usually, T can be derived analytically and $\overline{C}$ is easy to calculate numerically. Then, when working in this area, it is important to clarify which one is being used. Nevertheless, these two quantities reflect the same concept and, as it will be clear in the following sections, the mathematical differences will not be important for our purposes.

1.3 Brief history of network theory

1.3.1 The beginning

The legacy of Leonhard Euler (Basel 1707—St. Petersburg 1783) has never been equaled in quantity and quality along the history of Mathematics. He was publishing in many fields of Mathematics and Physics since 1726 (winning the French Academy Award) until he died. The 73 large volumes that comprise all his work, *Opera Omnia*, contain 886 books and articles written in Latin, French and German. Just the view of this work, shelf after shelf, is overwhelming.

Furthermore, besides quantity and quality, Euler always wrote to ease, not to obfuscate, the reading of his work. He was aware of the difficulties that many people find learning mathematics and he tried to be as kind as possible with his readers. The following generations of mathematicians appreciated this fact and they chose his notation to write their own results. Nowadays, his work still looks modern.

Among all the pages in *Opera Omnia*, there are seminal works which addressed new fields in mathematics, such as the variational calculus, complex analysis or differential equations. Actually, there are important theorems due to Euler almost in every mathematical area. In particular, he was the founder of the so–called *graph theory*, in which the term graph should be understood as synonymous of network (although some authors consider that only the mathematical abstraction of a real network is a graph).

Könisberg, now Kaliningrad (Russia), had in 1735 seven bridges to connect two islands to the margins of the river Pregel and between them (see Fig. 1.9). Many people who liked to go for a walk wondered if there was a route that crossed the seven bridges only once—this is referred to as the *Könisberg puzzle*.

When the citizens concluded that it was impossible, they presented the problem to Euler who, in turn, formulated a more general problem [35] that set the basis of graph theory:

> *Given any configuration of the river and the branches into which it may*
> *divide, as well as any number of bridges, to determine whether or not it*
> *is possible to cross each bridge exactly once.*

Figure 1.9. The old city of Königsberg. In 1735, Königsberg had seven bridges to connect the margins and the two islands in the middle of the river Pregel. Euler set the basis of graph theory when he was asked to answer the question: Is it possible to go for a walk using each bridge only once?

Euler's answer exemplifies how often the accurate formulation of a problem is almost its solution. He noted that only the constraints imposed by the bridges are important, not the distances. Thus he transformed the Könisberg puzzle into an equivalent topological problem that admitted an easy solution. Könisberg became a graph in Euler's mind. The edges were the bridges and the vertices were the islands and the margins of the river (see Fig. 1.10).
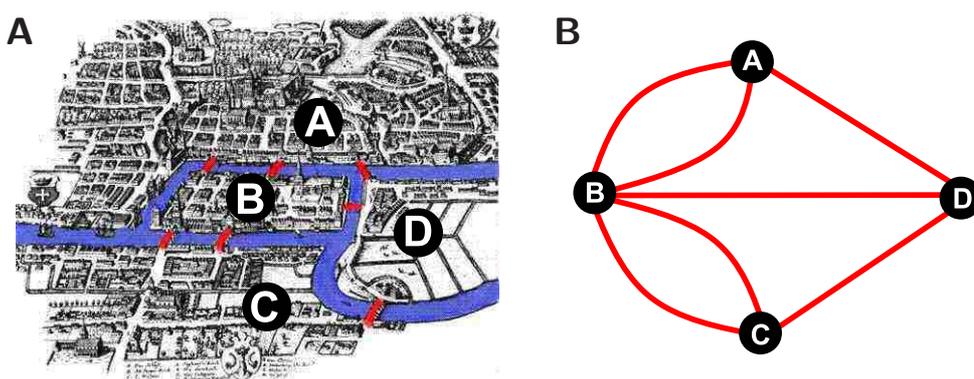
Figure 1.10. Königsberg puzzle solution. (A) Euler noted that distances are not important in this problem, thus he focused on the constraints: The margins (A and C), the islands (B and D) and the bridges (in red). (B) Graph rendering the city. Each link is a bridge and nodes are the four areas in which the river Pregel divides Königsberg.

Once the city is represented as a graph, the Königsberg puzzle can be formulated as follows: Is it possible to find a path between two nodes for which every link

appears exactly once? Such path is called an *Euler walk* in graph theory.

Euler proved that any graph with N nodes and L (undirected) links verifies that $\sum_{i=1}^{N} k_i = 2L$, where k_i is the degree of the node i. Hence, the sum of degrees is even and, consequently, the number of nodes with odd degree is even.

This simple result was enough for Euler to demonstrate that the solution depends on the number N_o of nodes with odd degree in this manner:

1. if $N_o > 2$, no Euler walk exists;

2. if $N_o = 2$, Euler walks only exist starting from one of the odd nodes;

3. if $N_o < 2$, there are Euler walks starting from any node.

Therefore, since Königsberg had four nodes with odd degree, there was no solution to the problem, that is, no Euler walk exists.

In this elegant manner, Euler was the first to show that graphs have intrinsic properties that may be hidden but allow or forbid certain events. Furthermore, the Königsberg puzzle is a good example of how small changes (i.e., adding or removing one bridge) may have global consequences (i.e., the existence or not of Euler walks).

1.3.2   Regular graphs

After the death of Euler, graph theory received many contributions from mathematicians such as Hamilton, Kirchhoff or Cayley. They mainly focused on finding and cataloguing the properties of regular graphs. Actually, several terms are named after them in graph theory such as a *Hamiltonian path*—a path in an undirected graph that visits each vertex exactly once—, a *Cayley graph*—a graph that encodes the structure of a group—, or the *Kirchhoff's matrix tree theorem*—a theorem about the number of spanning trees in a graph.

In a *regular graph*, all vertices have the same degree (i.e., the same number of neighbors). Then, a regular graph with vertices of degree K is called a *K–regular graph* or *regular graph of degree K*. Notice that the degree distribution of a K–regular graph is the Kronecker delta,

$$P(k') = \delta_{k',K} \equiv \begin{cases} 1 \text{ if } k' = K \\ 0 \text{ if } k' \neq K \end{cases}.$$

A widely studied regular network is the *nearest–neighbor coupled network*, also known as *lattice*, in which every node is connected only to its neighbors. A minimal lattice is obtained arranging the vertices in a straight line and connecting each node to the nearest neighbors (see Fig. 1.11A). However, it is often convenient, yet not strictly necessary, to apply periodic boundary conditions to the lattice, so that it becomes a ring (see Fig. 1.11B).

A very special case of lattice is the so–called *globally coupled network* or *fully connected graph*. In these graphs, there are N nodes and the $N(N-1)/2$ possible edges between them, that is, each node is linked to every other node (see Fig. 1.11C).
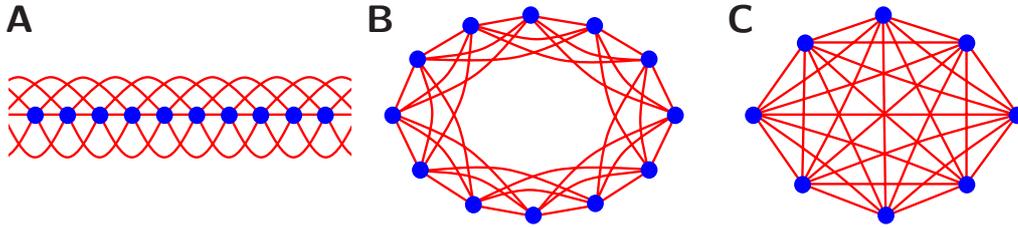
Figure 1.11. Lattices. (A) A one–dimensional lattice with each node linked to its 6 nearest neighbors (three on the left and three on the right). (B) The same lattice with periodic boundary conditions. Now, the nodes are arranged in a ring. (C) In a fully connected graph each vertex is linked to the rest.

In a lattice whose N nodes have degree $K < 2N/3$, which is true for almost all graphs, the clustering coefficient C is

$$C = \frac{3(K - 2d)}{4(K - d)},$$

where d is the dimension of the lattice [36]. Then, in general, lattices are highly clustered. For example, $C \geq 0.5$ in a one–dimensional lattice with $K \geq 4$ and only for $K = 2$ (i.e., when every node is just linked to one neighbor on each side) the clustering coefficient is small, in fact $C = 0$.

On the other hand, given the regularity of lattices, it is also easy to check that the average path length is

$$\ell \sim \sqrt[d]{\frac{N}{K}}.$$

Hence, the average path length in low dimensional lattices is large in general. Only if the degree is very large, $K \lesssim N$, it is small (i.e., in a globally coupled network $\ell = 1$ since $K = N$).

Although the analysis of regular graphs solved many and interesting problems from a mathematical viewpoint, nobody addressed the important question of how networks emerge. Graphs were just static entities without history. This problem was unanswered during two centuries until Paul Erdös proposed a theory to explain how graphs evolve.

1.3.3   Random graphs

Paul Erdös (Budapest 1913—Warsaw 1996) is indeed the most prolific mathematician in history after Euler. He published around 1500 articles in his lifetime about graph theory, number theory, classical analysis, approximation theory, set theory and probability theory. Standing out, especially, the development of Ramsey theory and the application of the probabilistic method.

However, while Euler was a family man and a sociable person, Erdös is famous by his eccentricities. As Erdös was never interested in possessions, he often donated

his awards and other earnings to charity. In fact, it is said that all his belongings
fitted in the suitcase that he used in his many travels. All his life was travelling
between scientific conferences and the homes of colleagues all over the world. He
typically said at a colleague's doorstep, "*my brain is open*", staying long enough to
"*turn coffee into theorems*" before moving on.

Erdös and his colleague Alfréd Rényi (ER) started working on graphs to un-
derstand the structure of social networks. To tackle this issue, they focused on the
so–called *random graphs* [37] in which the existence of a link between a pair of nodes
has probability p. This implies that, given a network with N nodes, the average
degree is

$$\langle k \rangle = p(N-1) \cong pN,$$

and the number of random connections between them is

$$\langle L \rangle = \frac{1}{2}pN(N-1) = \frac{1}{2}\langle k \rangle N.$$

A remarkable fact that ER found was that the important properties that a graph
exhibits appear suddenly [38]. They rigorously proved that a unique giant cluster
emerges, almost in every random graph, for probabilities greater than a certain
threshold

$$p_c \sim \frac{\ln N}{N}.$$

Precisely, for probabilities $p > p_c$, the number of nodes that are not in the giant
cluster decreases exponentially as new links are added.

Note that p_c corresponds to a rather low degree, $\langle k \rangle_c \sim \ln N$, thus it is very easy
that the majority of nodes in a random graph are connected, even for very large
networks.

Mathematicians call this phenomenon the emergence of the *giant connected com-
ponent* and physicists refer to it as *percolation*—the moment in which a phase tran-
sition occurs (see Fig. 1.12). In fact, if we choose the size of the giant cluster as
the order parameter, the transition at p_c has the typical features of a second order
phase transition.
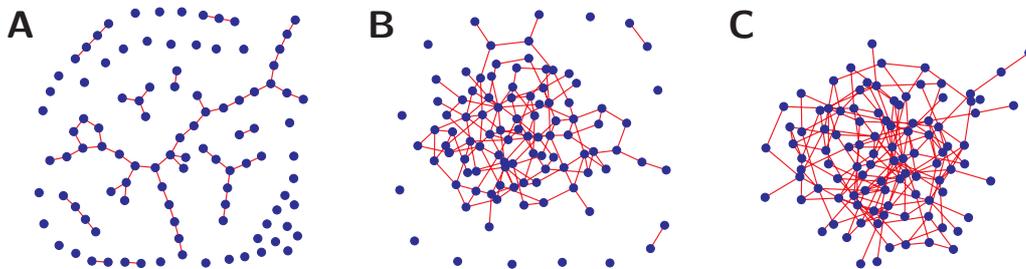
Figure 1.12. The emergence of the giant connected component. Here we show the
evolution of a graph with 100 nodes as the average degree is increased with new links
added randomly. (A) $\langle k \rangle = 1.5$, (B) $\langle k \rangle = 2.5$, and (C) $\langle k \rangle = 3.5$.

Given a random graph with $N \gg 1$ nodes and average degree $\langle k \rangle = p(N-1)$ fixed, the probability of a vertex having degree k is

$$P(k) = \binom{N}{k} p^k (1-p)^{N-k} \simeq \mathrm{e}^{-\langle k \rangle} \frac{\langle k \rangle^k}{k!},$$

where the approximation becomes exact when $N \to \infty$ but $\langle k \rangle$ remains fixed. That is, the degrees of a random graph follow a Poisson distribution [39].

A Poisson distribution has a well defined mean value (i.e., a natural scale) indicating that all nodes have essentially the same number of links. Nodes on either sides of the peak may have many more or fewer links than the average vertex, but these nodes are extremely rare since the distribution rapidly diminishes for values far from the mean.

In random graphs, the probability that two neighbors of a node are connected is the probability that two randomly chosen nodes are linked. Then, the clustering coefficient is simply

$$\overline{C} = p \cong \frac{\langle k \rangle}{N} \ll 1,$$

which means that large–scale random networks have no clustering in general.

Furthermore, clustering can only appear in a network if there is some type of *degree–degree correlation*—correlation in the degrees of two adjacent nodes. In the absence of correlations, clustering is only a finite size effect [40].

On the other hand, if the average degree in a a random graph is $\langle k \rangle$, every node has approximately $\langle k \rangle$ neighbors. Then, since each neighbor has in turn other $\langle k \rangle$ neighbors, every node has $\langle k \rangle^2$ second neighbors. Extending this argument, the number of links ℓ required to reach all nodes in the network is roughly estimated by the condition

$$\langle k \rangle^\ell \sim N \implies \ell \sim \frac{\ln N}{\ln \langle k \rangle},$$

which implies that the average distance in a random network is rather small, even for very large systems.

Notice that we can carry out this calculation because the clustering is small. In a network with large clustering, it is not true that node A has $\langle k \rangle^2$ second neighbors since many of those second neighbors are also themselves neighbors of node A. As a consequence, the number of second neighbors may be much smaller.

Generalized random graphs

Sometimes, the random graphs proposed by ER are called *Poisson random graphs* to avoid confusion with other random graphs whose degree distributions are non–Poisson. All these generalizations of the ER model, in which the degree distributions are arbitrarily fixed, are known as *generalized random graphs*.

There are mainly two methods to calculate the most important properties of a generalized random graph: The *configuration model* [41, 42] and the formalism

based on *probability generating functions* [43]. Although they are different methods, they coincide essentially in their results.

The configuration model can be used to determine when a generalized random graph with degree distribution $P(k)$ percolates. It is obtained that the giant cluster emerges, almost surely, when

$$\sum_{k=0}^{k_{\max}} k(k-2)P(k) > 0,$$

if the maximum degree $k_{\max}$ is not too large. Then, if we apply this result to the ER model (i.e., when $P(k)$ is a Poisson distribution), we find that the percolation occurs when

$$\langle k \rangle^2 - \langle k \rangle > 0 \Longleftrightarrow \langle k \rangle > 1,$$

which means that the giant cluster emerges at $p_c = 1/N$. This agrees with the conclusions of ER since $\ln N \sim 1$, given that $k_{\max}$ is not too large.

The method based on probability generating functions allows to calculate the following approximate formula for the average shortest path length,

$$\ell = 1 + \frac{\ln\left(N/z_1\right)}{\ln\left(z_2/z_1\right)},$$

where z_m is the average number of neighbors at distance m. To verify that this expression yields the average distance in a Poisson random graph, we just need to take into account that $z_1 = \langle k \rangle$ and $z_2 = \langle k \rangle^2$ in these networks, thus

$$\ell = 1 + \frac{\ln\left(N/\langle k \rangle\right)}{\ln\langle k \rangle} = \frac{\ln N}{\ln\langle k \rangle}.$$

Finally, the clustering coefficient in a generalized random graph is

$$\overline{C} = \frac{\langle k \rangle}{N} \left[\frac{\langle k^2 \rangle - \langle k \rangle}{\langle k \rangle^2} \right]^2,$$

regardless the method applied. Notice that it is the value $\overline{C}$ for the Poisson random graph times an extra factor which depends on $P(k)$. Then, although the clustering coefficient is large for finite (and not very large) random graphs with highly skewed degree distributions, in general, it is very small.

Therefore, generalized random graphs are not qualitatively different from the ER graphs. There is a probability at which a phase transition occurs and the clustering coefficient and the average distance between vertices are small for large systems.

The theory of random graphs is, in Erdös' words, "*written in the Book*"—an imaginary book in which God had written down the best and most elegant proofs for mathematical theorems. This theory gave insight into how networks emerge and, for the first time, their evolution was considered.

However, this approach to networks misidentified complexity with randomness without analyzing if real systems fitted into this description. In fact, although ER mentioned in their 1959 seminal paper [37] that

> *the evolution of graphs may be considered as a rather simplified model of the evolution of certain communication nets (railway, road or electric network systems, etc.),*

they were finally charmed more by the mathematical beauty of random graphs than by its applicability and they did not verify their own suggestion.

1.3.4 Small–world networks

Six degrees of separation

Stanley Milgram (New York 1933–New York 1984) was a controversial social psychologist who conducted an experiment in 1967 that is considered the first evidence of the so–called *small–world phenomenon* and the source of the *six degrees of separation concept* [44].

In a first attempt, Milgram sent letters to 60 people in Wichita (Kansas) in which they were asked to forward that letter to the wife of a Divinity student in Sharon (Massachusetts). They could only pass the letters to personal acquaintances who they thought might be able to reach the target—whether directly or via another friend. The result was that three letters of the 50 people who responded to the challenge reached their destination. Furthermore, one of these three letters required just two intermediaries and four days to be handed.

Next, Milgram introduced several changes in the methodology to improve the perceived value of the letter, which was an important factor to motivate people to pass it. In the subsequent experiment, 100 people in Omaha (Nebraska) received a letter whose target was a stock broker in Boston (Massachusetts). In this case, the number of letters that arrived at Boston was 39.

The analysis of the letters that completed the task revealed that the median number of intermediaries was 5.5, a very small number. In addition, Milgram found a *"funnelling"* effect, that is, there was a small group of people with high connectivity that were often one of the intermediaries along the path. For instance, he noted that in the first experiment *"two of the three completed chains went through the same people"*.

Some researchers casted doubts on the validity of the results since other experiments that tried to link people of different races showed clear differences (despite the race of the target was unknown). Others argued that the number 5.5 obtained by Milgram was an overestimation since the shortest paths could not be known in advance and, then, the actual ones were longer.

Nevertheless, Milgram's result showed that, although the precise value might be different of 5.5, the separation between any person and everybody else in a social network was much smaller than the number of people in it. In fact, Milgram never rounded up his result to talk about "six degrees of separation" since he was aware that it was just a rough estimate. This term was born in 1991 when John Guare used this appealing idea about our close interconnectedness in a play with that title, which was eventually made into a homonym movie due to its success on Broadway.

Sometimes, two people who meet for the first time are amazed at knowing that they share a friend and cheer: *"What a small world!"* This smallness of our world is precisely what Milgram showed and from which the experiment takes its name. But, is this result only a property of social networks? Is this "small–world" phenomenon uniquely human or some subtle, but general, principle is at work?

Small worlds

A first example of the "small–world" phenomenon is a network inspired in the outstanding output of Erdös. His friends created the so–called *Erdös number* to keep track humorously of their distance from him. He has assigned the Erdös number zero. His immediate collaborators have Erdös number one. Those who write a paper with any Erdös coauthor are Erdös number two, and so on. The 90% of the world's active mathematicians have an Erdös number smaller than eight, being typically between three to five.

Furthermore, although the initial scope of the Erdös number was the mathematical community, finally it went beyond this field. Thus, we can find small Erdös numbers between physicists (Albert Einstein, two), economists (Paul Samuelson, five) or linguists (Noam Chomsky, four). Even William (Bill) Gates, founder of Microsoft, has an Erdös number of four. This smallness of most Erdös numbers shows that the scientific community is a highly interconnected network [45].

Another, and somewhat frivolous, example is the parlor game *"The six degrees of Kevin Bacon"* in which Kevin Bacon is linked to almost any actor through two or three movies. For instance, Brigitte Bardot played in *Shalako* with Sean Connery, who played in *The first great train robbery* with Donald Sutherland, who in turn played in *Animal house* with Kevin Bacon (see Fig. 1.13). Then, using the Erdös number analogy, Bardot has Bacon number three. Amazingly, even actors dead more than 75 years ago can be connected to him by few links (e.g., Rudolph Valentino has Bacon number three).

Figure 1.13. The six degrees of Kevin Bacon. Brigitte Bardot has Bacon number three since she played in *Shalako* with Sean Connery, who played in *The first great train robbery* with Donald Sutherland, who played in *Animal house* with Kevin Bacon.

However, although Kevin Bacon is a famous actor, he does not occupy a special place between actors. When Brett Tjaden and his colleague Glen Wasson managed

to gather the complete database of all actors and movies ever released [46], they found that all actors are separated on average by only three links. That is, the network of actors also shows the "small–world" phenomenon.

Nowadays, it is known that Milgram's experiment unveiled a property that has been found in a large number of systems. As Table 1.1 shows, the average path length in many real networks is rather small. Notice that, although the median separation in these networks is not six degrees, the "six degrees of separation" concept can be still used to emphasize the striking closeness between their nodes.

NETWORK	SIZE	$\langle k \rangle$	ℓ	ℓ_{rnd}	C	C_{rnd}
1. Movie actors [31]	225 226	61.0	3.65	2.99	0.79	0.00027
2. Power grid [31]	4 941	2.67	18.7	12.4	0.08	0.00054
3. WWW site level (undir.) [47]	153 127	35.2	3.10	3.35	0.11	0.00023
4. Words (co–ocurrence) [13]	460 902	70.1	2.67	3.03	0.44	0.00015
5. LANL co–authorship [25]	52 909	9.70	5.90	4.79	0.43	0.00018
6. MEDLINE co–authorship [25]	1 520 251	18.1	4.60	4.91	0.07	0.00001
7. Math. co–authorship [48]	70 975	3.90	9.50	8.21	0.59	0.00005

Table 1.1. Clustering coefficient and average path length of real networks. For each network, the number of nodes (size), the average degree $\langle k \rangle$, the average path length ℓ and the clustering coefficient C are shown. If we compare this values to the average path length ℓ_{rnd} and the clustering coefficient C_{rnd} of a random graph with the same size and average degree, we find that $\ell \sim \ell_{\text{rnd}}$ but $C \gg C_{\text{rnd}}$.

Interestingly, the average path length in these networks is roughly the corresponding to a random graph with the same number of nodes and average degree. This fact can be used to define mathematically the "small–world" phenomenon in the following manner.

If we compare the average shortest path length in a random graph, $\ell_{\text{rnd}} \sim \ln N$, to the expression $\ell_{\text{lat}} \sim \sqrt[d]{N}$ for a d–dimensional lattice, we find that the size dependence $\ell(N)$ is slower in random graphs than in lattices. This growth of $\ell(N)$ slower than any positive power of N is what we call the "small–world" phenomenon and networks with this characteristic are referred to as *small worlds* [40].

However, if we carefully analyze the networks on Table 1.1, we can see that their clustering coefficients are much larger than in a Poisson random graph with the same number of nodes and average degree. Actually, all of them have a clustering of the order of a lattice. For example, a three–dimensional lattice with the degree of the LANL co–authorship network has $\overline{C} = 0.41$ and a one–dimensional lattice with the degree of the movie actors network has $\overline{C} = 0.74$, which are approximately the real values. Therefore, most of complex systems are both small worlds, as random graphs, and highly clustered networks, as lattices.

Nevertheless, we can obtain a large clustering coefficient, while the average path length remains small, in a generalized random graph with a highly skewed degree distribution. Is it possible that complex systems are random graphs with awkward degree distributions?

On the other hand, if the dimension d of a lattice is large, its average path length becomes a slowly increasing function of N, $\ell_{lat} \sim \sqrt[d]{N}$. Then, a d–dimensional lattice whose average degree is much larger than $2d$ shows a small average path length and a high clustering coefficient. Despite this requieres a large average degree, could it be that real networks are high dimensional lattices?

Although both possibilities are reasonable for some networks, none is actually regarded as the answer. Real networks cannot be described neither as random graphs nor lattices, but they lie somehow between both of them, between order and disorder. This type of networks in which these two apparently irreconcilable terms coexist are called *small–world networks*.

At this point, it is important to remark that small worlds are not the same as small–world networks. Small worlds are a wide class of networks more compact than any finite–dimensional lattice. Small–world networks are small worlds with the typical high clustering of a lattice [40].

The Watts–Strogatz model

The first model that conciliated the existence of a large clustering with a small average path length was proposed by Duncan J. Watts and Steven Strogatz (WS) in 1998 [31].

They start from a low–dimensional lattice with N nodes and L links (a ring, for example). Then, each link is "rewired" with probability p, that is, one of its ends is randomly reassigned to a new node—with the constraints that any pair of nodes cannot have more than one edge and no node is linked to itself (see Fig. 1.14).

In this manner, the WS model continuously interpolates between the two limiting cases of a regular lattice ($p = 0$) and a random graph ($p = 1$). And consequently, we can consider that both the clustering coefficient and the average path length are functions of the rewiring probability p.
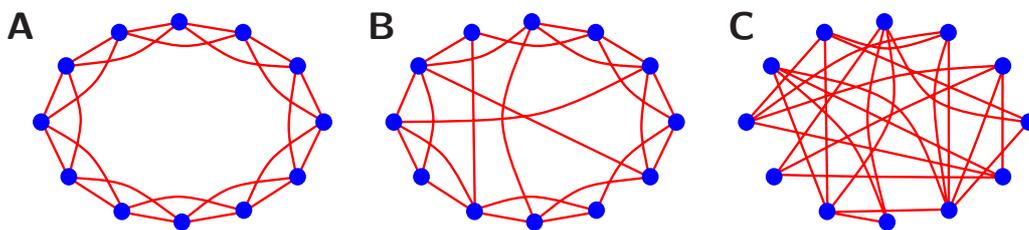
Figure 1.14. The Watts–Strogatz model. Here we show how a ring with 12 nodes and 24 links can be continuously transformed into a random graph by "rewiring" the ends of each link with probability p. The initial regular lattice (A) becomes a small–world network for halfway probabilities (B), and finally transforms into a random graph (C).

The interesting finding of WS was that only a few extra links are enough to reduce the average path length between nodes without changing the clustering coefficient significantly. In other words, they realized that there is an interval of rewiring

probabilities in which the clustering coefficient is still the corresponding to a lattice but the average path length is similar to a random graph (see Fig. 1.15).
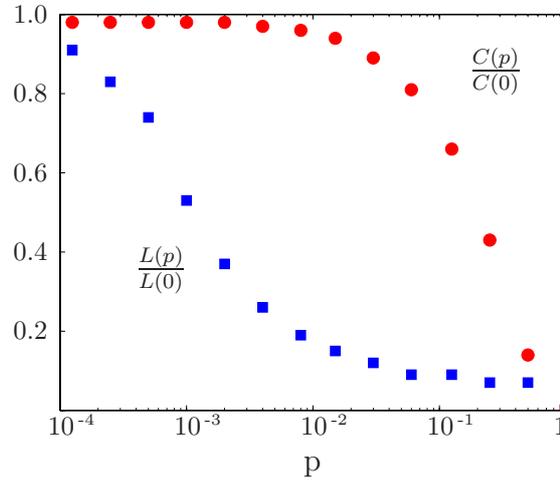
Figure 1.15. Small–world networks. As the probability p of rewiring increases from zero to one, we move from a regular lattice ($p = 0$) to a random graph ($p = 1$). Interestingly, the distance between nodes rapidly drops, thus there is an interval of probabilities in which the network is a small world and highly clustered, that is, a small–world network. After [31].

This result simply reflects that, although a few random links are enough to reduce the separation between nodes (since remote areas of a lattice are now connected), they are insufficient to change the local properties of a lattice and, in particular, its clustering coefficient. Hence, the "six degrees of separation" phenomenon is rooted in the fact that, even if most of people are very provincial in choosing their friends, a small fraction of the population with long–range links is enough to have a small world.

The WS model has many technical difficulties that prevent its analytical study, thus other equivalent models have been proposed in the literature to ease the mathematical treatment of small–world networks. A typical variant is the model independently developed by Monasson [49] and Newman and Watts [50] in which, rather than moving the edges between nearest neighbors, new links are added with probability p—these long–range connections (i.e., links between nodes that are not neighbors) are also known as *shortcuts*.

Since any pair of nodes cannot have more than one edge and no node is linked to itself, the Newman and Watts (NW) model interpolates between a lattice ($p = 0$) and a fully connected graph ($p = 1$). Then, while the WS model may lead to the formation of isolated clusters, the NW model has the desirable property that all vertices are always connected in one cluster and, consequently, it is easier to analyze. Nevertheless, despite these differences, both models are essentially equivalent and the results obtained for one of them can be applied to the other [36].

A first question prompted by Fig. 1.15 is when small–world networks emerges.

Numerical and theoretical studies show that the small–world regime appears when the probability p of having long–range connections verifies that $pN \sim O(1)$ [51, 52, 53]. Since the NW model is roughly a random graph on a lattice, the probability $p \sim 1/N$ coincides with the onset of the giant connected component associated to the links randomly added (i.e., without taking into account the edges between nearest neighbors).

If the initial lattice is one–dimensional, the clustering coefficient can be easily calculated [53, 54]. Thus, while the WS model has

$$\overline{C} = \frac{3(K-1)}{2(2K-1)}(1-p)^3,$$

the NW models verifies that

$$\overline{C} = \frac{3(K-1)}{2(2K-1) + 4Kp(p+2)},$$

being K the average degree in the initial lattice and p the rewiring (or adding) probability.

On the other hand, it is now widely accepted that, although the average path length has no exact solution, it has the general scaling form

$$\ell = \frac{N}{K}F(pKN^d),$$

where N is the number of nodes, K is the average degree in the initial d–dimensional lattice, p is the adding probability and $F(x)$ is a universal scaling function that asymptotically behaves as

$$F(x) \propto \left\{ \begin{array}{ll} 1 & \text{if } x \ll 1 \\ \ln(x)/x & \text{if } x \gg 1 \end{array} \right.$$

Notice that this form of F is reasonable since the small–world network model becomes a random graph for large p (in which ℓ scales logarithmically with system size) or a lattice for small p (in which ℓ scales linearly).

The variable pKN^d that appears as the argument of the scaling function is simply two times the mean number of shortcuts in the model and $F(x)$ is the average fraction by which the vertex–vertex distance is reduced for the given value of x. Then, ℓ basically depends on how many shortcuts there are for a given K.

The scaling function $F(x)$ can be calculated for one–dimensional networks (i.e., $d = 1$) using a mean–field approximation [55],

$$F(x) = \frac{4}{\sqrt{x^2 + 4x}} \tanh^{-1}\left(\frac{x}{\sqrt{x^2 + 4x}}\right),$$

which is exact for small and large values of x but only approximate when $x \simeq 1$.

Finally, although these two models of small–world networks explain the large clustering coefficient and average distance between nodes of real systems, they are
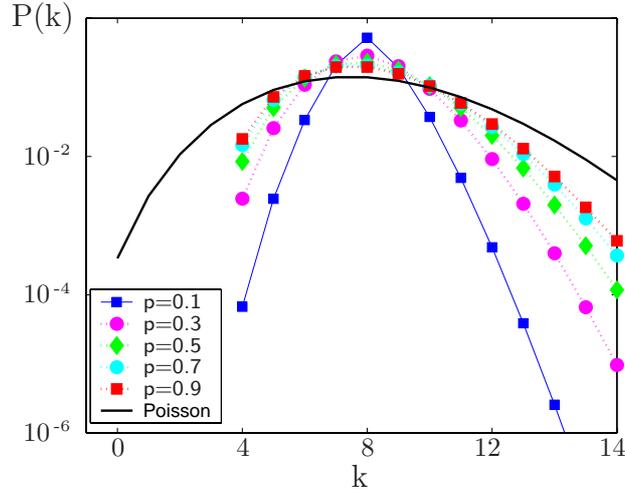
Figure 1.16. Degree distribution of the WS model for $K = 8$ and different rewiring probabilities p. Since the rewiring process only reallocates the existing edges, all distributions have the same average degree $\langle k \rangle = 8$ and the minimum number of links that a node has is $k_{\min} = K/2 = 4$. The black curve is a Poisson distribution with average degree eight as the others.

essentially random graphs from the viewpoint of their degree distributions (see Fig. 1.16). That is, they have a pronounced peak at their average value and their tails decay relatively fast.

In both models, all vertices have approximately the same number of connections since they present a pronounced peak at $\langle k \rangle = K$ and decay exponentially for large k—such networks are called *exponential networks*.

In fact, if the initial lattice has average degree K, the degree distribution of the WS model is [53]

$$P(k) = \begin{cases} 0 & \text{if } k < \frac{K}{2} \\ \sum_{i=0}^{\min\left\{k-\frac{K}{2}, \frac{K}{2}\right\}} \binom{\frac{K}{2}}{i} \frac{\left(\frac{1}{2}pK\right)^{k-\frac{K}{2}-i}}{\left(k-\frac{K}{2}-i\right)!} (1-p)^i \, p^{\frac{K}{2}-i} \, e^{-\frac{1}{2}pK} & \text{otherwise} \end{cases}$$

being p the rewiring probability (see Fig. 1.16), and the degree distribution of the NW model is

$$P(k) = \begin{cases} 0 & \text{if } k < K \\ \binom{N}{k-K} \left(\frac{pK}{N}\right)^{k-K} \left(1 - \frac{pK}{N}\right)^{N-k-K} & \text{otherwise} \end{cases}$$

where p is the adding probability.

1.3.5 Scale–free networks

Power–law degree distributions

In 1999, Albert–László Barabási and coworkers found [56, 57] that the degree distribution of some complex systems were *power laws* (i.e., $P(k) \sim k^{-\gamma}$) instead of

being Poisson–like as in exponential networks (see Fig. 1.17).
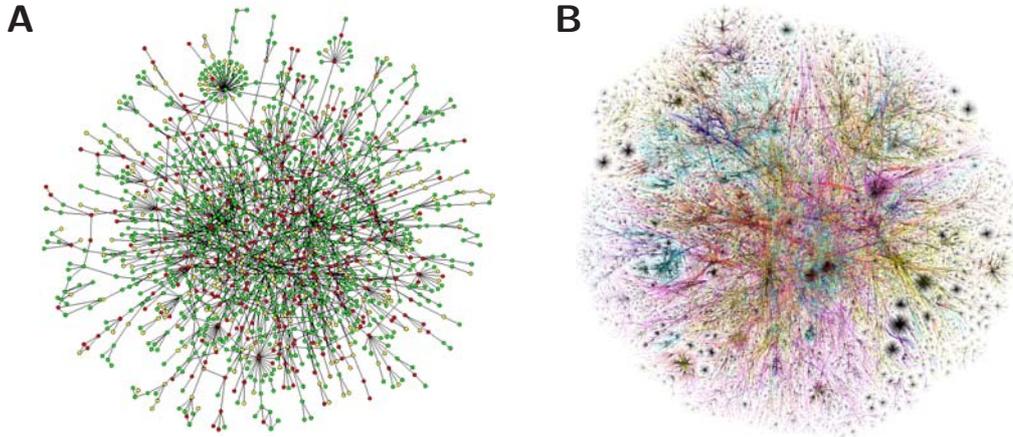
Figure 1.17. Scale–free networks. (A) The largest cluster of the yeast protein–protein interaction network is shown. The color of a node indicates the effect of removing the corresponding protein (red=lethal, green=non–lethal, orange=slow growth, yellow=unknown). After [58]. (B) A graph of Internet based on IP addresses. Each color represents a geographical localization: Asia Pacific = cyan, Europe/Middle East/Central Asia/Africa = magenta, North America = yellow, Latin American and Caribbean = blue, Unknown = Black. From the Opte Project.

This was an important (and unexpected) finding in the field of complex networks since power laws have two distinguishing features that makes them very different from Poisson–like distributions:

Power laws are relatively slow decreasing functions. Given the slow decay rate of a power law, the likelihood of extreme events is much greater than in Poisson–like distributions. For example, the distribution of wealth in most of European countries is a power law, meaning that many people possess relatively little wealth while a minority are extremely wealthy. This "explains" why it is easy to find people who is three or four orders of magnitude richer than others but it is inconceivable a human being even twice taller than the average. Whereas the distribution of wealth is a power law, the distribution of human heights is Gaussian.

A power–law distribution has no peak at its average value. Due to the fat tail that a power–law distribution has, the mean is much higher than what we would consider its "typical" value and, consequently, it is not very meaningful. Thus, the absence of a peak in the wealth distribution implies that there is no a characteristic individual but, on the contrary, a continuous hierarchy of them, spanning from the rare superrich to the numerous poor.

A network whose degree distribution is a power law is referred to as a *scale–free network* due to the lack of a characteristic scale. Actually, the important feature

that describes the distribution of these networks is the exponent γ which essentially reflects how the distribution changes as a function of the underlying variable.

Nowadays, it is known that the initial observation of Barabási and his colleagues was not an exception (see Table 1.2). Many empirical results show that real networks are often scale–free. This result implies that networks can be found both following power laws and exponential distributions.

NETWORK	SIZE	κ	$\gamma_{\text{in}}/\gamma_{\text{out}}$
1. Movie actors [57]	212 250	900	2.3
2. WWW [59]	$2 \cdot 10^8$	4000	2.7/2.1
3. Internet, router [60]	260 000	—	—/1.94
4. Words (co–ocurrence) [13]	460 902	—	2.7
5. Neuro. co–authorship [61]	209 293	400	2.1
6. SPIRES co–authorship [48]	56 627	1100	1.2
7. E-mail messages [62]	59 912	—	1.5/2.0
8. Metabollic network [63]	778	110	2.2

Table 1.2. Degree distributions of real networks. Nowadays, it is well known that many real–world networks are scale–free, that is, their degree distributions are power laws, $P(k) \sim k^{-\gamma}$. Since all empirical power law has a cut–off that may prevent its observation, it is important that this cut–off is not too small. This table shows, for eight networks, the number of nodes (size), the cut–off κ and the exponent γ. If the network is directed, both the in–degree and the out–degree are listed.

Notice that, although the finite size of a network is problematic for any degree distribution, it is particularly troubling for power laws since vertices with large degree are absent and, consequently, the degree distribution $P(k)$ always presents a cut–off κ. This cut–off is so important in networks with few nodes that the accurate observation of the degree distribution may be impossible. Then, the effect of the finite size of a network must be carefully analyzed to affirm confidently that a network is scale–free and not exponential [40].

The Barabási–Albert model

Although it is possible to construct a generalized random graph with a power–law degree distribution, reducing complex networks to sheer randomness cannot be the solution in general. We need a new paradigm to answer the important question of how scale–free networks emerge.

In 1999, Barabási and Reka Albert (BA) proposed a new model to explain the origin of power–law degree distributions in complex networks [57]. They started noting that other models had not considered two important features of real–world networks.

First, although edges could be added or rearranged in exponential models networks, they had a fixed number of nodes, contrary to most real networks that are

open and in continuous change. For example, the World Wide Web is endlessly adding, removing and reallocating web pages, thus neither nodes nor links are fixed.

Second, both random and small–world networks show a well defined scale due to the fact that each new link is created according to a uniform random distribution. However, an important consequence of having a power–law degree distribution is that some nodes, referred to as *hubs*, are much more connected than others.

Then, BA proceeded to show that scale–free structures emerge because of two factors: Growth and *preferential attachment*. Precisely, scale–free distributions appear when a network is continuously grown by adding new vertices (growth) that are linked to existing nodes proportionally to their degrees (preferential attachment). Consequently, hubs attract new connections with higher probability—this is the so–called *"rich gets richer" phenomenon*.

Once a small initial number N_0 of nodes is defined, the algorithm to obtain a BA model network has the following two steps:

Growth. A new node is added and linked to $n \leq N_0$ of the other nodes. Notice that, after t time steps, the number of nodes is $N(t) = t + N_0$ and the number of edges is $L(t) = nt$, thus the average degree asymptotically tends to

$$\langle k \rangle = \frac{nt}{t + N_0} \sim n.$$

Preferential attachment. The vertices to which the new node is attached are randomly chosen according to the *preference function*

$$p_i = \frac{k_i}{\sum_{j=1}^{N(t)} k_j},$$

where p_i is the probability that node $i = 1, ..., N(t)$ has of being linked and k_j the degree of node j.

If these steps are iteratively repeated (see Fig. 1.18), the degree distribution finally stabilizes in a power law with exponent $\gamma = 3$, being independent of n which is the only parameter in the model.

If we consider a model in which, at every time step t, a new node is linked to n old vertices without preferential attachment, we can assume that this new node is connected to node i following an uniform distribution (i.e., independent of k_i),

$$p_i = \frac{1}{N_0 + t},$$

where N_0 is the initial number of nodes. In this case, it can be analytically proved [57] that the resulting degree distribution decays exponentially, $P(k) \sim \exp(-k/n)$, as t tends to infinity.

On the other hand, if we start with a fixed number N of nodes and no edges, but we create new links by preferential attachment, numerical simulations show that the
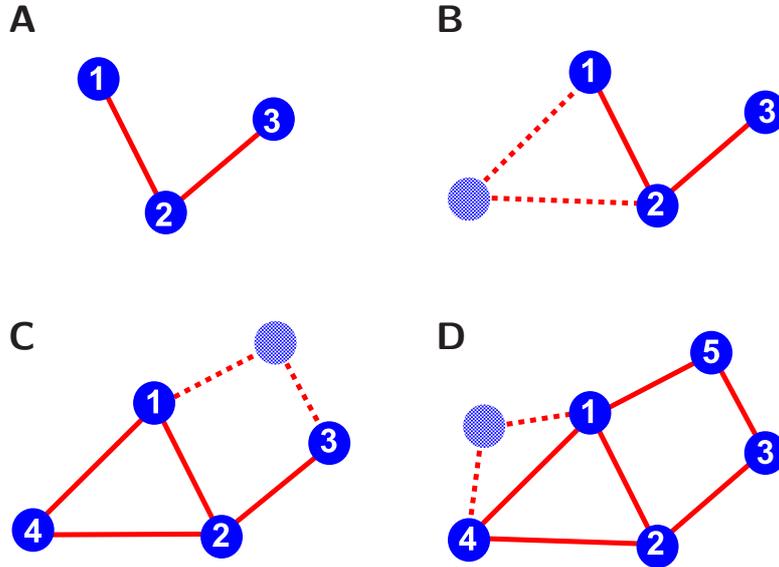
Figure 1.18. The Barabási–Albert model. (A) The network has initially $N_0 = 3$ nodes and two links. (B) Then, a fourth node is linked to $n = 2 < N_0$ out of the three existing vertices with probability proportional to their degrees (i.e., $p_{i=1...3} = \{1/4, 1/2, 1/4\}$). (C) At the following step, a fifth node is attached to $n = 2$ out of the four existing nodes with probabilities $p_{i=1...4} = \{2/8, 3/8, 1/8, 2/8\}$. (D) If we repeatedly iterate this procedure, a heterogeneous degree distribution is finally obtained since nodes with more connections have a higher probability of being linked to new vertices.

scale–free behavior only exists at early times [64]. Precisely, after a transient time of $t \approx N^2$ steps in which the degree distribution is a power law, the network becomes a fully connected graph (since N is constant but the number of edges increases) in which any node is characterized by a Gaussian distribution with mean degree

$$k_i(t) = \frac{2}{N} t.$$

Therefore, both growth and preferential attachment are required simultaneously to obtain a power law. The absence of one of them derives in an exponential network rather than in a scale–free structure. Then, an interesting question is if the BA preference function is unique or others also produce power laws.

Although the amount of papers on that issue is impressive (see [61, 18, 65] for an exhaustive and exhausting description of many of them), the main result is that scale–free degree distributions emerge only if the preference function p_i (i.e., the probability that a new edge is linked to node i with degree k_i) is linear,

$$p_i = \frac{\eta_i k_i + c_i}{\sum_{j=1}^{N(t)} \eta_j k_j + c_j},$$

where η_i is a *fitness constant* that measures the intrinsic ability of a node to attract

connections (e.g., new scientific articles can be more cited than old ones, if they are more interesting), and c_i is the *initial attractiveness* of node i. Depending on the concrete parameter values of the model, any $\gamma \geq 2$ can be obtained with this form of preferential attachment, contrary to the original BA model which has always $\gamma = 3$.

When the preference function is non–linear, the scale–free nature of the network is destroyed. Thus, while a sub–linear preference function produces a exponential degree distribution, a super–linear preference function leads to a network in which one node is nearly linked to all other vertices—this known as the *"winner–takes–all" phenomenon*.

It is important to remark that the preferential attachment is incorporated in the model with no explanation for its origin. In fact, although several "microscopic" mechanisms have been proposed to justify the existence of the preferential attachment (e.g., *copying mechanism* [66], *edge redirection* [67], *walking on a network* [68], or *attaching to edges* [69]), it is widely accepted that there is no universal answer to this question but it is model dependent.

Another interesting fact is that the BA model generates a small world as the behavior of its average path length ℓ shows. Actually, analytical results [70] prove that any network with a power law distribution is a small world since they grow slower than any power of N,

$$\ell \sim \begin{cases} \ln \ln N & \text{if } 2 < \lambda < 3 \\ \ln N / \ln \ln N & \text{if } \lambda = 3 \\ \ln N & \text{if } \lambda > 3 \end{cases}$$

Note that, for $\lambda = 3$ (i.e., the BA model), the double logarithmic correction to the logarithmic N dependence is a constant in practice.

Finally, although there is no analytical prediction for the BA model, numerical simulations show that its clustering coefficient approximately follows a power law, $\overline{C} \sim N^{-0.75}$ [61]. This decay is slower than in random graphs (i.e., $\overline{C} \sim N^{-1}$) but it is still different from the constant value obtained for the WS model.

Getting rich can be hard

We have seen that both the scale–free model of Barabási and Albert and the model proposed by Watts and Strogatz are small–world networks since they are small worlds with a large clustering coefficient. Note that scale–free networks are small–world networks but the inverse is not true in general.

However, empirical data suggest that the differences between their degree distributions are irreducible and the existence of the following three classes of small–world networks cannot be neglected [71]:

1. Single–scale networks, characterized by a degree distribution with a fast decaying tail, such as exponential or Gaussian.

2. Scale-free networks.

3. *Truncated scale–free networks*, characterized by a degree distribution that has a power–law regime followed by a sharp cut–off that is not due to the finite size of the network.

This fact arises the interesting question of how this three type of small–world networks are related. In 2000, Luís A. N. Amaral and coworkers found this relation when they noted that the governing principle in a scale–free network (i.e., the preferential attachment) can be overridden by other stronger factors, preventing the emergence of a power law [71]. These factors are mainly the following:

Aging. In some cases, a node (even a hub) may be part of a network and contributing to network statistics without receiving new links. This can be found in networks in which the probability of connection of the new site with some old one is proportional not only to the connectivity of the old site but also to some function of its age. For example, researchers in a citation network only receive links (i.e., citations) as long as their work is considered not "too old". When this occurs, these authors and their citations remain in the network but the "preferential attachment" no longer applies to them.

Cost of adding links and limited capacity. The "preferential attachment" principle implicitly assumes that connections are costless, thus nodes can have any degree regardless the difficulty of establishing (or maintaining) them. This can be true for the WWW but not for human, technical or biological networks. For instance, the number of friends that a person has is not limited by the size of the global population but by the energy and time they require. Hence, the "preferential attachment" principle in a network of acquittance (i.e., "popularity is attractive") only works while nodes are not saturated, after which time newcomers will tend to befriend other more accesible people.

Limits on information and access. Even though the creation of a connection has no cost, it is generally false that a new node can know the degrees of any other node in the network to establish its links by "preferential attachment" [72]. New nodes appear in a particular part of the network and it is required a costly process of search to find out how the rest of the network is. For example, the outgoing links in a web page may well be directed to pages with many ingoing links (i.e., preferential attachment) but only among those that the new web page knows.

Bibliography

[1] P.W. ANDERSON. *More is different.* Science 177, 393–396 (1972).

[2] S. SOLOMON AND E. SHIR. *Complexity: A science at 30.* Europhysics News 34(2), 54 (2003).

[3] G.L. BAKER AND J.P. GOLLUB. *Chaotic dynamics: An introduction,* Cambridge University Press, Cambridge, 1990.

[4] H.E. STANLEY. *Exotic statistical physics: Applications to biology, medicine and economics.* Physica A 285, 1–17 (2000).

[5] B. DENNIS, R.A. DESHARNAIS, J.M. CUSHING, S.M. HENSON, R.F. COSTANTINO. *Estimating chaos and complex dynamics in an insect population.* Ecological Monographs 71(2), 277-303 (2001).

[6] R. LEWIN. *Complexity: Life at the edge of chaos,* University of Chicago Press, Chicago, 2000.

[7] H.E. STANLEY. *Introduction to phase transitions and critical phenomena,* Oxford University Press, Oxford, 1971.

[8] L.A.N. AMARAL AND J.M. OTTINO. *Complex networks.* European Physical Journal B 38, p147–162 (2004).

[9] D.J. WATTS. *Six degrees: The science of a connected age,* W.W. Norton & Company, Inc., New York, 2003.

[10] D.J. WATTS. *Small worlds: The dynamics of networks between order and randomness,* Princeton University Press, Princeton, New Jersey, 1999.

[11] M. FALOUTSOS, P. FALOUTSOS AND C. FALOUTSOS. *On power–law relationships of the Internet topology.* Comput. Commun. Rev. 29, 251–262 (1999).

[12] J.E. COHEN, F. BRIAND AND C.M. NEWMAN. *Community food webs: Data and theory,* Springer–Verlag, Berlin, 1990.

[13] R. FERRER I CANCHO AND R.V. SOLÉ. *The small–world of human language.* Proceedings of the Royal Society of London B 268(1482), 2261–2265 (2001).

[14] J. SCOTT. *Social network analysis: A handbook,* Sage, London, 2000.

[15] J.G. WHITE, E. SOUTHGATE, J.N. THOMPSON AND S. BRENNER. *The structure of the nervous system of the nematode C. Elegans.* Philos. Trans. Roy. Soc. London 314, 1–340 (1986).

[16] E. RAVASZ, A.L. SOMERA, D.A. MONGRU, Z.N. OLTVAI AND A.-L. BARABÁSI. *Hierarchical Organization of Modularity in Metabolic Networks.* Science 297, 1551–1555 (2002).

[17] P.S. Bearman, J. Moody and K. Stovel. *Chains of affection: The structure of adolescent romantic and sexual networks*. American Journal of Sociology 100, 44–91 (2004).

[18] S. Boccaletti, V. Latora, Y. Moreno, M. Chavez and D.-U. Hwang. *Complex networks: Structure and dynamics*. Physics Reports 424, 175–308 (2006).

[19] M. Granovetter. *The strength of weak ties*. American Journal of Sociology 78, p1360–1380 (1973).

[20] A.-L. Barabási, H. Jeong, R. Ravasz, Z. Neda, A. Schubert and T. Vicsek. *Evolution of the social network of scientific collaborations*. Physica A 311, 590–614 (2002).

[21] R. Pastor-Satorras and A. Vespignani. *Evolution and structure of the Internet: A statistical physics approach*, Cambridge University Press, Cambridge, 2004.

[22] A.E. Krause, K. A. Frank, D.M. Mason, R.E. Ulanowicz and W.W. Taylor. *Compartments revealed in food–web structure*. Nature 426, 282–285 (2003).

[23] J. Galaskiewicz and P.W. Marsden. *Interorganizational resource networks: Formal patterns of overlap*. Social Sci. Res. 7, 89–107 (1978).

[24] G.F. Davis and H.R. Greve. *Corporate elite networks and governance changes in the 1980s*. American Journal of Sociology 103, 1–37 (1997).

[25] M.E.J. Newman. *The structure of scientific collaboration networks*. PNAS USA 98, p404–409 (2001).

[26] G. Ergün. *Human sexual contact network as a bipartite graph*. Physica A 308, p483–488 (2002).

[27] I. Farkas, I. Derényi, A.-L. Barabási and T. Vicsek. *Spectra of "real–world" graphs: Beyond the semi-circle law*. Physical Review E 64, 026704 (2004).

[28] K.-I. Goh, B. Kahng and D. Kim. *Spectra and eigenvectors of scale–free networks*. Physical Review E 64, 051903 (2001).

[29] X.F. Wang. *Complex networks: Topology, dynamics and synchronization*. International Journal of Bifurcation and Chaos 12(5), 885–916 (2002).

[30] V. Latora and M. Marchiori. *Efficient behavior of small–world networks*. Physical Review Letters 87, 057105 (2001).

[31] D.J. Watts and S.H. Strogatz. *Collective dynamics of "small–world" networks*. Nature 393, p440–442 (1998).

[32] A. Barrat, M. Barthélemy, R. Pastor-Satorras and A. Vespignani. *The architecture of complex weighted networks*. PNAS USA 101, 3747–3752 (2004).

[33] J.P. Onnela, J. Jari Saramäki, J. Kertész and K. Kaski. *Intensity and coherence of motifs in weighted complex networks*. Physical Review E 71, 065103 (2005).

[34] M.E.J. Newman. *The structure and function of Complex Networks.* SIAM Review 45, p167–256 (2003).

[35] L. Euler. *Solutio problematis ad geometriam situs pertinentis.* Opera Omnia 1(7), 1–10 (1736).

[36] M.E.J. Newman. *Models of the Small World: A review.* Journal of Statistical Physics 101, 819–841 (2000).

[37] P. Erdös and A. Rényi. *On random graphs.* Publicationes Mathematicae Debrecen 6, 290–297 (1959).

[38] P. Erdös and A. Rényi. *On the evolution of random graphs.* Publ. Math. Inst. Hung. Acad. Sci. 5, 17–60 (1959).

[39] B. Bollobás. *Random graphs*, Academic Press, New York, 1985.

[40] S.N. Dorogovtsev and J.F.F. Mendes. *The shortest path to complex networks.* arXiv.org:cond-mat/0404593 (2004).

[41] E.A. Bender and E.R. Canfield. *The asymptotic number of labelled graphs with given degree sequences.* Journal of Combinatorial Theory A 24, 296–307 (1978).

[42] M. Molloy and B. Reed. *The size of the largest component of a random graph on a fixed degree sequence.* Combinatorics, Probability and Computing 7, 295–306 (1998).

[43] M.E.J. Newman, S.H. Strogatz and D.J. Watts. *Random graphs with arbitrary degree distributions and their applications.* Physical Review E 64, 026118 (2001).

[44] S. Milgram. *The small–world problem.* Physiology Today 2, 60–67 (1967).

[45] A.-L. Barabási. *Linked: The new science of networks*, Perseus Publishing, Cambridge, Massachusetts, 2002.

[46] B. Tjaden and G. Wasson. Available at http://www.cs.virginia.edu/oracle/ (1997).

[47] L.A. Adamic. *Proceedings of the Third European Conference*, Springer–Verlag, Berlin, Germany, 1999.

[48] M.E.J. Newman. *Scientific collaboration networks I: Network construction and fundamental results.* Physical Review E 64, 016131 (2001).

[49] R. Monasson. *Diffusion, localization and dispersion relations on "small–world" lattices.* European Physical Journal B 12, 555–567 (1999).

[50] M.E.J. Newman and D.J. Watts. *Renormalization group analysis of the small–world network model.* Physics Letters A 263, 341–346 (1999).

[51] M. Barthélemy and L.A.N. Amaral. *Small–world networks: Evidence for a crossover picture.* Physical Review Letters 82, 3180–3183 (1999).

[52] M. Barthélemy and L.A.N. Amaral. *Erratum: Small–world networks: Evidence for a crossover picture.* Physical Review Letters 82, 5180 (1999).

[53] A. Barrat and M. Weigt. *On the properties of small–world networks.* European Physical Journal B 13, 547–560 (2000).

[54] M.E.J. Newman. *The structure and function of networks.* Comput. Phys. Comm. 147, 40–45 (2002).

[55] M.E.J. Newman, C. Moore and D.J. Watts. *Mean–field solution of the small–world network model.* Physical Review Letters 84, 3201–3204 (2000).

[56] R. Albert, H. Jeong and A.-L. Barabási. *Diameter of the world–wide web.* Nature 401, 130–131 (1999).

[57] A.-L. Barabási and R. Albert. *Emergence of scaling in random networks.* Science 286, 509–512 (1999).

[58] H. Jeong, S.P. Mason, A.-L. Barabasi and Z.N. Oltvai. *Lethality and centrality in protein networks.* Nature 411, 41–42 (2001).

[59] A. Broder, R. Kumar, F. Maghoul, P. Raghavan, S. Rajagopalan, R. Stata, A. Tomkins and J. Wiener. *Graph structure in the web.* Computer Networks 33, 309–320 (2000).

[60] L.A. Adamic and B.A. Huberman. *Power-Law Distribution of the World Wide Web.* Science 287, 2115 (2000).

[61] R. Albert and A.-L. Barabási. *Statistical mechanics of complex networks.* Review of Modern Physics 74, 47–97 (2002).

[62] H. Ebel, L.-I. Mielsch and S. Bornholdt. *Scale–free topology of e-mail networks.* Physical Review E 66, 035103 (2002)

[63] H. Jeong, B. Tombor, R. Albert, Z.N. Oltvai and A.-L. Barabasi. *The large–scale organization of metabolic networks.* Nature 407, 651–654 (2000).

[64] A.-L. Barabási, R. Albert and H. Jeong. *Mean–field theory for scale–free random networks.* Physica A 272, 173–187 (1999).

[65] S.N. Dorogovtsev and J.F.F. Mendes. *Evolution of networks: From biological nets to the Internet and WWW,* Oxford University Press, Oxford, 2003.

[66] J. Kleinberg, S.R. Kumar, P. Raghavan, S. Rajagopalan and A. Tomkins. *The Web as a graph: Measurements, models and methods.* Proceedings of the International Conference on Combinatorics and Computing, Lecture Notes in Computer Science 1627, Springer–Verlag, Berlin, 1999.

[67] P.L. Krapivsky and S. Redner. *Organization of growing random networks.* Physical Review E 63, 066123 (2001).

[68] A. VAZQUEZ. *Disordered networks generated by recursive searches.* Europhysics Letters 54, 430–435 (2001)

[69] S.N. DOROGOVTSEV AND J.F.F. MENDES. *Scaling properties of scale–free evolving networks: Continuous approach.* Physical Review E 63, 056125 (2001)

[70] R. COHEN AND S. HAVLIN. *Scale–free networks are ultrasmall.* Physical Review Letters 90, 058701 (2003).

[71] L.A.N. AMARAL, A. SCALA, M. BARTHÉLEMY AND H.E. STANLEY. *Classes of small–world networks.* PNAS USA 97, 11149–11152 (2000).

[72] S. MOSSA, M. BARTHÉLEMY, H.E. STANLEY AND L.A.N. AMARAL. *Truncation of power law behavior in scale–free network models due to information filtering.* Physical Review Letters 88, 138701 (2002).

Chapter 2

A real complex network: The 5th Framework Programme

2.1 Introduction

Understanding the relationship between research and industry is essential to improve the quality of life in any modern society. Ranging from faster application of new discoveries to knowing whether or where investment should be employed, this flow of knowledge between research and industry has long been of general interest.

However, knowledge is a very special resource whose study demands new techniques. The traditional approach to resources is based on the concept of scarcity since they are usually finite. But knowledge cannot be seen this way because it grows, and the more it is used the more it spreads [1]. In addition, existing studies on the research and industry interplay have neglected its network character [2, 3, 4].

We address in this chapter this relationship between research and applications by means of the complex networks theory [5]. As it was explained in Chapter 1, many other real systems (e.g., Internet, biological or social networks) are now best understood from this point of view. This is indeed the reason why investigations on this subject have been attracting so much attention in the past few years [6, 7, 8, 9].

We also explained in Chapter 1 that the success of this novel approach to Nature is based on the fact that the comprehension of a real complex system cannot be reduced to the study of its constituent elements. That is, it is necessary a complete analysis of the relations between all its components.

This can be done in two main ways, either proposing theoretical models or investigating real systems. This chapter corresponds to the latter case since we focus on an initiative that sets out the priorities for the European Union's research and technological development: the *Framework Programme* (FP).

The Framework Programme (FP) is a system in which structure and information flow affect each other simultaneously, which is interesting since it is usual to find that either the topology of a network constrains the flow of information on it [9] or the information stored in the network defines its topology [10].

Currently, the 6th programme is under execution and the 7th is being planned, thus we focus our investigation in the 5th Framework Programme (FP5), corresponding to the period $1998 - 2002$, in order to analyze a completely finished programme.

The first step to study this network is to fix the vertices and the property determining if there exists a connection between any couple of them. In our case, it is natural to consider that each vertex is a participant in the Programme and each edge represents two participants collaborating in a project.

Once the vertices and the edges of the network are defined, the data to generate the graph can be obtained from CORDIS [11]. This information is not given in the form of a database, thus it is necessary to program a robot to gather it. The result is a large database made of 15 776 projects, from which it is derived a graph with 25 287 nodes (participants) and 329 636 edges (collaborations).

Despite the presence of more than 25 000 participants, they can be split in two major groups: Companies and Universities. The first is made of over 16 700 companies and other industry related participants who expect their investments in R+D+I to be profitable. The second group can be regarded as the opposite, more than 8 500 participants involved in some type of research for whom results do not necessarily return income (see Appendix).

Exploring the relationship between these two groups not only provides a good example of the interplay between structure and information flow, but also offers a glimpse on how research links with innovation and if the distance between basic research, applications and products reduces [12].

At this point, it is important to remark that we are mainly interested in the capacity of the FP5 to create and transfer information and nothing can be said about this question inside each node. Notice that some participants are large institutions or companies with complex organization charts and if they have several projects, their coordination cannot be guaranteed in general. However, our concern is how to set the means to integrate research, development and innovation efficiently, not if these means are successfully used.

To characterize the FP5, we compute five important features in any network: degree distribution, shortest path distribution, betweenness, clustering coefficient and the degree–degree correlation. The detailed description of the dataset can be found in the Appendix.

2.2   Degree distribution

We find that the degree distribution of the FP5 follows a power–law, $P(k) \sim k^{-\gamma}$, with a striking maximum degree $k_{\max} = 2\,784$ and average degree $\langle k \rangle = 26.1$ (see Fig. 2.1A).

In general, the observation of a power–law is troubling because it may be hindered by the fluctuations at large degrees [13]. Then, to measure the degree distribution confidently, it is required that $N \gtrsim 10^3$ when $\gamma < 2$ or $N \gtrsim 10^{2.5(\gamma-1)}$ when $\gamma > 2$. Consequently, the scale–free behavior of the FP5 can only be assured if the points are fitted to a power law with $\gamma < 2.7$.

But if a linear regression is calculated for all the points lying on the right of the maximum, the FP5 fits a power law $P(k) \sim k^{-\gamma}$ with $\gamma = 1.86 \pm 0.02$ and a correlation coefficient $R = 0.92$, which is an exponent smaller than the threshold

discussed previously.

Likewise, the probability that a University collaborates with k other Universities is a power law with $\gamma_u = 1.56 \pm 0.03$ and a correlation coefficient $R = 0.93$, and the degree distribution of Companies is also a power law with $\gamma_c = 2.32 \pm 0.07$ and $R = 0.94$ (see Fig. 2.1B).

These results imply that the FP5 has a scale–free topology that Universities and Companies share [14]. Then, collaborations within these networks were established following some type of preferential attachment during their growth. In other words, participants with more collaborations establish new ones at higher rate than participants with few connections. As a consequence, the so–called "rich–get–richer" phenomenon arises, in which the most connected participants increase their collaborations at the expense of the latecomers.
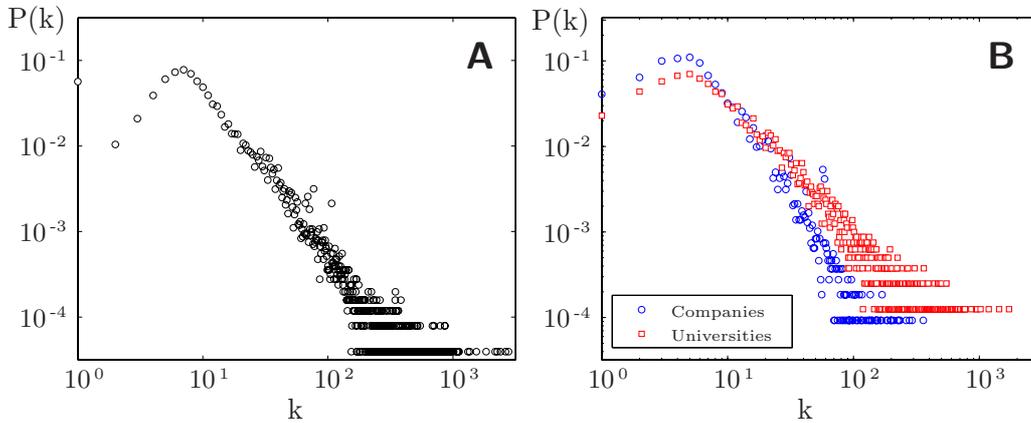
Figure 2.1. Degree distributions. (A) The FP5 network. The average degree is $k = 26.1$ and the maximum degree is a striking $k_{max} = 2\,784$. The points lying on the right of the maximum fit well a power–law, $P(k) \sim k^{-\gamma}$, where $\gamma = 1.86 \pm 0.02$ with a correlation coefficient $R = 0.92$. Consequently, the FP5 is scale–free. (B) We find that both Universities (red squares) and Companies (blue circles) follow a power law, $P(k) \sim k^{-\gamma}$, thus having a scale–free topology. If a linear regression is calculated as before, we obtain that $\gamma_u = 1.56 \pm 0.03$ with a correlation coefficient $R = 0.93$ for Universities, and $\gamma_c = 2.32 \pm 0.07$ with $R = 0.94$ for Companies. The fact that Universities show $\gamma_u < 2$ whereas Companies have $\gamma_c > 2$ implies that the mean degree of Universities grows in time but not the mean degree of Companies. From this result we conclude that some form of synergy encourages the creation of new collaborations between Universities but not between Companies.

Nevertheless, the main result is not the concrete value of γ since, as a consequence of the finite size of a network, there is always a cutoff region that makes difficult to derive it accurately. The main result is that the degree distributions of the FP5 and Universities are power laws with exponents smaller than two. This is interesting since it means that their average degrees diverge as the networks grow.

A possibility to explain this result is that they are accelerated growing networks [13]. In these networks, the total number of edges grows faster than a linear function of the total number of vertices and, consequently, it may be verified that

$1 < \gamma < 2$.

To elucidate this issue, we can compute the average degree $\langle k \rangle$ during several years to check its tendency. Although we have only the data corresponding to four years (Table 2.1), they are enough to confirm the existence of an accelerated growth since $\langle k \rangle$ is not constant but it grows.

Year	N Univ–Comp	(Total)	⟨k⟩ Univ–Comp	(Total)	C Univ–Comp	(Total)
1999	3 075– 4 658	(7 733)	17.2–6.2	(16.30)	0.65–0.58	(0.87)
2000	5 377– 9 359	(14 736)	21.9–6.8	(19.25)	0.66–0.53	(0.86)
2001	7 355–13 905	(21 260)	27.7–7.9	(23.56)	0.67–0.53	(0.86)
2002	8 522–16 765	(25 287)	31.9–8.2	(26.07)	0.68–0.59	(0.85)

Table 2.1. Evolution of Universities and Companies in the FP5. Here we show the total number of vertices N, the average degree $\langle k \rangle$ and the average clustering coefficient $\overline{C}$ during the four years that the FP5 lasted. This data let us conclude that there is an accelerated growth in the network since the average degree is not constant but it grows.

But if collaborations grow faster than proportional to the number of participants, it is because they do not emerge by the mere increase of participants. Not only new participants contribute to increase the number of collaborations, but also the old ones. Then, some form of synergy exists that encourages the creation of new collaborations.

However, the average degree of Companies is practically constant during the four years that the FP5 lasted (table 2.1). Then, although the creation of collaborations is encouraged (e.g., when the FP5 was finished the mean number of collaborations had risen from 10 to 26 and some participants had surpassed 2 500 collaborations), these results reveal that the synergy exists only between Universities. In this sense, the FP5 fails to improve the network of Companies and only Universities use this opportunity to create new collaborations.

2.3   Shortest paths

Although the FP5 network is not completely connected, we find that its giant connected component (GCC) spans 91.17% of the nodes (23 055 vertices). Likewise, the GCC of the network including only Universities spans 7 987 vertices (i.e., 93.7% of them) and the GCC of Companies is made of 10 801 nodes (i.e., 64.4%).

Hence, while most of Universities are linked between them, Companies are more fragmented and one third of them fall in other smaller components (actually, the second biggest component contains only 48 participants). This result shows that Universities are important to compact the FP5 network since its GCC comprises 88.7% of Companies and 96.0% of Universities.

In addition, we can obtain the distribution of shortest paths $P(d)$ as follows:

$$P(d) = \frac{2N(d)}{N_{gcc}(N_{gcc} - 1)},$$

where N_{gcc} is the number of vertices in the GCC and $N(d)$ is the number of times a distance d occurs in this component. Once $P(d)$ is known, we can easily derive the average distance in this manner:

$$\ell = \sum_{i>j} \frac{2d_{ij}}{N_{gcc}(N_{gcc}-1)} = \sum_{d>0} P(d)d,$$

where vertices i and j belong to the GCC.

In Fig. 2.2A, we plot the shortest paths distribution $P(d)$ to show the large compactness of the FP5 network, which is indeed useful to integrate the R+D+I in Europe. The greatest distance in the network is only 8 and the average distance is $\ell = 3.14$.

Likewise, we find that the farthest pair of Companies is separated by 14 edges and the average distance is $\ell_c = 5.67$, in contrast with the network of Universities in which the greatest distance is 7 and the average distance is $\ell_u = 3.34$ (see Fig. 2.2B). Thus also here Universities are essential for Companies to reduce the separation between them.
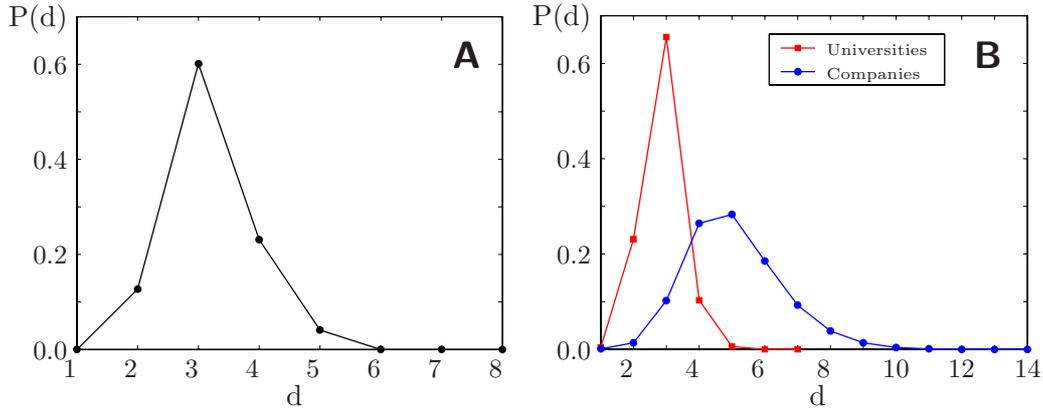
Figure 2.2. The distribution of shortest paths. (A) The $P(\ell)$ in the giant connected component of the FP5 is shown. The mean value is $\ell = 3.14$ and the farthest pair of nodes in the graph is separated by only 8 edges. (B) The distribution of shortest paths in the GCC of Universities (red squares) and Companies (blue circles) is shown. The mean value is $\ell_u = 3.34$ for Universities and $\ell_c = 5.67$ for Companies. Furthermore, while the farthest pair of Companies has 13 intermediaries, for Universities the maximum separation is 7 edges.

Notice that the average distances obtained are approximately the value obtained for a random graph [15] with the same number of nodes and average degree (i.e., $\ell \approx \ln N/\ln\langle k \rangle = 2.61$ for Universities, $\ell = 4.62$ for Companies and $\ell = 3.11$ for the whole network).

It is also possible to calculate the average distance of a vertex of degree k to all other vertices in the GCC [16]. To obtain $\ell(k)$, one first calculates the average

distance from vertex i to all other vertices j in the GCC:

$$\ell_i = \sum_{j \neq i} \frac{d_{ij}}{N_{gcc} - 1},$$

and then takes the average of ℓ_i over all vertices i that have $k_i = k$:

$$\ell(k) = \sum_{\{i:k_i=k\}} \frac{\ell_i}{N_{gcc} P(k)}.$$

We note that, within the GCC of the FP5, $\ell(k)$ has a logarithmic dependence on k since we can fit $\ell(k) \sim -\beta \log k$ with $\beta = 0.555 \pm 0.004$ and a correlation coefficient $R = 0.986$ (see Fig. 2.3A). Also, we find this logarithmic dependence in the GCC of Universities, being $\beta_u = 0.503 \pm 0.003$ with $R = 0.994$, and within the GCC of Companies in which $\beta_c = 1.13 \pm 0.03$ with $R = 0.958$ (see Fig. 2.3B).
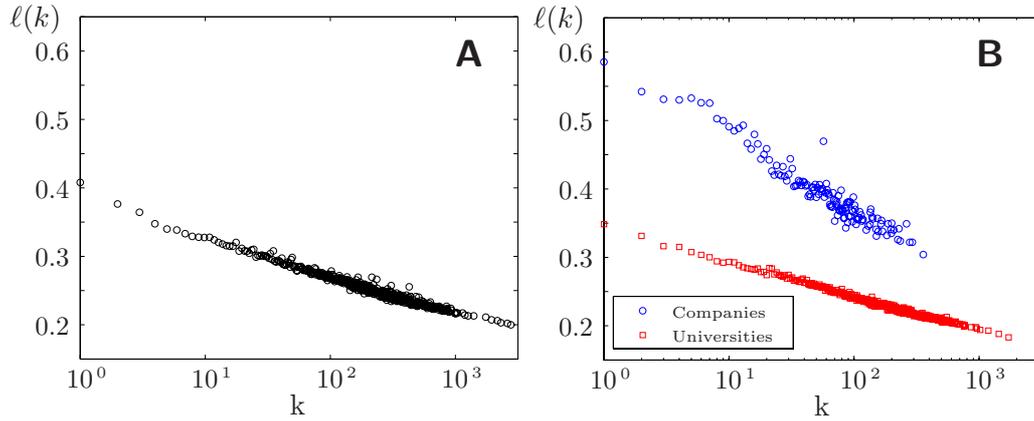
Figure 2.3. The average distance of a vertex of degree k to all other vertices. (A) The logarithmic dependence of ℓ within the GCC of the FP5 is shown: $\ell(k) \sim \log k^{-\beta}$ where $\beta = 0.555 \pm 0.004$ with $R = 0.986$. (B) This figure depicts the logarithmic dependence $\ell(k)$ $\ell \sim -\beta \log k$ in the GCC of Universities with red squares ($\beta_u = 0.503 \pm 0.003$ with $R = 0.994$) and in the GCC of Companies with blue circles ($\beta_c = 1.13 \pm 0.03$ with $R = 0.958$). Note that the lowest degree vertices in the network of Universities show a distance to other vertices comparable to the one of the highest degree vertices in the network of Companies.

Since the three networks have power–law degree distributions, it is easy to prove that

$$\ell = \sum_k P(k)\ell(k) \sim -\beta \sum_k P(k) \log k \sim -\beta \log k_{max} \sim \frac{\beta}{\gamma - 1} \log k_{max}^{1-\gamma}.$$

Then, if we take into account that the maximum degree k_{max} in a scale–free network with N nodes verifies $N \sim k_{max}^{1-\gamma}$ [13], we obtain that

$$\ell \sim \frac{\beta}{\gamma - 1} \log N.$$

Therefore, the logarithmical dependence of $\ell(k)$ within the three networks implies that they all display the small–world effect, that is, they are small worlds [17].

Therefore, the presence of Universities eases the flow of information since they are much closer to each other than Companies. This could be expected since the main purpose of a company is to satisfy its shareholders, which does not include the spread of information from which competitors can take advantage.

But, interestingly, the consequences of this fact go beyond. When Universities are excluded from the projects, Companies become isolated despite Universities are only one third of the participants. Companies tend to form clusters, turning difficult (if not impossible) the communication between them and, consequently, little can be developed or innovated since other results are not available to work with. Thus the natural tendency of Companies to protect their findings would finish killing R+D+I. The presence of Universities contributes to moderate this.

2.4   Betweenness

To further investigate the interplay between Companies and Universities, we can also measure the betweenness in the FP5 [8]. The *betweenness* σ_m of vertex m measures the extent to which m lies on the paths between other participants. Then, since it accounts for the influence of a participant between other two distant participants, it is a measure that relates the local structure and the global topology of the network. It is defined as

$$\sigma_m = \frac{1}{(N-1)(N-2)} \sum_{i,j:i\neq j\neq m} \frac{B(i,m,j)}{B(i,j)},$$

where $B(i,j)$ is the number of shortest paths between nodes i and j, $B(i,m,j)$ is the number of such shortest paths passing through vertex m, and the sum is taken over all pairs of vertices i and j that do not include m. The pre–factor, where N is the total number of nodes, accounts for normalization, so that $0 \leq \sigma_m \leq 1$.

Since the computation of the betweenness for the whole FP5 is an extremely time–consuming task, we focus our study on one of its subprograms: 'Small and Medium sized Enterprises' (SME), which is formed by 195 research institutions and 212 Companies (see Appendix).

Given our ability to split the SME into Universities and Companies, several different situations are considered. The average betweenness of the SME, taken over all its vertices, turns out to be $\langle\sigma\rangle = 5.19 \cdot 10^{-3}$. Considering only those vertices m that are Universities, we find that their average betweenness among all other vertices in the SME is $\langle\sigma_u\rangle = 6.76\cdot10^{-3}$. Likewise, we obtain $\langle\sigma_c\rangle = 3.74\cdot10^{-3}$ for Companies.

Now, if we only take into account those shortest paths whose endpoints are Companies, the betweenness measures the role Universities play in linking Companies: $\langle\sigma_{cuc}\rangle = 5.44 \cdot 10^{-3}$; on the other hand, when the endpoints are Universities, the average betweenness of Companies is $\langle\sigma_{ucu}\rangle = 2.34 \cdot 10^{-3}$.

Thus, we see that the role Universities play between Companies is just above twice the one played by Companies between Universities. Moreover, given that

$\langle \sigma_u \rangle > \langle \sigma \rangle > \langle \sigma_c \rangle$), we observe again the central function played by research institutions in the FP5 network.

2.5   Clustering coefficient

The first finding is the large average clustering coefficient that the three networks possess: $\overline{C} = 0.85$ in the FP5 network, $\overline{C} = 0.68$ for Universities and $\overline{C} = 0.59$ for Companies. In fact, they are 3 orders of magnitude higher than the clustering coefficient of an Erdös–Rényi graph with the same N and $\langle k \rangle$ (i.e., $\overline{C} \cong \langle k \rangle / N$ [15]).

Moreover, $\overline{C}$ is independent of the number N of participants in all cases (see Table 2.1), in contrast with the prediction of a scale–free model [14] where $\overline{C} \sim N^{-0.75}$ [5]. This high and size–independent average clustering coefficient evidences the organization of Universities and Companies in modules.

To further analyze this issue, we have measured the clustering coefficient $C(k)$ as a function of the degree k. This function is obtained by considering all vertices with degree k and, for these vertices, computing the average value of C_i:

$$C(k) = \frac{1}{NP(k)} \sum_{\{i:k_i=k\}} C_i.$$

The function $C(k)$ for the FP5, after the region of low values of k in which $C(k)$ is approximately constant, decays as a power law (see Fig. 2.4A). Thus, if the initial plateau is not considered, the FP5 network verifies that $C(k) \sim k^{-\alpha}$, where $\alpha = 0.77 \pm 0.01$ with a correlation coefficient $R = 0.94$. Similarly, $C(k)$ is a power law $C(k) \sim k^{-\alpha}$ for Universities, where $\alpha_u = 0.54 \pm 0.01$ with $R = 0.97$, and for Companies, where $\alpha_c = 1.05 \pm 0.06$ with $R = 0.86$ (see Fig. 2.4B).

Therefore, these networks have hierarchical modularity because both scale–free and modular networks are degree–independent, whereas hierarchical modularity is characterized by the scaling law $C(k) \sim k^{-1}$ [18].

This result suggests that Universities and Companies have an inherent self–similar structure [19], being made of many highly connected small modules, which integrate into larger modules, which in turn group into even larger modules.

But this is certainly true since $16\,313$ of the vertices in the FP5 have local clustering coefficient $C_i = 1$, indicating the presence of many completely connected clusters (see Fig. 2.5A). This is due to the fact that $15\,814$ of these entities participate only in one project, having as neighbors other vertices, which in turn are all connected between them by virtue of the participation in the project.

Furthermore, given that this result suggests that they have weak geographical constraints [20], we searched for communities in them [21] and found precisely that they were not based on nationality (see Fig. 2.5B), whence, the FP is successfully applying a policy that avoids its segregation by nationality.

Finally, since the hierarchical organization of a network is a poorly defined term, we study this question through the notion of *hierarchical path* [23] because it is uncorrelated with $C(k)$. A path is said hierarchical if the degrees of the vertices along this path vary monotonously or they grow monotonously up to some maximum
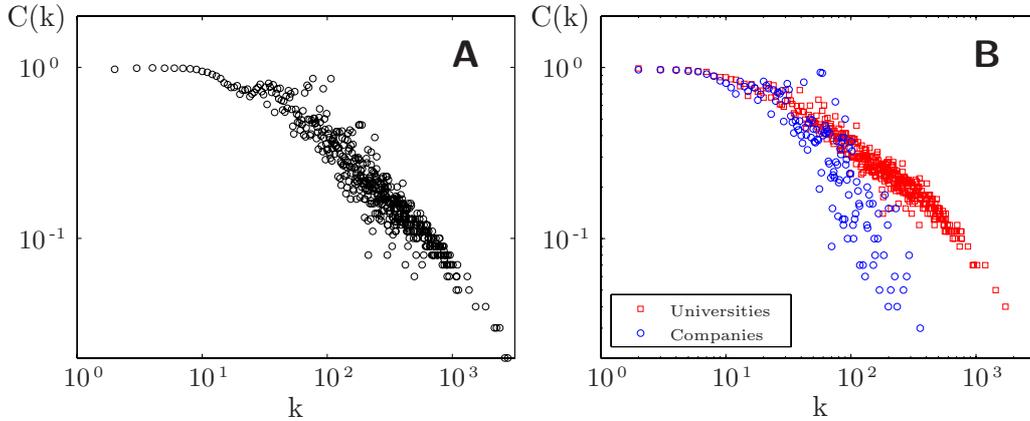
Figure 2.4. The clustering coefficient as a function of k is shown. From these figures, we conclude that the three networks have hierarchical modularity since scale–free and modular networks are degree–independent, whereas hierarchical modularity is characterized by the scaling law $C(k) \sim k^{-1}$. After the initial plateau, where $C(k)$ is approximately constant, it decays as a power law $C(k) \sim k^{-\alpha}$ where (A) $\alpha = 0.77 \pm 0.01$ with $R = 0.94$ for the FP5, (B) $\alpha_u = 0.54 \pm 0.01$ with $R = 0.97$ for Universities (red squares), and $\alpha_c = 1.05 \pm 0.06$ with $R = 0.86$ for Companies (blue circles).
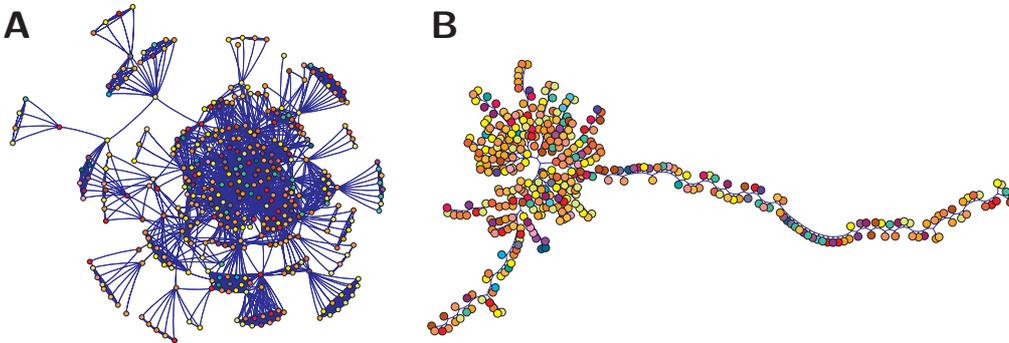
Figure 2.5. The existence of hierarchical modularity in the networks of Universities and Companies suggests that they have a self–similar structure. (A) Since projects in the FP are classified in 8 subprograms depending on their objectives, we choose, for clarity, to illustrate this self–similar structure with the smallest one (SME). (B) To verify if there is a bias by nationality in the collaborations, we searched for communities reflecting groups of participants collaborating strongly among them. The result is that all networks (even when analyzed by subprograms) behave as this one, corresponding to the SME subprogram. If we color each node according to its nationalities and arrange all of them with a standard algorithm [22], we find that they are all mixed.

value, from which decrease monotonously. Then, the fraction H of shortest paths that are hierarchical can be used as a metric of a hierarchical topology [24]. We find that the FP5 has $H = 0.91$, which confirms the hierarchical structure of the FP5. Actually, the distribution of hierarchical shortest paths is rather similar to the

distribution of all shortest paths. And this implies that most of the shortest paths between nodes are hierarchical.

2.6 Degree–degree correlation

An interesting question is which vertices pair up with which others. It may happen that vertices connect randomly, no matter how different they are. But usually there is a selective linking, there is some feature that makes more (or less) likely the connection [10]. If nodes with the same feature tend to link among them, the situation is called *assortative mixing*. In the opposite case, when vertices with some feature do not tend to connect among them, we have *disassortative mixing*.

A property that is usually used to investigate the presence of assortative mixing is the degree correlation. In this case, we say that there is assortative mixing when the nearest neighbors of vertices with high degree have also high degree. And there is disassortative mixing when the nearest neighbors of vertices with high degree have low degree [25, 26].

To analyze the degree correlations, we carry out three calculations: the joint degree–degree distribution, the mean degree $\bar{k}_{nn}(k)$ of the nearest neighbors of a vertex of degree k and the assortativity coefficient.

Figure 2.6. Joint degree–degree distribution of the FP5 network. The X and Y axes represent the degrees k and k' and the Z axis gives the corresponding joint degree–degree probability in per mill. The range is limited from 0 to 200 to illustrate a clearer picture. The distribution peaks on the line $k = k'$ which implies that the FP5 shows assortative mixing.

2.6.1 Joint degree–degree distribution

A first approach to elucidate this issue is by means of the *joint degree–degree distribution $P(k, k')$*, which gives us the probability of finding an edge connecting vertices of degree k and k'.

When we measure $P(k, k')$ for the FP5 network, it is found that $P(k, k')$ has sharp peaks for $k = k'$, suggesting that the FP5 presents assortative mixing. This

means that if one chooses at random a vertex of degree k then, with great probability, it will be connected to vertices of degree $k = k'$. The result for $k < 200$ is depicted in Fig. 2.6, where X and Y axes represent the degrees k and k', and Z axis gives the corresponding probability in per mill.

However, this assortative mixing is mainly due to Companies. In effect, we can see that Companies have sharp peaks at $k = k'$, meaning that Companies present assortative mixing (see Fig. 2.7A). In other words, Companies with similar degree tend to collaborate more frequently than Companies with different degrees.

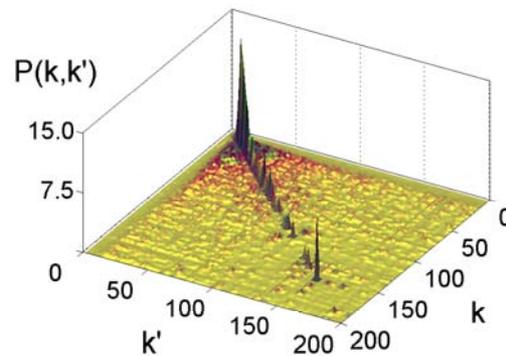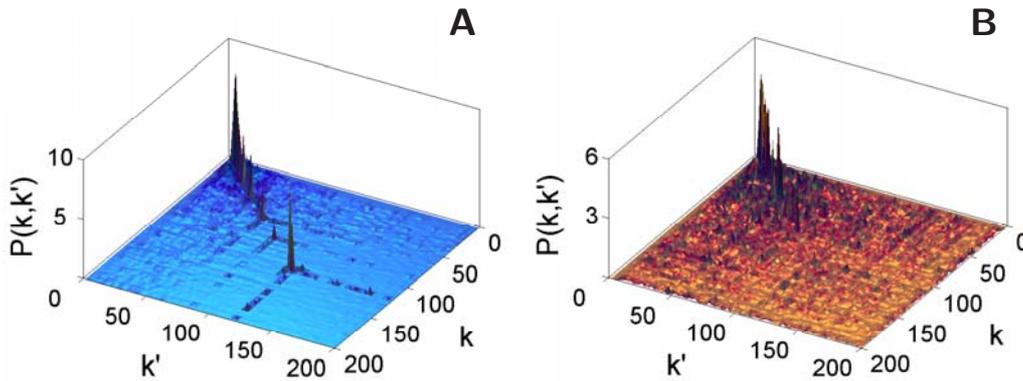**Figure 2.7.** Determination of the mixing through the joint degree–degree distribution. The X and Y axes represent the degrees k and k' and the Z axis gives the corresponding joint degree–degree probability in per mill. The range is limited from 0 to 200 for clarity. The joint degree–degree distribution of Companies (A) peaks on the line $k = k'$ which implies that the mixing is assortative. Since the number of links held by a participant is related to its size, we infer that Companies with similar sizes tend to collaborate more frequently than Companies with different sizes. The joint degree–degree distribution of Universities (B) is distributed throughout the X–Y plane which suggests that Universities do not have assortative mixing. Hence, we conclude that Universities choose their collaborators independently of their sizes.

But commonly, when a Company has high degree it is due to being involved in many projects. Therefore it is reasonable to assume that nodes with high degree represent large institutions, given that only these can deal with many projects at the same time. Then, the observed assortativity means that the spread of information between Companies depends on the institution's size.

On the contrary, Universities are distributed throughout the plane $k - k'$ (see Fig. 2.7B). While there are still peaks along the line $k = k'$, the presence of many others for $k \neq k'$ is clear, suggesting that Universities choose their partners independently of their sizes.

2.6.2 $\bar{k}_{nn}(k)$ distribution

It is important to remark that the joint degree–degree distribution requires many points to obtain good statistics. For example, if we focus our analysis in the range

$[0, 200]$, we need about 200×200 points, otherwise fluctuations are important and the plot is far from smooth [27]. To avoid this problem, it is used the mean degree $\bar{k}_{nn}(k)$ of the nearest neighbors of a vertex of degree k, which is a coarser but less fluctuating feature. To compute $\bar{k}_{nn}(k)$ we have only to find all nodes with degree k, and then, the average degree of all their neighbors is calculated.

The result for the complete FP5 network is shown in Fig. 2.8A. Interestingly, we find that the picture presents two regions with different behaviors that approximately overlap on $k \approx 200$. While for high degrees ($k \gtrsim 200$) the mixing is disassortative, for low degrees ($k \lesssim 200$) it is slightly assortative. However, the points on the right–hand side correspond to degrees where the finite size of the network is important, thus we cannot conclude that over $k = 200$ there is disassortative mixing.

To show this fact we have represented as green crosses those points calculated from only 1 or 2 participants (indicating the proximity to the cutoff) and the rest of the points as magenta circles. It can be seen that the majority of points over $k = 200$ are green crosses, that is, the $\bar{k}_{nn}(k)$ obtained for participants with high degrees is biased by the presence of the cutoff. This is reasonable since participants with $k \approx 1000$ could only have the value of $\bar{k}_{nn}(k)$ that the tendency imposes, if they had many neighbors with even higher degrees, but the finite size of the network impedes this.

Then, if we only consider the points below $k \gtrsim 200$ (i.e., the magenta circles), the mixing is slightly assortative. Nonetheless, another measure of the mixing will be helpful to determine the assortativity of the FP5.

The results for Universities and Companies support those obtained through the joint degree–degree distributions (see Fig. 2.8B). To emphasize the presence of the cut–off due to the finite size of the network, the points obtained from less than 10 observations are plotted as crosses (Universities in red and Companies in blue) and the rest of the points as red squares (Universities) or blue circles (Companies). Then, if we only consider the circles and the squares, we confirm that collaborations between Companies are size–dependent whereas those between Universities are much less size–dependent.

It is also interesting to analyze how Universities and Companies link each other, which can be done as follows. We search for all Companies with k links and then compute the average degree of all their neighboring Universities. Notice that the former degrees are always calculated in the corresponding network, thus a Company with degree k has k neighbor Companies, although it may have more links (with Universities). Analogously, we can look for all Universities with k links to average the degrees of all neighbor Companies.

If we plot again as squares (Universities) or circles (Companies) the points obtained from more than 10 observations to identify the region where the tendency is well defined. We find that, while Companies link to Universities independently of their degrees, Universities with high degree prefer to collaborate with Companies of large degree (see Fig. 2.9).
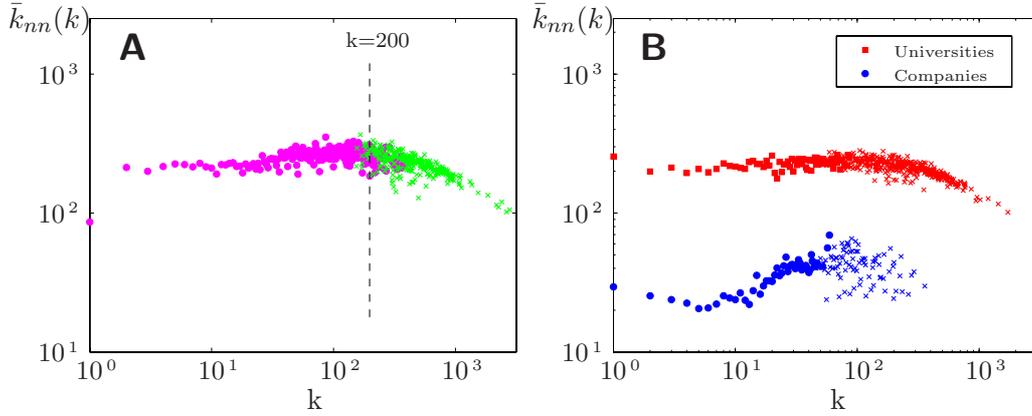
Figure 2.8. Plot of the mean degree of the nearest neighbors $\bar{k}_{nn}(k)$ of a vertex of degree k. (A) The complete FP5 network. Apparently, the behavior below $k \approx 200$ is slightly assortative and disassortative for higher degrees. However, only the region below $k \approx 200$ must be considered because the region apparently disassortative is where the finite size of the network is important. If the green crosses are points calculated from only 1 or 2 participants and the rest of the points are magenta circles, it can be seen that the region with disassortative mixing is essentially made of green crosses. (B) Universities and Companies. To mark the proximity to the cut–off, the points obtained from less than 10 observations are plotted as crosses (Universities in red and Companies in blue) and the remaining points as red squares (Universities) or blue circles (Companies). In this manner, it can be seen that these points are biased downwards because of the finite size of the network. Then, once we focus our attention on the circles and the squares, we find that Companies have assortative mixing, while links between Universities are much less size–dependent.

2.6.3 Assortativity coefficient

Another way to quantify the mixing in the FP5 is by means of the *assortativity coefficient* [25]. In this case, we obtain what type of mixing takes place in the network by means of a single number instead of a distribution.

If e_{jk} is the probability that a randomly chosen edge has vertices with degree j and k at either end, the assortativity coefficient takes the following form:

$$r = \frac{\sum_{jk} jk(e_{jk} - q_j q_k)}{\sum_k k^2 q_k - \left(\sum_k k q_k\right)^2}$$

where $q_k = \sum_j e_{jk}$ and $q_j = \sum_k e_{jk}$. This coefficient verifies that $-1 \leq r \leq 1$, being positive when the network is assortative and negative when it is disassortative.

The FP5 has assortative mixing since $r = 0.25$, which is close to the coefficients obtained for other social networks [26]. Also Universities and Companies have assortative mixing, although it is higher in Companies $r_c = 0.51$ than in Universities $r_u = 0.34$. Note that the whole FP5 has a smaller coefficient than the networks of Companies or Universities, indicating that the collaborations between Companies and Universities reduce the assortativity.
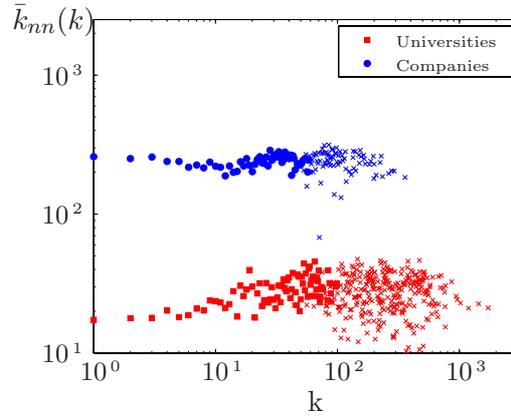
Figure 2.9. Here we plot the average degree of the nearest Companies of a University with k links to other Universities (red squares) and the average degree of the nearest Universities of a Company with k links to other Companies (blue circles). As before, if we only consider the circles and the squares, we find that Companies link to Universities independently of their degrees while Universities with high degree collaborate mainly with Companies that have also high degree.

Therefore, Companies and Universities differ in the way they establish collaborations. Companies are organized hierarchically, where positions in that hierarchy are related to the size: Large corporations are reluctant to choose as partners small companies. Between Universities, however, size is not important and it is common to find a large institution collaborating with a small one.

But if we analyze which partners Universities choose among Companies, we check that large institutions in Universities prefer working with large Companies. On the contrary, Companies select their collaborators between Universities regardless of their sizes. Then, we can conclude that large Companies are indeed the stars featuring the FP5 but Universities play the role of bridges between participants who are separated in the hierarchical structure of Companies.

2.7   Conclusions

We have thoroughly analyzed the complex network constituted by the scientific collaborations of the fifth Framework Programme to study the interplay between research and industry. This study uses the methods coming from the field of complex networks to derive several measures that allow us to quantify the features of this relationship and assess their potential improvements.

The FP5 network is scale–free with an accelerated growth, which means that new collaborations are created at a faster rate than usual. We have also concluded that some sort of synergy among the participants exists since new collaborations appear.

However, the fact that only Universities use the different programmes to create new collaborations shows that this is not enough to assure the transfer of knowledge.

While the network of Universities is well integrated and established in accordance to what is observed for other social networks, the same does not seem to be true for the Companies network, mainly due to its relatively small largest connected component. Competition is probably the origin of this effect, which is moderated by the presence of Universities.

We find that the transmission of information is more efficient between Universities than among Companies. Furthermore, when Universities are excluded from the projects, Companies tend to form clusters, turning difficult (if not impossible) the communication between them. These results point to the central function played by Universities in the FP5 network to reduce the distance between research and applications.

We also show that Companies and Universities are organized differently. Large corporations are reluctant to choose as partners small companies, whereas size is not important between Universities. But if we analyze how Universities and Companies cooperate; the result is that large Universities prefer working with large Companies, while Companies select their collaborators between Universities regardless of their sizes.

Therefore, while Companies exhibit a hierarchical structure, Universities do not. Then, although Universities contribute to approach Companies which would be separated otherwise, small Companies are not well integrated yet. Therefore, we believe that the industry–industry and industry–research interactions should be particularly encouraged, while maintaining the investment in the research–research interplay.

These findings have potential implications for future programmes, as well as for new policies and services aiming at research, development and innovation in general.

Appendix: Classification of participants into Companies and Universities

The Framework Programme (FP) sets out the priorities for the European Union's research and technological development. These priorities are defined following a set of criteria that pursue an increase of the industrial competitiveness and the quality of life for European citizens.

A fact that shows the effort made by the European Union to promote this global policy for knowledge is the budget devoted to these programmes. For example, the FP5 (1998-2002) was implemented by means of 13 700 million euros and the FP6 (2002-2006) has assigned a budget of 17 883 million euros.

All projects in the FP5 are organized in eight specific programmes which can be classified as follows. There are five focused Thematic Programmes implementing research, technological development and demonstration activities:

- QOL: Quality of life and management of living resources (2 524 projects).

- IST: User–friendly information society (2 382 projects).

- GROWTH: Competitive and sustainable growth (2 014 projects).

- EESD: Energy, environment and sustainable development (1 772 projects).

- NUKE: Research and Training in the field of Nuclear Energy (1 032 projects).

And there are three Horizontal Programmes to cover the common needs across all research areas:

- INCO: Confirming the international role of Community research (1 034 projects).

- SME: Encouragement of small and medium enterprises participation (142 projects).

- HPOT: Improving human research potential and the socio–economic knowledge base (4 876 projects).

The data to analyze the FP5 as a complex network were obtained from the web pages of CORDIS [11] with a robot implemented in Perl. The result was a database with 15 776 records as follows:

Programme | Year | Participant1 - Nation - Dedication | Participant2 - Nation - Dedication | ...

The first field refers to the specific programme to which the project belongs and the second field informs us about the year in which it started. The following fields are the participants in the project with their corresponding nationality and dedication ('research', 'education', 'industry'...).

Note that we have a bipartite graph [5, 13] since there are two kinds of vertices (participants and projects) and each edge links a participant with a project. To obtain the graph with 25 287 participants (nodes) and 329 636 collaborations (edges) used throughout the text, we have only to project it onto the participants.

The names of the participants were not free of typos since we collected them as they were in the web. The consequence of this fact was that sometimes the same participant appeared in two projects with different names and, consequently, it was recorded twice in the data. For instance, 'François Company of Something, Ltd.' and 'Francois Company of SOMETHING LTD' would be recorded as different. To avoid these duplications, we used a parser covering many possibilities that could lead to false entries. Nevertheless, despite our efforts, not all duplications have been eliminated. However, after a visual inspection of the data, we estimate that the error is below 10%.

To split the participants in Universities and Companies, we considered the organization type reported in the project. This information is encoded in the field 'Dedication', in which we found 11 levels: 'Commission External Service', 'Commission Service', 'Consultancy', 'Education', 'Industry', 'Non Commercial', 'Not Available', 'Other', 'Research', 'Technology Transfer' and ⟨Void⟩.

The level 'Not available' means that the FP itself was not able to obtain the information and it is shown in this manner. In addition, ⟨Void⟩ means that no information at all is given, i.e. our robot found nothing (not even 'Not Available').

The first step to define only two groups was to reduce the number of levels in 'Dedication'. We found that eight levels could be merged to define a new one, called 'Non Companies'. It was not homogeneous since we found consultancies, universities, hospitals, institutes, laboratories, observatories, museums, technological parks even cities. However, they all were participants involved in some type of research for whom results do not necessarily return income. This new level was, basically, the union of 'Research' and 'Education' since the other six levels appeared few times in the data: 'Commission External Service' (4 records), 'Commission Service' (8 records), 'Consultancy' (49 records), 'Non Commercial' (389 records), 'Technology Transfer' (1 record) and ⟨Void⟩ (1 record). The record with ⟨Void⟩ was identified as 'Non Company' by direct inspection.

Therefore, all records could be classified in one of the following levels: 'Non Companies' (41 317), 'Industry' (6 447), 'Other' (17 588) and 'Not Available' (12 346). The total number of records (77 698) is larger than the number of participants (25 287) since many of them collaborate in several projects. Then, it was necessary to verify if repeated records were always classified in the same level of 'Dedication'.

We found that many participants were classified in different levels, thus we had to define a set of rules that eliminated this ambiguity. Hence, the following step was to study each level to understand their composition. For every level, we chose 100 records randomly to check by direct inspection their dedication. The result was that all selected records in 'Industry' were companies, any in 'Non Companies', 95 in 'Other' and 55 in 'Not Available'.

With the former information, we proceeded as follows. We first defined for each participant a vector D={'Non Companies', 'Industry', 'Other', 'Not Available'}, where the components are the number of times that it is classified in that level. For instance, D={17, 0, 8, 4} means that the participant appears 17 times as 'Non Company', 8 as 'Other' and 4 as 'Not Available'. Then, we decided that vectors in the form {a, 0, 0, 0} or {a, 0, 0, d} were Universities and vectors in the form {0, b, c, d}, {0, b, c, 0}, {0, b, 0, d} and {0, b, 0, 0} were Companies. With only these sensible rules, we managed to classify 22 001 participants (87%).

In order to confirm this result and to classify the remaining 3 286 entities, we defined a filter based in keywords relative to the Universities group, such as 'univer', 'schule', 'laborato'... When we focused our attention in the group of 22 001 participants classified using 'Dedication', we found that those classified as Universities according to the filter were also Universities according to 'Dedication'. Since the filter was a completely different manner of splitting the dataset, we could use it for the rest of the entries. Note that we only believed the result of the filter if it was University, not if the result was Company. This is reasonable since the filter was designed to identify terms related to Universities, not to Companies.

By means of the filter we classified all participants but 309. To place these entities, we paid attention to which value was higher: 'Non Companies' or 'Industry', independently of the other two values. If the value 'Non Companies' was higher, it was a University, otherwise it was a Company.

Bibliography

[1] D. Amidon. *In the Knowledge Zone: Modern Policies for Innovation Strategy.* Baltic Dynamics 2004 Conference, Riga, 2004.

[2] L.M. Branscomb, F. Kodama and R.L. Florida. *Industrializing Knowledge: University–Industry Linkages in Japan and the United States*, MIT Press, Cambridge, 1999.

[3] Y. Caloghirou, A. Tsakanikas and N.S. Vonortas. *University–Industry Cooperation in the Context of the European Framework Programmes.* Journal of Technology Transfer 26, 153 (2001).

[4] F. Meyer–Krahmer and U. Schmoch. *Science–based technologies: university–industry interactions in four fields.* Research Policy 27, 835–851 (1998).

[5] R. Albert and A.-L. Barabási. *Statistical mechanics of complex networks.* Review of Modern Physics 74, 47–97 (2002).

[6] R. Guimerà and L.A.N. Amaral. *Functional cartography of complex metabolic networks.* Nature 433, 895–900 (2005).

[7] H. Jeong, B. Tombor, R. Albert, Z.N. Oltvai and A.-L. Barabasi. *The large–scale organization of metabolic networks.* Nature 407, 651–654 (2000).

[8] S.N. Dorogovtsev and J.F.F. Mendes. *Evolution of networks: From biological nets to the Internet and WWW*, Oxford University Press, Oxford, 2003.

[9] J. Balthrop, S. Forrest, M.E.J. Newman and M.M. Williamson. *Technological Networks and the Spread of Computer Viruses.* Science 304, 527–529 (2004).

[10] M.E.J. Newman. *The structure and function of complex networks.* SIAM Review 45, 167–256 (2003).

[11] Community Research and Development Information Service: http://www.cordis.lu/

[12] H. Wigzell. *Framework programmes evolve.* Science Editorial 295, 443–445 (2002).

[13] S.N. Dorogovtsev and J.F.F. Mendes. *Evolution of networks.* Adv. Phys. 51, 1079–1145 (2002).

[14] A.-L. Barabási and R. Albert. *Emergence of scaling in random networks.* Science 286, 509–512 (1999).

[15] B. Bollobas. *Random graphs.* Academic Press, London, 1985.

[16] S.N. Dorogovtsev, J.F.F. Mendes and J.G. Oliveira. *Degree–dependent intervertex separation in complex networks.* Physical Review E 73, 056122 (2006)

[17] S.H. Strogatz. *Exploring complex networks.* Nature 410, 268–276 (2001).

[18] E. RAVASZ, A.L. SOMERA, D.A. MONGRU, Z.N. OLTVAI AND A.-L. BARABÁSI. *Hierarchical organization of modularity in metabolic networks.* Science 297, 1551–1555 (2002).

[19] S. CHAOMING, S. HAVLIN AND H.E. MAKSE. *Self–similarity of complex networks.* Nature 433, 392–395 (2005).

[20] E. RAVASZ AND A.-L. BARABÁSI. *Hierarchical organization in complex networks.* Physical Review E 67, 026112 (2003).

[21] M.E.J. NEWMAN. *Fast algorithm for detecting community structure in networks.* Physical Review E 69, 066133 (2004).

[22] The algorithm package PAJEK can be found at http://vlado.fmf.uni-lj.si/pub/networks/pajek/

[23] L. GAO. *On inferring autonomous system relationships in the Internet.* IEEE/ACM Transactions on networking 9, 733–745 (2001).

[24] A. TRUSINA, S. MASLOV, P. MINNHABEN AND K. SNEPPEN. *Hierarchy measures in complex networks.* Physical Review Letters 92, 178702 (2004).

[25] M.E.J. NEWMAN. *Assortative Mixing in Networks.* Physical Review Letters 89, 208701 (2002).

[26] M.E.J. NEWMAN. *Mixing patterns in networks.* Physical Review E 67, 026126 (2003).

[27] M. BOGUÑÁ, R. PASTOR–SATORRAS AND A. VESPIGNANI. *Cut–offs and finite size effects in scale–free networks.* European Physical Journal B 38, 205–210 (2004).

Chapter 3

Spreading processes in complex networks

3.1 Introduction

Network analysis is a tool that has been successfully used in different scientific fields, such as neurobiology [1], Internet [2], or the financial markets [3]. But, one of the most important, and historically one of the first, reasons to study networks is to understand the mechanisms by which information, rumors or computer viruses spread over them.

In this Chapter we follow the methodology explained in Chapter 1, in which we describe a social group as a complex network whose nodes may be friends or employees and the links could be the social relations or the information transfer between them.

We focus our attention on two questions. First, we are interested in the study and characterization of the information flow between members of a social group hierarchically organized when the information spreads with degradation (i.e., the transmission is not perfect).

For this purpose, we analyze different aspects of a generalized hierarchical topology that we propose to describe the relationships between them. In this model, we assume that each person in the group, except for the top leader, is subordinated to a boss. Additionally, we also consider that all people directed by the same boss are connected.

The second question, related to the first one, is what happens when the spread of information is perfect (i.e., no degradation) but the access to this information is restricted by some physical constraint (e.g., time, storage,...).

It is well known that whenever a common resource is scarce, a set of rules are needed to share it in a fairly way. However, most control schemes assume that people will behave in a cooperative way, without taking care of guaranteeing that they will not act in a selfish manner.

Then, a fundamental issue is to evaluate the impact of cheating. This can be done from the point of view of game theory and, more precisely, using the concept of *Nash equilibrium*. Nash equilibrium implies that nobody can take advantage by unilaterally deviating from this stable state, even in the presence of selfish people.

57

In particular, we are interested in knowing if it is possible to define a control scheme that does not depend on the previous behavior of the people in the group— this type of control scheme is called *oblivious*.

3.2   Information flow in generalized hierarchical networks

Traditionally, the research in graph theory has assumed that information in a graph travels through edges without degradation. This approach is useful to model some particular types of phenomena, like disease spread [4] or virus infection in a group and error propagation in computer networks [5].

Nevertheless, this is not appropriate when trying to model processes that take place in collaborative social networks. In order to create a model for this particular situation, we define a quantity that we call the *coordination degree*, which measures the ability of the vertices in a graph to interchange information. There are several manners to model this magnitude, but one of the easiest ways is to consider the coordination degree to be exponentially related to the distance between the vertices [6]. In this way, we define the coordination degree γ_{ij} between two vertices i and j as

$$\gamma_{ij} = \mathrm{e}^{-\xi d_{ij}},$$

where d_{ij} is the distance between the two vertices and ξ is a real positive constant, measuring the strength of the relationship which we call the *coordination strength.*

Quantities similar to the coordination degree have been already discussed in the literature. The most remarkable work in this field is the one by Katz [7], in which the author considers the sum of $e^{-\xi d_{ij}}$ over all paths to a particular vertex. However, our model postulates that only the shortest paths are appropriate for this purpose. We think that our model is more appropriate than the one proposed by Katz for several reasons.

First, the Katz measure can only be expressed in terms of the adjacency matrix of the graph, making the analysis and computations much more complex.

Second, the fact that all the paths have the same priority for the spread of information produces some inconsistencies in the interpretation of the results, mainly when considering closed loops, since the information can be somehow amplified using this approach.

Opposite to this, the coordination degree may be easily evaluated and can be considered as a very good approximation in sparse graphs, just by considering that the information travelling through secondary routes is negligible.

Accepting these assumptions, we can define the *total coordination degree of a vertex i* in a graph as the sum of all the coordination degrees between that particular vertex and the rest,

$$\Gamma_i = \sum_{j=1}^{N} \gamma_{ij},$$

where N is the order of the graph (the total number of vertices in that particular graph). The total coordination degree of a vertex is a measure of the amount of

information that the vertex is able to receive belonging to that particular network.

In the same way, we define the *average coordination degree of the graph* as

$$\overline{\Gamma} = \frac{1}{N} \sum_{i=1}^{N} \Gamma_i,$$

which can be interpreted as a measure of the efficiency of a particular community or organization, since it suggests how much an individual contributes to the community.

3.2.1 The law of diminishing marginal returns

When analyzing the efficiency of social networks in terms of the average coordination degree, an interesting phenomenon appears (see Fig. 3.1). The efficiency of networks does not vary linearly with the order, but it tends to saturate to a value which depends on the topology of the network.
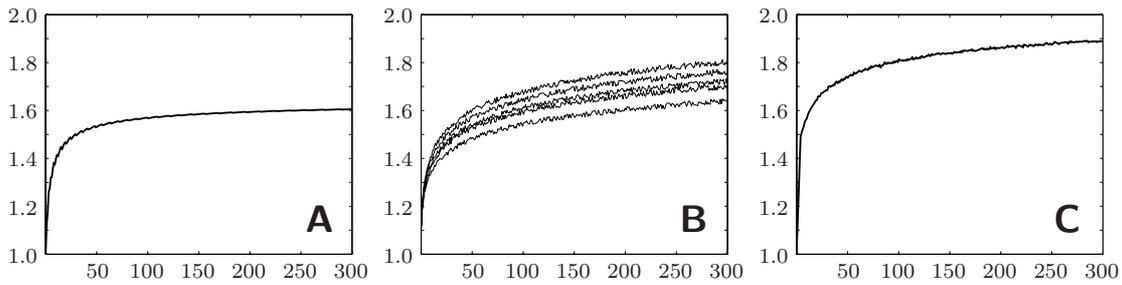
Figure 3.1. The average coordination degree for three different graphs with $k = 4$ and $\xi = 2$ is shown. Whereas the X axis is the order of the graph (i.e., the number of nodes), the Y axis is the average coordination degree $\overline{\Gamma}$. (A) A two dimensional regular lattice. (B) Different small–world networks. (C) A random graph.

This result can be seen from the point of view of the well known *law of diminishing marginal returns*. This law states that when the amount of a variable resource is increased, while other resources are kept fixed, the resulting change in the output will eventually diminish.

This is precisely what occurs in the models, more members in the organization does not produce an increase in the average coordination degree. This means that the increase in information of each individual diminishes as the number of members grows. As a consequence, it is reasonable to think that there exist a maximum group size, since values greater than a certain N imply marginal returns close to zero.

Actually, some scientists propose the existence of this limit in the maximum number of members of a social group by other means. Probably the most important work in this direction is the one carried out by the British anthropologist R. Dunbar [8], who related the size of the neocortex (a part of the brain related to social and language capabilities) and the maximum group size for primates. When applying this relation for the Homo sapiens, the group estimate maximum size is 147.8, or roughly 150.

Nevertheless, the analysis we have performed shows that the size of an organization cannot be only understood in terms of the intrinsic psychological properties of its members. The relational structure and the properties of the information transfer on the network may also play a definitive role.

3.2.2   Information in hierarchical networks

Here, we focus on the analysis of social networks having hierarchical topologies [9]. Examples of graphs having this structure are regular trees. A *regular tree* is a regular graph (all vertices have the same degree c) that is connected (there is a path joining any two of its vertices) and that contains no circuits (there is no path going from one actor to itself that does not visit the same vertex twice). Every regular tree has a particular vertex, called *root node* or *top of the tree*, that is the most central vertex in the graph.

In order to generalize hierarchical topologies based on regular trees, we work with a regular tree that each vertex has $c - 1$ order one–lower neighbors and $c - 2$ order 1 neighbors in the same level (see Fig. 3.2). The edges that link vertices in different levels and the edges that link vertices in the same level have different coordination strength, and hence, there are two different coordination degrees.
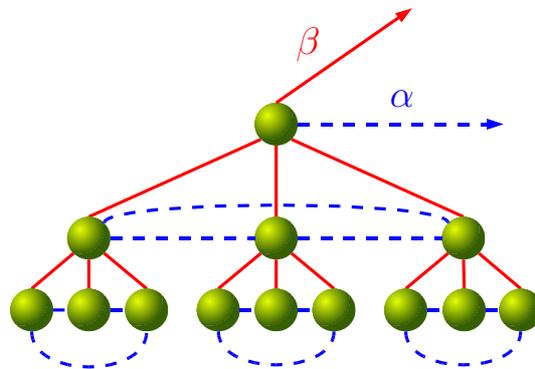
Figure 3.2. Representation of a hierarchical topology with links between members of the same group. Notice that there are two different coordination degrees α, between members of the same level in the hierarchy, and β, between members of different levels.

Let ξ and ζ be the coordination strength that measures the strength of the relationship between vertices in different levels and vertices in the same level, respectively. Then, the coordination degree between two vertices order 1 neighbors in the same level is $\alpha = e^{-\zeta}$, and the coordination degree between two vertices order 1 neighbors in different levels is $\beta = e^{-\xi}$. Our objective is to obtain a formula giving the information flow, for the former topology representing social networks, in terms of the coordination degrees α and β.

As it is mentioned in the introduction of this section, we assume that the information travels through the shortest path. This implies that α has really an effect on

the model only when $\alpha > \beta^2$. In that case, the following formula for the coordination degree is obtained

$$
\widetilde{\Gamma}_i(\alpha,\beta) = \left\{
\begin{array}{ll}
\left.
\begin{array}{l}
\frac{(c-2)\alpha}{1-(c-1)\beta}\left[\frac{\beta-\beta^{N-i}}{1-\beta} - \frac{1-[(c-1)\beta^2]^{N-i-1}}{1-(c-1)\beta^2}(c-1)^{i+1}\beta^{i+2}\right] \\
+\frac{\beta-\beta^{N-i+1}}{1-\beta} + [1+(c-2)\alpha]\frac{1-[(c-1)\beta]^i}{1-(c-1)\beta}
\end{array}
\right\} & i \leq N-1 \\[2em]
\frac{1-[(c-1)\beta]^i}{1-(c-1)\beta} & i = N
\end{array}
\right.
$$

(3.1)

When $\alpha < \beta^2$, the shortest path is through the one–order upper neighbor, as in a traditional hierarchical tree. Consequently, the former equation cannot be used to compute the coordination degree. However, from Eq. (3.1) it is possible to derive the coordination degree in a traditional hierarchical tree, by introducing the following change $\alpha \to \beta^2$. Hence, the coordination degree in our model can be written in the following terms

$$
\Gamma_i(\alpha,\beta) = \left\{
\begin{array}{ll}
\widetilde{\Gamma}_i(\alpha,\beta) & \alpha > \beta^2 \\
\widetilde{\Gamma}_i(\beta^2,\beta) & \alpha \leq \beta^2
\end{array}
\right.
$$

As a basic ingredient of our model, it is important to remark the common perception that the number of close relationships a person may have within a community is necessary limited to a quite small number, independently on the type of organization. This may be the consequence of the fact that establishing close relationships with people is normally very time consuming, and time is a limited resource for every individual.
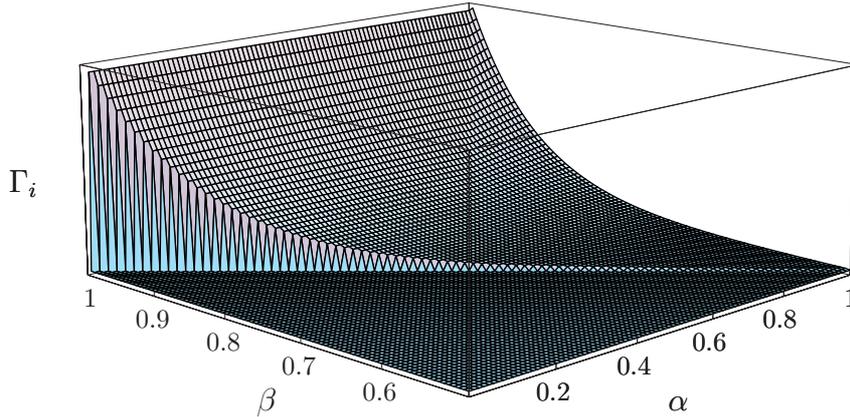
Figure 3.3. When the constraint $(c-2)\alpha + c\beta = cons.$ is included in the model, the coordination degree is a curve depending on α and β whose maximum is at $\alpha = 0$. This implies that the maximum information is received when each node only pays attention to neighbors in upper levels in the hierarchy.

Therefore, we can consider that each member devotes time to his neighbors proportionally to the information obtained. That is, each actor shares his time

between neighbors in the same level and neighbors in different levels, proportional to α and β respectively.

Thus, there is a constraint on α and β given by $(c-2)\alpha + c\beta = const$, which is a plane in the space $\{\alpha, \beta, \Gamma_i\}$. Hence, the coordination degree is a curve, the intersection of that plane and the surface defined by Γ_i (see fig. 3.3). And the result is that the maximum information is received when each actor devotes all his time to neighbors in upper levels.

3.3 Congestion Schemes and Nash Equilibrium

The problem of control schemes constitutes a largely studied issue in the past few years [10, 11, 12, 13, 14, 15, 16]. Many systems nowadays are based on the principle of sharing a common resource, e.g., a communication link, among different users. Consequently one of the main objectives of such schemes is to establish a number of rules guaranteeing that the common resources are shared in a fair way among users.

However, most of these schemes require users to behave in a cooperative way, so that they respect some "social responsible" rules. Moreover, without forcing end users to adopt a centralized mandated policy controlling their behavior, it is not possible to guarantee that they will not act in a selfish manner. Then, it seems a main issue to evaluate the impact of having users acting this way.

An example that illustrates the above mentioned scenario is the control scheme used by the TCP/IP protocol, which is currently the dominant protocol in the internet. By using it, users control the injection rate of packets into the communication network by means of a pair of parameters. When users detect that the network is overloaded, by means of control messages, they decrease their injection rate by a half, thus alleviating the network's load.

However, the adherence to this scheme is voluntarily in nature, and some users may decide to act in a selfish manner and not to decrease its injection rate. As it has been evaluated by several authors [17, 18], this may lead to a congestion collapse that only benefits selfish users. Therefore, it is interesting to know how cooperative users may "fight back" against unsupportive ones.

Another example can be found in social networks, mainly when they are based on the traditional hierarchical paradigm. Despite the problems of this topology, large companies prefer a hierarchical organization because it is the only way to keep their activities under a strict control (see Section 3.2).

But with the growth of the companies, the number of specialized activities grows also, and it is a need the introduction of a non–hierarchical communication to maintain the efficiency.

However, nobody knows how to control a non–hierarchical organization. The hope is that some global "self–organizing" order emerges by means of a horizontal interaction protocol [19]. Consequently, it is important to analyze the features that such a successful protocol must have.

Game theory constitutes a good mathematical tool for analyzing the interaction of decision makers with conflicting interests [20, 21]. From a game–theoretic per-

spective, users are considered as the *game players* and congestion control schemes establish the *game rules*.

We regard *players* are agents that issue requests for a common resource selfishly (i.e., they are only concerned about their own good). Hence, the utility function of each player, which is the parameter to be maximized, is assumed to be equal to the number of requests that have been served per unit time.

The *rules* of the game are determined by the management policy of the common resource. Here, we consider policies that are *oblivious*, i.e., that do not differentiate between requests belonging to different agents, and that have a limited storage capacity for pending requests. Moreover, requests issued after such a limit is reached are simply discarded. Figure 3.4 shows an illustration of the above mentioned scenario.
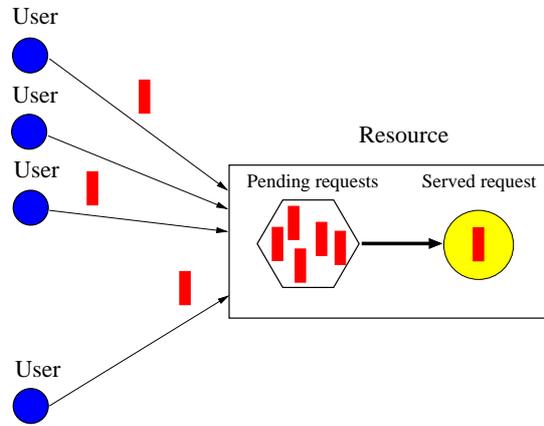
Figure 3.4. The requests sent to use the common resource are represented here with filled rectangles. These requests are stored up to a certain limit until they are chosen obliviously to be served, one at each time.

Once the players and the rules have been fixed, the next step is the definition of a utility function. But the problem here is that its concrete form depends on the assumptions made for the network under analysis.

For example, if we consider N players in a communication network, the request rate of the ith player (also referred to as *load*) can be modelled by a Poisson process with average rate λ_i and the utility function (also known as the *goodput*) can be written as [22]

$$\mu_i = \lambda_i(1 - p(\lambda)),$$

where $p(\lambda)$ is the discarding probability due to an average aggregate load of

$$\lambda \equiv \sum_{i=1}^{N} \lambda_i$$

and an average service time of unity[1].

---

[1]Note that there is no loss of generality if it is assumed that the service rate of the system is normalized to 1.

Although the utility function is different for many other problems, in the rest of the chapter it is used the goodput given in the former example to ease the reading. Nonetheless, we will show that the results derived from this particular goodput can be generalized to a broad set of utility functions.

An important concept in game theory is the *Nash equilibrium*. In our context, a Nash equilibrium is a scenario in which no selfish user has a reason to unilaterally deviate from its current state, because he is acting in an optimal way. Clearly, being in a Nash equilibrium means that we are in a stable state in the presence of selfish users.

In a Nash equilibrium, no player can increase his goodput by either increasing or decreasing their request rate λ_i. Then, the following condition must be satisfied

$$\left.\frac{\partial \mu_i}{\partial \lambda_i}\right|_{\lambda^*} = 0, \qquad i = 1, \ldots, N,$$

where λ^* is the average aggregate request rate at equilibrium. This condition can be rewritten as

$$q(\lambda^*) + \lambda_i^* q'(\lambda^*) = 0,$$

where $q(\lambda) \equiv 1 - p(\lambda)$ for simplicity.

Since we are interested in a *symmetric equilibrium*, which imposes $\lambda_i^* = \lambda^*/N$, the Nash condition becomes

$$q(\lambda^*) + \frac{\lambda^*}{N} q'(\lambda^*) = 0. \tag{3.2}$$

It is interesting to note that this symmetry condition implies that the goodput at equilibrium is the same for all players, which is the only way to guarantee that the obtained policy is fair.

On the other hand, given a solution for the Nash condition, it is also desirable that such a solution has a good efficiency. A solution is *efficient* when the aggregate goodput at equilibrium μ^*, which is defined as

$$\mu^* \equiv \sum_{i=1}^{N} \mu_i^* = \sum_{i=1}^{N} \lambda_i^* q(\lambda^*) = \lambda^* q(\lambda^*),$$

verifies that $\lim_{N \to \infty} \mu^*$ is a positive constant, otherwise it means that no requests are being processed.

Observing Eq. 3.2 we must remark that λ^* is, in general, a function of the number N. Hence, the load of any of the players at equilibrium λ_i^* also depends on N. In this situation, it is interesting to define a parameter measuring the increase on λ_i^* when N changes. With this purpose, we use the *sensitivity coefficient* $\Delta_i(N)$, which can be defined as [23]

$$\Delta_i(N) = \lambda_i^*(N) - \lambda_i^*(N - 1).$$

Note that $\Delta_i(N)$ is a measurement of how difficult is for player i to reach a new equilibrium when the number of users increases from $N - 1$ to N. For practical

purposes, it will be interesting to obtain oblivious policies having no sensitivity to N, that is, $\Delta_i(N) = 0$.

We say that a policy is *reachable* in a practical situation if it has no sensitivity to N. This would guarantee that, once all players have reached the equilibrium, they will be able to maintain it without the need of passing a transient period of time searching their new Nash conditions.

3.3.1 Efficient Solutions to the Nash Condition

As it has been stated previously, the average aggregate load at equilibrium λ^* derived from the Nash condition depends on N, the number of agents involved in the network. Hence, λ^* is a discrete function $\lambda^* : \mathbb{N} \to \mathbb{R}^+$, which for every value of N returns the λ^* imposed by the Nash condition for N agents.

However, although λ^* is a discrete function of N, it is always possible to regard λ^* as a twice differentiated function $f : [1, \infty) \to \mathbb{R}^+$ such that $f(N) = \lambda^*(N)$ for all positive integer N. Note that the function λ^* can be geometrically seen as a set of points in the plane located at $(N, \lambda^*(N))$, where N is an integer. Then, the definition of f simply reflects the fact that we can always draw a curve (twice differentiated, for technical reasons that will be clear later) passing through them.

Therefore, when this continuum limit is taken, Eq. 3.2 can be seen as the following condition, which holds for all $v \geq 1$,

$$q[f(v)] + \frac{f(v)}{v} q'[f(v)] = 0,$$

where, according to the definition of f, the derivative must be understood as $()' \equiv \frac{d}{df}()$.

Consequently, if it is used the notation $\dot{()} \equiv \frac{d}{dv}()$ and $q(v) \equiv q[f(v)]$ for simplicity, the Nash condition in the continuum limit is written as the following first order ordinary differential equation

$$q(v) + \frac{f(v)}{v} \frac{\dot{q}(v)}{\dot{f}(v)} = 0,$$

whose solution can be written formally as

$$q(v) = \mathrm{D}\, \mathrm{e}^{-I(v)}, \tag{3.3}$$

where D is a constant of integration and $I(v)$ is defined in this manner

$$I(v) \equiv \int \frac{\dot{f}(v)}{f(v)} v \, dv.$$

Although Eq. 3.3 is a formal solution to the Nash condition, it is enough to demonstrate that any efficient solution has to tend asymptotically to a positive constant (see Appendix A). Namely, $f(v)$ must verify

$$0 < \lim_{v \to \infty} f(v) < \infty.$$

This implies that $f(v)$ can always be written as

$$f(v) \equiv f_\infty[1 + \tilde{f}(v)], \tag{3.4}$$

with f_∞ a positive constant and $\tilde{f}(v)$ a twice differentiated function verifying $\lim_{v \to \infty} \tilde{f}(v) = 0$ and $\tilde{f}(v) > -1$, for all $v \geq 1$.

However, not all $f(v)$ verifying Eq. 3.4 is an efficient solution. Hence, we need more conditions to fix the set of efficient solutions. There are two results that are useful for this purpose.

The first one is a sufficient condition (see Appendix B) that states that if $\tilde{f}(v)$ is a twice differentiated function behaving asymptotically as

$$\dot{\tilde{f}}(v)v^2 \sim \frac{1}{v^\alpha} \qquad \text{with } \alpha > 0,$$

then, an efficient solution is derived.

The second result is a necessary condition (see Appendix C) that states that if the Nash condition is efficiently verified, the following equation holds

$$\lim_{v \to \infty} \dot{\tilde{f}}(v)v^2 = 0.$$

Notice that because both conditions are similar but not equal, nothing can be said about some functions. The following function is an example,

$$\tilde{f}(v) = \frac{-1}{v \ln v} \implies \dot{\tilde{f}}(v)v^2 = \frac{1 + \ln v}{(\ln v)^2} \sim \frac{1}{\ln v}.$$

Nevertheless, the set of efficient solutions are functions such that asymptotically tend to a constant faster than $1/v$. Then, in terms of the load, this result tells us that, at equilibrium, any efficient solution must have a λ^* that falls with N to a constant value faster than $1/N$.

Then, as our equilibrium is assumed to be symmetric, the load of any of the players at equilibrium asymptotically changes in the form $\lambda_i^*(N) \sim 1/N$. Hence, the sensitivity coefficient for any player behaves like $\Delta_i(N) \sim \frac{1}{N} - \frac{1}{N-1} \sim \frac{1}{N^2}$ in that limit.

This allows us to conclude that, in situations in which the number of players rapidly changes, which occurs often, the efficient equilibrium of any oblivious efficient policy is not easily reachable, because the load of players strongly depends on the number of current players.

At this point, we have to remark that it is possible to have situations with an efficient Nash equilibrium. What we prove here is that, in order to remain in an efficient equilibrium, users must adapt their request rate whenever the number of users changes. Furthermore, such an adaptation will be very significant and, consequently, it will likely require some time to be realized.

Therefore, if the number of users rapidly changes, the system will be always evolving from one equilibrium state to another, without reaching any of them (or being in equilibrium only during a short time interval). That is, the system would be always out of equilibrium.

3.3.2 Real–World Congestion Schemes

Here, we analyze two real–world congestion schemes to show how their behavior can be greatly affected by the result we have just derived.

The TCP/IP Protocol

As it has been pointed out previously, the TCP/IP protocol is the dominant protocol in the Internet. Furthermore, most of the current scheduling policies in Internet are oblivious, e.g., FIFO (First In First Out). Therefore, taking into account that the adherence to the TCP/IP control scheme is voluntarily in nature, our result shows that, in the presence of selfish users, TCP/IP control schemes cannot impose a Nash equilibrium.

To assess the importance of the above mentioned effect in real situation, we note that there are already protocols, patented and owned by commercial companies [24], that "exploit" the "weakness" of TCP/IP protocol by means of behaving in a selfish manner. Such protocols offer goodputs (i.e., number of requests served per unit time) that are higher than the offered by the TCP/IP protocol, but at a cost of penalizing the performance of the latter.

Unfortunately, our result implies that it is not possible to obtain an internet router capable of providing an equilibrium state without maintaining a record of the requests performed by each user.

A result somehow similar to ours, when focussed in communication systems, has been reported by other authors. For example, Dutta et al. [23] assume that the discarding probability must be a non–decreasing and convex function. Furthermore, they assumed that their sensitivity coefficient depends on the number of flows in an exponential fashion.

Such assumptions, although simplify the proofs, are arbitrary. On the contrary, our result is completely general. Surprisingly, we noted that their assumption about the sensitivity coefficient constitutes a sufficient condition to obtain an efficient solution.

Altman et al. [25] present a detailed analysis when the utility function of each user is taken as the ratio of some positive power of the total throughput of that user to the average delay seen by the user. Also, they consider a routing problem in networks defined by a directed graph with a polynomial cost function [26]. However, when all these utility functions are studied for a symmetric equilibrium, they are functions of only one parameter, being particular instances of our result.

Social Networks

Several papers [14] have appeared in the literature reporting that social networks and computer networks share similar features in terms of information transfer. Some recent work [9] remarks that the problem of congestion often arises in social networks, mainly when these are based on the traditional hierarchical paradigms used by companies and organizations.

Illustrative examples are telecommunication or digital cable/satellite TV companies. Usually, installers must communicate with a central site in order to validate new services, e.g., a home installation. At the central site, requests are queued and managed in the receiving order, but only up to a certain threshold, above it, the installer is required to communicate later on (i.e., the request is dropped).

Clearly, the number of requests may have peaks at given moments. If installers act in a cooperative way, they will communicate again after some time. But some of them may act unfairly and communicate immediately, trying to reduce their waiting time, at a cost of increasing the waiting time of the other employees.

The only way to attain a reachable and efficient equilibrium, being fair at the same time (i.e., giving equal opportunities to any requester) is to track their activities over time measuring their individual degrees of cooperation, and acting accordingly to these measurements. Namely, any strategy taking into account only the current state and not the individual past will fail.

3.4   Conclusions

We have derived the existence of a natural limit in the size of a group due to the limitation in the amount of information that the group can deal.

Additionally, we have found that hierarchical networks are so spread because this structure arises when each actor only looks for maximizing his information. The result is a structure that mainly benefits the higher levels, by providing them a higher information centrality and improving their dominance of information.

When edges, between vertices with the same upper neighbor, are added to a hierarchical tree, we show that the information each actor manages decreases. This means that a hierarchical tree is a stable network against relationships between members of the same group.

This stability can be seen as another reason that explains why hierarchical trees are so spread in companies all over the world. A hierarchical tree backs the leader's superiority of information despite the strength of the relationship that links the members of a group.

Nevertheless, it should be noticed that in our model edges between vertices in the same level with different upper neighbor are not included, or between vertices in different levels. This study may yield a different result.

When we assume that the transmission of information is perfect, without degradation, but the access to this information is somehow restricted, the problem is how to fairly share it, if some users act in a selfish manner.

We have shown that, if the policy used to manage the common resource is oblivious (i.e., if it does not differentiate between requests belonging to different users) then any efficient Nash equilibrium will highly depend on the number of users, in the sense that they must adapt their request rate in a significant manner.

Taking into account that, in many realistic situations, the number of users changes rapidly and that the time needed to adapt from one equilibrium to another one can be significant, this means that the system will be most of time out

of equilibrium. Actually, as illustrative examples, we point out a pair of congestion schemes in which the above mentioned effect may have a real impact.

Appendix A

Lemma 1: If $f(v)$ is a solution to the Nash condition, it is verified:

$$\lim_{v \to \infty} f(v) > 0.$$

Proof: Any solution to the Nash condition must be such that the resulting $q(v)$ of Eq. 3.3 is a well defined probability. Then, we can use Appendix D in which it is proven that we can write

$$f(v) = \text{D' } e^{J(v)}, \tag{A1}$$

with D'> 0 and

$$J(v) \equiv \frac{I_+(v)}{v} + \int_1^v \frac{I_+(z)}{z^2} \, dz,$$

being $I_+(v) \geq 0$ for all $v \geq 1$.

We have that $J(v) \geq 0$ for all $v \geq 1$ because it is the sum of two positive terms, thus $f(v) \geq$ D' for all $v \geq 1$ and, as a consequence, $\lim_{v \to \infty} f(v) > 0$ because $D' > 0$.

Lemma 2: If $f(v)$ is an efficient solution to the Nash condition, it is verified:

$$\lim_{v \to \infty} f(v) < \infty.$$

Proof: It is done by *reductio ad absurdum.*

Since any solution $f(v)$ must result in a well defined probability function $q(v)$, it is proven in Appendix D that it takes the form given by Eq. A1. Thus if we suppose that $\lim_{v \to \infty} f(v) = \infty$, it is because $\lim_{v \to \infty} J(v) = \infty$.

If such a solution is also efficient, the following condition must hold

$$0 < \lim_{v \to \infty} \lambda^*(v) \, q[\lambda(v)] < \infty,$$

which in the continuum limit implies that

$$0 < \lim_{v \to \infty} f(v) \, e^{-I_+(v)} < \infty.$$

Taking into account A1, the former condition can be written as

$$0 < \lim_{v \to \infty} e^{J(v)} \, e^{-I_+(v)} < \infty$$

which can only be true if

$$\lim_{v \to \infty} J(v) - I_+(v) \neq \pm\infty. \tag{A2}$$

Since $\lim_{v \to \infty} J(v) = \infty$, Eq. A2 can only be satisfied if $\lim_{v \to \infty} I_+(v) = \infty$. But, if it is verified that $\lim_{v \to \infty} J(v) - I_+(v) = $ constant, with $\lim_{v \to \infty} J(v) = \infty$ and $\lim_{v \to \infty} I_+(v) = \infty$, it is easy to check that

$$\lim_{v \to \infty} \frac{J(v)}{I_+(v)} = 1,$$

which implies, by definition of $J(v)$, that

$$\lim_{v \to \infty} \frac{1}{I_+(v)} \int_1^v \frac{I_+(z)}{z^2} \, dz = 1. \tag{A3}$$

Let us define the function $s(v)$ as follows:

$$s(v) \equiv \frac{1}{I_+(v)} \int_1^v \frac{I_+(z)}{z^2} \, dz.$$

We have that Eq. A3 imposes on $s(v)$ the condition $\lim_{v \to \infty} s(v) = 1$. Since it is also true that $\lim_{v \to \infty} 1/s(v) = 1$, there exists some $V \geq 1$ such that, for all $v > V$,

$$\frac{1}{s(v)} < 1 + \epsilon. \tag{A4}$$

where ϵ is a positive real number.

On the other hand, by definition of $s(v)$, its derivative with respect to v is the following

$$\frac{I_+}{v^2} = \dot{s}(v) I_+ + s(v) \dot{I}_+.$$

Then, the following ordinary differential equation is obtained

$$\frac{\dot{I}_+}{I_+} = \frac{1}{s(v)v^2} - \frac{\dot{s}(v)}{s(v)},$$

whose solution can be written formally as

$$I_+(v) = \frac{C}{s(v)} \, \exp\left[\int \frac{dv}{s(v)v^2}\right],$$

where C is a constant of integration.

If Eq. A4 is considered, we have that, for all $v > V$,

$$I_+(v) < C \, (1 + \epsilon) \, \exp\left[\int \frac{1 + \epsilon}{v^2} \, dv\right] = C \, (1 + \epsilon) \, \exp\left[C' - \frac{1 + \epsilon}{v}\right],$$

where C' is a constant of integration. As a consequence, it is derived that, for all $v > V$

$$I_+(v) < C \, (1 + \epsilon) \, \exp\left[C' - \frac{1 + \epsilon}{V}\right] = C'',$$

where C'' is a constant.

Therefore, it is obtained that $\lim_{v \to \infty} I_+(v) < \infty$. However, this contradicts the result derived from Eq. A2 (i.e., $\lim_{v \to \infty} I_+(v) = \infty$). Then, we conclude that no efficient solution to the Nash condition can verify that $\lim_{v \to \infty} f(v) = \infty$.

Appendix B

Lemma: If $\tilde{f}(v)$ is a twice differentiated function that behaves asymptotically as

$$\dot{\tilde{f}}(v)v \sim \frac{1}{v^{1+\alpha}} \qquad \text{with } \alpha > 0,$$

it is an efficient solution to the Nash condition.

   Proof: By definition of $\tilde{f}(v)$, it is easy to check that

$$\lim_{v \to \infty} \frac{1}{1 + \tilde{f}(v)} = 1.$$

Thus, given any $\epsilon > 0$, there exists some $V \geq 1$ such that, for all $v > V$,

$$\left| \frac{1}{1 + \tilde{f}(v)} \right| < 1 + \epsilon.$$

   Then, it is deduced that

$$\left| \int_1^\infty \frac{\dot{\tilde{f}}(v)}{1 + \tilde{f}(v)} v \; dv \right| < \int_1^\infty \left| \frac{\dot{\tilde{f}}(v)}{1 + \tilde{f}(v)} v \right| dv < \mathrm{B} + (1 + \epsilon) \int_V^\infty |\dot{\tilde{f}}(v)| v \; dv,$$

where B is a real number defined as

$$\int_1^V \left| \frac{\dot{\tilde{f}}(v)}{1 + \tilde{f}(v)} v \right| dv.$$

   If $\dot{\tilde{f}}(v)v \sim v^{-(1+\alpha)}$ with $\alpha > 0$, and taking into account that the integration of a function that asymptotically behaves as $v^{-(1+\alpha)}$ is a function that tends to zero as $v \to \infty$, it is straightforward to check that

$$\int_V^\infty |\dot{\tilde{f}}(v)| v \; dv = \mathrm{B'},$$

with B' being a constant.

   Therefore, it is deduced that

$$\left| \int_1^\infty \frac{\dot{\tilde{f}}(v)}{1 + \tilde{f}(v)} v \; dv \right| < \mathrm{B} + (1 + \epsilon)\mathrm{B'} < \infty,$$

which implies that there exists an efficient solution (see Appendix E).

Appendix C

Lemma: If the Nash condition is verified efficiently, the following equation holds:

$$\lim_{v \to \infty} \dot{\tilde{f}}(v)v^2 = 0.$$

Proof: Assume that $\lim_{v \to \infty} \dot{\tilde{f}}(v)v^2 = A' > 0$. Then, for every $A'' \in (0,A')$, it is always possible to find a $V_1 \geq 1$ such that $\dot{\tilde{f}}(v)v^2 \geq A''$, for all $v > V_1$. On the other hand, $\lim_{t \to \infty} \tilde{f}(v) = 0$. Thus for every $\epsilon \in (0,1)$ there exists a $V_2 \geq 1$ such that

$$\frac{1}{1 + \tilde{f}} > 1 - \epsilon,$$

for all $v > V_2$.

Then, we deduce by means of Appendix E that, for all $v > V \equiv \max\{V_1, V_2\}$,

$$\text{cons} = \int_1^\infty \frac{\dot{\tilde{f}}(v)v^2}{1 + \tilde{f}(v)} \frac{dv}{v} \geq A + A'' \int_V^\infty \frac{1}{1 + \tilde{f}(v)} \frac{dv}{v}$$

$$\geq A + A''(1 - \epsilon) \int_V^\infty \frac{dv}{v} = \infty,$$

because A is a constant defined as

$$A \equiv \int_1^V \frac{\dot{\tilde{f}}(v)}{1 + \tilde{f}(v)} v \, dv.$$

This contradiction arises because it was supposed that $\lim_{v \to \infty} \dot{\tilde{f}}(v)v^2 > 0$.

Similarly, when $\lim_{t \to \infty} \dot{\tilde{f}}(v)v^2 = -A' < 0$, for every $A'' \in (0,A')$, there exists some $V_1 \geq 1$ such that $\dot{\tilde{f}}(v)v^2 \leq -A''$, for all $v > V_1$. In addition, $\lim_{v \to \infty} \tilde{f}(v) = 0$. Thus given any $\epsilon > 0$ there exists some $V_2 \geq 1$ such that

$$\frac{1}{1 + \tilde{f}} < 1 + \epsilon,$$

for all $v > V_2$.

Then, it is derived from Appendix E that, for all $v > V \equiv \max\{V_1, V_2\}$,

$$\text{cons} = \int_1^\infty \frac{\dot{\tilde{f}}(v)v^2}{1 + \tilde{f}(v)} \frac{dv}{v} \leq A - A'' \int_V^\infty \frac{1}{1 + \tilde{f}(v)} \frac{dv}{v}$$

$$\leq A - A''(1 + \epsilon) \int_V^\infty \frac{dv}{v} = -\infty.$$

Such a contradiction only disappears when the condition $\lim_{v \to \infty} \dot{\tilde{f}}(v)v^2 < 0$ is rejected.

Notice that it is only possible to find an A">0 when A' is not zero. If A' is zero the former reasoning fails because the first case results in cons$< \infty$ and the second one derives in cons$> -\infty$ and nothing can be argued.

These results imply that, given an efficient solution to the Nash condition, it is not feasible that $\lim_{v\to\infty} \dot{\tilde{f}}(v)v^2 \neq 0$. But, it could be possible that the condition $\lim_{v\to\infty} \dot{\tilde{f}}(v)v^2 = 0$ was also rejected. In that case, it would derive that there is no efficient solution to the Nash condition.

However, in the Appendix B we demonstrate that the functions $\tilde{f}(v)$ that behave asymptotically as $\dot{\tilde{f}}(v)v \sim v^{-(1+\alpha)}$, with $\alpha > 0$, are efficient solutions. But these functions verify that $\lim_{v\to\infty} \dot{\tilde{f}}(v)v^2 = 0$, thus this condition defines a non–empty set of efficient solutions. Therefore, it can be affirmed that $\lim_{v\to\infty} \dot{\tilde{f}}(v)v^2 = 0$ is a necessary condition to obtain an efficient solution to the Nash condition.

Appendix D

Lemma: The function $q(v)$ is well defined probability if and only if the solution to the Nash condition can be written as

$$f(v) = \text{D' } e^{J(v)}, \tag{D1}$$

with D'> 0 and

$$J(v) \equiv \frac{I_+(v)}{v} + \int_1^v \frac{I_+(z)}{z^2}\, dz,$$

being $I_+(v) \geq 0$ for all $v \geq 1$.

Proof: Assume that $q(v)$ is a probability that verifies the Nash condition for all $v \geq 1$. Then, from Eq. 3.3 we derive that $I(v) \neq -\infty$ for all $v \geq 1$ (otherwise, $q(v) > 1$ and it would not be a probability). Therefore, we can define a new function $I_+(v)$ such that $I(v) \equiv -M + I_+(v)$, with $0 \leq M < \infty$ and $I_+(v) \geq 0$ for all $v \geq 1$.

The definition of $I_+(v)$ implies that

$$\dot{I}_+(v) = \frac{\dot{f}(v)}{f(v)}v,$$

which is an ordinary differential equation easily integrable in this manner

$$\ln\left[\frac{f(v)}{f(1)}\right] = \int_1^v \frac{\dot{I}_+(z)}{z}\, dz = \frac{I_+(v)}{v} - I_+(1) + \int_1^v \frac{I_+(z)}{z^2}\, dz,$$

where the right hand side of the equation is obtained from the integration by parts.

Therefore, if $q(v)$ is a well defined probability for all $v \geq 1$, the function $f(v)$ can be written as

$$f(v) = \text{D' } e^{J(v)},$$

where the function $J(v)$ is

$$J(v) \equiv \frac{I_+(v)}{v} + \int_1^v \frac{I_+(z)}{z^2}\, dz,$$

and D' $\equiv f(1)\, \mathrm{e}^{-I_+(1)}$ is a positive constant because $f(1) = \lambda^*(1) > 0$.

Now, assume that the function $f(v)$ is the one described by Eq. D1. It is easy to verify that

$$I(v) = \int \frac{\dot{f}(v)}{f(v)} v\ dv = I_+(v) + \mathrm{D''},$$

where D'' is another constant of integration. Consequently, $q(v)$ can be written as

$$q(v) = \mathrm{D}\, \mathrm{e}^{-\mathrm{D''}}\, \mathrm{e}^{-I_+(v)}.$$

But we have that $I_+(v) \geq 0$ for all $v \geq 1$, which implies that $\mathrm{e}^{-I_+(v)} \leq 1$ for all $v \geq 1$. Likewise, the constant $\mathrm{D}\, \mathrm{e}^{-\mathrm{D''}}$ is an arbitrary constant since D is also arbitrary. Then, D can be defined to keep $q(v)$ in the interval $[0,1]$ for all $v \geq 1$ and, therefore, it is obtained a well defined probability.

Appendix E

Lemma: There exists an efficient solution to the Nash condition if and only if

$$\int_1^\infty \frac{\dot{\tilde{f}}(v)}{1 + \tilde{f}(v)} v\ dv \neq \pm\infty. \tag{E1}$$

Proof: The function f must be such that the result of Eq. 3.3 is a well defined probability (i.e. in the range $[0,1]$). Then, f is a solution to the Nash condition if and only if $I(v) \neq -\infty$ for all $v \geq 1$.

But from the mean–value theorem for integrals [27], it is derived that $I(v)$ is a constant for all $1 \leq v < \infty$. Note that it is the integration of a continuous function in a finite interval (recall that $f(v)$ is defined as twice differentiated). Hence, in order to obtain a solution to the Nash condition, it is not necessary to verify that $I(v) > -\infty$ for all $v \geq 1$ but to check that $\lim_{v\to\infty} I(v) \neq -\infty$.

On the other hand, since $\lim_{v\to\infty} f(v) = f_\infty$, the condition of efficiency is verified when $\lim_{v\to\infty} q(v) \neq 0$. Then, from Eq. 3.3 is deduced that the efficiency is guaranteed if and only if $\lim_{v\to\infty} I(v) \neq \infty$.

Therefore, the condition $\lim_{v\to\infty} I(v) \neq \pm\infty$ is satisfied if and only if $f(v)$ is an efficient solution. Thus writing $I(v)$ in terms of the $\tilde{f}(v)$ defined in Eq. 3.4, the following condition must hold

$$\pm\infty \neq \lim_{v\to\infty} I(v) = \mathrm{cons} + \lim_{v\to\infty} \int_1^v \frac{\dot{\tilde{f}}(z)}{1 + \tilde{f}(z)} z\ dz,$$

which is equivalent to Eq. E1.

Bibliography

[1] D. Golomb and D. Hansel. *The Number of Synaptic Inputs and the Synchrony of Large, Sparse Neuronal Networks.* Neural Computation 12, 1095–1139 (2000).

[2] M. Faloutsos, P. Faloutsos and C. Faloutsos. *On power–law relationships of the Internet topology.* Comput. Commun. Rev. 29, 251–262 (1999).

[3] A. Kirman, C. Oddou and S. Weber. *Stochastic Communication and Coalition Formation.* Econometrica 54, 129–138 (1986)

[4] F. Ball, J. Mollison and G. Scalia–Tomba. *Epidemics with two levels of mixing.* Annals of Applied Probability 7, 46–89 (1997)

[5] R. Albert, H. Jeong and A.-L. Barabási. *Error and attack tolerance in complex networks.* Nature 406, 387–482 (2000).

[6] L. López and M.A.F. Sanjuán. *Relation between structure and size in social networks.* Physical Review E 65, 036107 (2002).

[7] L. Katz. *A New Status Index Derived from Sociometric Data Analysis.* Psychometrika 18, 34–43 (1953).

[8] R.I.M. Dunbar. *Co–evolution of neocortex size, group size and language in humans.* Behavioral and Brain Sciences 16, 681 (1993).

[9] L. López, J.F.F. Mendes and M.A.F. Sanjuan. *Hierarchical social networks and information flow.* Physica A 316, 591–604, (2002).

[10] R. Guimerà, A. Díaz–Guilera, F. Vega–Redondo, A. Cabrales and A. Arenas. *Optimal network topologies for local search with congestion.* Physical Review Letters 89, 248701 (2002).

[11] A. Arenas, A. Díaz–Guilera and R. Guimerà. *Communication in networks with hierarchical branching.* Physical Review Letters 86, 3196 (2001).

[12] R. Guimerà, A. Arenas and A. Díaz–Guilera. *Communication and optimal hierarchical networks.* Physica A 299, 247–252 (2001).

[13] T. Ohira and R. Sawatari. *Phase transition in computer network traffic model.* Physical Review E 58(1), 193–195 (1998).

[14] B. Wellman. *Computer networks as social networks.* Science 293, 2031–2034 (2001).

[15] R.V. Solé and S. Valverde. *Information transfer and phase transitions in a model of internet traffic.* Physica A 289, 595–605 (2001).

[16] S. Valverde and R.V. Solé. *Self-organized critical traffic in parallel computer networks.* Physica A 312, 636–648 (2002).

[17] A. Akella, S. Seshan, R. Karp, S. Shenker and C. Papadimitriou. *Selfish behavior and stability of the internet: a game-theoretic analysis of TCP.* Proceedings of the 2002 Conference on Applications, Technologies, Architectures, and Protocols for Computer Communications, ACM Press, p117–130, 2002.

[18] R. Garg, A. Kamra and V. Khurana. *A game–theoretic approach towards congestion control in communication networks.* ACM Computer Communication Review 32(3), p47–61 (2002).

[19] S. Solomon and E. Shir. *Complexity: A science at 30.* Europhysics News 34(2), 54 (2003).

[20] D. Fudenberg and J. Tirol. *Game Theory.* MIT Press, Cambridge, Massachusetts, 1991.

[21] G. Owen. *Game Theory.* Academic Press, New York, 1995.

[22] L. Kleinrock. *Queueing Theory (Volume 1).* Wiley, New York, 1967.

[23] D. Dutta, A. Goel and J. Heidemann. *Oblivious AQM and Nash Equilibria.* INFOCOM 2003. Twenty–Second Annual Joint Conference of the IEEE Computer and Communications Societies, p106–113, 2003.

[24] J. Byers, M. Luby and M. Mitzenmacher. *A digital fountain approach to the reliable distribution of bulk data.* IEEE Journal on Selected Areas in Communications 20(8), 1528–1540, (2002).

[25] E. Altman, T. Basar and R. Srikant. *Nash equilibria for combined flow control and routing in networks.* IEEE Transactions on Automatic Control 47(6), 917–930 (2002).

[26] E. Altman, T. Basar, T. Jiménez and N. Shimkin. *Competitive routing in networks with polynomial costs.* IEEE Transactions on Automatic Control 47(1), 92–96 (2002).

[27] T. Apostol. *Mathematical Analysis.* Addison Wesley, 1974.

Chapter 4

Classical approach to dynamical systems

4.1 Introduction

The study of how an ensemble of dynamical systems becomes synchronized is one of the most active and fruitful fields of research in Physics. Given two or more systems, which evolve in different attractors when they are disconnected, we say that they are synchronized when one or more of their variables converge in a common behavior as a consequence of some type of link between them.

On the other hand, complex networks can also be used to study ensembles of dynamical systems. Note that, following [1], we distinguish between dynamics *of* networks and dynamics *in* networks. While the first one is focused on how networks evolve, the later analyzes what happens when each node is a dynamical system.

Both the studies on synchronization and dynamics in networks pursue to understand complex systems better (e.g., neural networks, food–webs or cellular systems). Then, an interesting question to investigate is synchronization in networks of dynamical systems, in which the interplay between the intrinsic dynamics of each element in the network and the links among them notably affects the global dynamics.

However, before delving into the importance of the topology in this issue, we should justify why a new methodology is required to analyze complex systems. To this purpose, we explain in this chapter the classical approach to dynamical systems based on the idea of a constant of motion for a differential equation. This viewpoint will lead us to investigate the essence of integrability, its geometrical relevance and dynamical consequences.

Integrability is analyzed using the powerful *Lie theory for differential equations*. Actually, different techniques developed to solve certain types of equations (e.g., separable or exact equations) are regarded in this theory as special cases of a general integration method.

Lie theory allows determining when the equation is integrable and its symmetry group. Basically, a symmetry group of a differential equation is a group that transforms solutions to other solutions of the equation. In the case of an ordinary differential equation, this is useful to integrate it, since invariance under a symmetry implies that the order of the equation can be reduced by one. Hence, two symme-

tries are needed to integrate a second order equation and to write the solution in terms of known functions.

Chaotic aspects of certain dynamical systems are better understood when the analytical structure is known [2] since it comprises information about the integrability of the model, which is useful to assure whether chaos is possible or not. This link between integrability and chaotic motion has been analyzed for several models, for instance, the Lorenz model [3] or the Hénon–Heiles Hamiltonian [4].

4.1.1   Non–linear oscillators

Oscillations and waves are ubiquitous in nature and are easily modelled through differential equations. The general equation for the one–dimensional oscillatory motion of a unit mass particle, can be easily understood using a mechanical analogy. Assume that the particle moves in a force field, which is generated by the potential $V(x)$, then the general equation of motion may be written as

$$\ddot{x} + \frac{dV}{dx} = 0. \tag{4.1}$$

Stated the problem this way, different oscillators may be obtained, depending on the potential $V(x)$ acting on the particle. Assuming $V(x)$ to be a polynomial function in x, very few cases with analytical solutions have been studied. Among them the *Duffing oscillator*, with a nonlinear term of fourth order, and the *Helmholtz oscillator* [5] when the cubic term is used. Obviously higher order terms may be considered, which in general lead to rather complicated mathematical solutions. These are the nonlinear versions of the oscillator given by Eq. 4.1. If only the quadratic term is taken into account obviously the *harmonic oscillator* is derived. Another simple case with a non–polynomial potential $V(x) = -\cos x$ is the pendulum equation.

In order to be more specific, this chapter will be focused on the Helmholtz oscillator since it is the simplest non–linear oscillator. The dynamics of this oscillator mimics the dynamics of certain prestressed structures, the capsize of a ship [6] and the nonlinear dynamics of a drop in a time–periodic flow [7] or in a time–periodic electric field [8]. It appears also in relation to the randomization of solitary–like waves in boundary–layer flows [9] and in the three–wave interaction, also referred as to *resonant triads* [10].

If it is included a linear friction and a periodic forcing in Eq. 4.1, it is obtained

$$\ddot{x} + \delta \dot{x} + \frac{dV}{dx} = \gamma \cos \omega t,$$

where the inclusion of friction and forcing on the system bestows rather different dynamical behavior as compared with the case without them.

Even though an analysis in absence of friction has been accomplished for the pendulum equation [11, 12], as well as for the Duffing oscillator [13], no similar results are known for the Helmholtz oscillator. In spite of that, when friction is considered, this system has received some attention by different authors [5, 6, 14].

4.2 Dynamics of the Helmholtz Oscillator

The equation of motion of a particle of unit mass that undergoes a periodic forcing in a cubic single–well potential with friction, reads

$$\ddot{x} + \delta\dot{x} + \alpha x - \beta x^2 = \gamma \cos \omega t, \tag{4.2}$$

where δ, α, β, γ and ω are positive constants.

A Hamiltonian and Lagrangian formalism can be used [15] to derive the equation of a particle in a potential $V(x)$ with a linear friction and a periodic forcing. The particular case given by Eq. 4.2 is derived from a time–dependent Hamiltonian and Lagrangian of the following form

$$H(p, x, t) = \frac{1}{2}p^2 e^{-\delta t} + e^{\delta t} V(x, t), \tag{4.3}$$

$$L(\dot{x}, x, t) = e^{\delta t} \left[\frac{1}{2}\dot{x}^2 - V(x, t) \right],$$

where $V(x, t)$ is the following generalized potential for the whole system

$$V(x, t) = \frac{\alpha x^2}{2} - \frac{\beta x^3}{3} - \gamma x \cos \omega t.$$

In this section, it is considered that $\delta = 0$ (i.e., there is no friction). Hence, the equation to analyze is

$$\ddot{x} + \alpha x - \beta x^2 = \gamma \cos \omega t,$$

and therefore, Eq. 4.3 becomes

$$H(p, x, t) = \frac{1}{2}p^2 + V(x, t), \tag{4.4}$$

$$L(\dot{x}, x, t) = \frac{1}{2}\dot{x}^2 - V(x, t),$$

which will be particularly useful to compute the so–called separatrix map. This map yields a lot of information about the effect of a periodic forcing on the Helmholtz oscillator (in particular, about the possibility of transient chaos as a consequence of the forcing).

4.2.1 Single–well potential

When $\gamma = 0$, the equation of a conservative oscillator is obtained. This oscillator may be understood as a particle that is situated in a single potential well $V(x)$ defined as

$$V(x) = \frac{\alpha x^2}{2} - \frac{\beta x^3}{3}.$$

One important feature of this system, easily seen in Fig. 4.1, is that according to the initial condition and the energy of the particle, the orbits may be bounded or
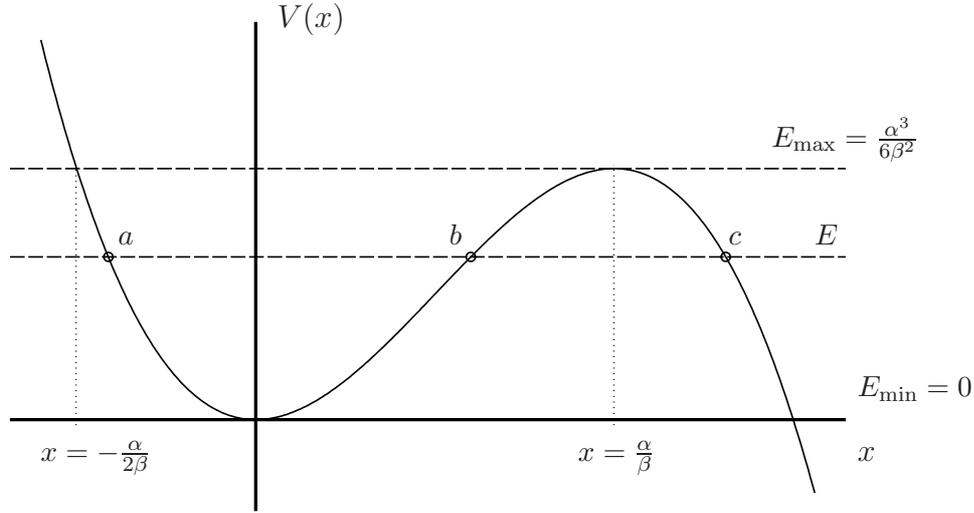
Figure 4.1. Potential energy associated to the Helmholtz oscillator, which may be seen as the simplest potential with an escape. Notice that the potential has been chosen to be $V(x) = \frac{\alpha}{2}x^2 - \frac{\beta}{3}x^3$, because in this way α and β are positive constants. The orbits will be bounded only when $-\frac{\alpha}{2\beta} < x < \frac{\alpha}{\beta}$ and $0 < E < E_{\max}$. For instance, the bounded orbit with energy E is comprised within $[a, b]$. If $x > c$ then the orbit is unbounded.

unbounded. When the value of the energy $E_{\min} = 0 \leq E \leq E_{\max} = \frac{\alpha^3}{6\beta^2}$, then there exist possibilities of bounded motions and hence, oscillations, while for $E > E_{\max}$ the motion of the particle is unbounded, i.e., the particle escapes to infinity.

When the particle has energy E in the range $[E_{\min}, E_{\max}]$, then the cubic equation $E - V(x) = 0$ provides three real roots a, b and c, $(a < b < c)$, which represent physically the *turning points*, i.e., the points where the velocity of the particle changes sign.

These roots verify the following relationships that will be important for further results:

$$a + b + c = \frac{3\alpha}{2\beta}, \quad ab + bc + ac = 0, \quad abc = -\frac{3E}{\beta}, \tag{4.5}$$

and their general expressions are

$$a = \frac{\alpha}{2\beta} + (-1 - m)\frac{\lambda}{3}, \quad b = \frac{\alpha}{2\beta} + (2m - 1)\frac{\lambda}{3}, \quad c = \frac{\alpha}{2\beta} + (2 - m)\frac{\lambda}{3}, \tag{4.6}$$

where to obtain the former results, the following parameters are used

$$m = \frac{b - a}{c - a}, \quad \lambda = c - a. \tag{4.7}$$

If it is defined also

$$\Delta^2 = 1 - m + m^2, \tag{4.8}$$

then, from the Eqs. 4.5, it is derived that

$$\frac{\alpha}{2\beta} = \frac{\lambda\Delta}{3};$$

a useful expression that allows to express the values of the roots in terms only of the parameter m

$$a = \frac{\alpha}{2\beta} - \frac{(1+m)\alpha}{2\beta\Delta}, \quad b = \frac{\alpha}{2\beta} + \frac{(2m-1)\alpha}{2\beta\Delta}, \quad c = \frac{\alpha}{2\beta} + \frac{(2-m)\alpha}{2\beta\Delta}. \tag{4.9}$$

4.2.2 Analytical solution

Now the equation of motion Eq. 4.2 can be solved exactly in the conservative case, i.e., in the absence of friction and periodic forcing. Hence, the analytical solutions of the periodic orbits inside the single well will be derived.

The conservation of energy can be used to set the problem in terms of the three roots of $E - V(x) = 0$ in the following way

$$\frac{\dot{x}^2}{2} = \frac{\beta}{3}(x-a)(x-b)(x-c).$$

The terms can be rearranged into

$$\frac{dx}{dt} = \sqrt{\frac{2\beta}{3}}\sqrt{(x-a)(x-b)(x-c)},$$

and now after a simple integration of the above equation it is achieved the following result

$$t - t_0 = \sqrt{\frac{3}{2\beta}} \int_a^x \frac{dx}{\sqrt{(x-a)(x-b)(x-c)}}, \tag{4.10}$$

where it is assumed that the particle lies in $x = a$ for the initial time t_0. Now assume the following change of variable

$$x = a + (b-a)\sin^2\theta,$$

and introducing this result into Eq. 4.10 it is obtained that

$$t - t_0 = \sqrt{\frac{6}{\beta(c-a)}} \int_0^\phi \frac{d\theta}{\sqrt{1 - m\sin^2\theta}}.$$

The solution of the integral in the right–hand side is given by the *sine amplitude* of a Jacobian elliptic function [16] from which it is deduced that

$$\sqrt{\frac{\beta(c-a)}{6}}(t - t_0) = \int_0^\phi \frac{d\theta}{\sqrt{1 - m\sin^2\theta}} = \mathrm{sn}^{-1}(\sin\phi|m),$$

where ϕ is the *elliptic amplitude* and m is the *elliptic parameter*.

There is a lot of confusion in the literature about the use of the *elliptic parameter* m and the *elliptic modulus* k, which are related by the expression $k^2 = m$. The notation of [16] is followed here, in which $\mathrm{sn}(u|k)$ represents the sine amplitude

when the elliptic modulus is used, while $\text{sn}(u|m)$ when the elliptic parameter is used. For simplicity, the elliptic parameter is used throughout.

Thus, from the last equation is inferred

$$\sin \phi = \text{sn} \left(\sqrt{\frac{\beta(c-a)}{6}}(t-t_0)|m \right),$$

and if the change of variable used before is taken into account, the following solution is obtained

$$x(t) = a + (b-a) \, \text{sn}^2 \left(\sqrt{\frac{\beta(c-a)}{6}}(t-t_0)|m \right),$$

which is the general solution for all the periodic orbits lying within the single well.

Note that all orbits are labelled by the elliptic parameter m. This parameter m, which ranges from $0 \leq m \leq 1$, is in fact the same previously defined in Eq. 4.7 in relation to the turning points of motion in the potential well. It labels the energy of each periodic orbit inside the potential well.

4.2.3   Period of the orbits

It is also interesting to calculate the period of each and everyone of the orbits inside the potential well. For this purpose the following integral has to be worked out

$$T(m) = 2\sqrt{\frac{3}{2\beta}} \int_b^c \frac{dx}{\sqrt{(x-a)(x-b)(x-c)}} = \sqrt{\frac{6}{\beta(c-a)}} \int_0^{\frac{\pi}{2}} \frac{d\theta}{\sqrt{1-m\sin^2\theta}}.$$

The last integral represents exactly the *complete elliptic integral of the first kind* $K(m)$ [16], so that

$$T(m) = \sqrt{\frac{24}{\beta(c-a)}} K(m).$$

For orbits whose energy is very small in absolute terms, i.e., $m \to 0$, the complete elliptic integral of first kind $K(m) \to \pi/2$ and then the period becomes $T \to 2\pi/\sqrt{\alpha}$. This is obviously the period for the linear oscillations around the elliptic fixed point $(0,0)$.

However for values of the energy close to the separatrix, which means $m \to 1$, the complete elliptic integral of the first kind diverges logarithmically in this way

$$K(m) \approx \frac{1}{2} \ln \left(\frac{16}{1-m} \right),$$

and this means that the period also diverges logarithmically for values of m close to unity

$$T(m) = \frac{2}{\sqrt{\alpha}} \ln \left(\frac{16}{1-m} \right).$$

4.2.4 Equation of the separatrix

From the general solution obtained before is rather easy to derive the equation of the separatrix orbit. In fact the separatrix orbit is the orbit with energy corresponding to the parameter $m = 1$ and that possesses a period infinity. The sine amplitude of the Jacobian elliptic function has two natural limiting functions depending on the limit values of m. These limiting functions are $\mathrm{sn}(u|m) \to \sin u$, for $m \to 0$ and $\mathrm{sn}(u|m) \to \tanh u$, for $m \to 1$.

Moreover, if $m = 1$, then $\Delta = 1$, $a = -\frac{\alpha}{2\beta}$ and $b = c = \frac{\alpha}{\beta}$ from Eq. 4.8 and Eqs. 4.9. Hence, the equations in phase space are given by

$$x_{sx}(t) = \frac{3\alpha}{2\beta}\left[\frac{2}{3} - \cosh^{-2}\left(\sqrt{\frac{\alpha}{4}}\,(t - t_0)\right)\right],$$

$$y_{sx}(t) = \frac{3}{2}\sqrt{\frac{\alpha^3}{\beta^2}}\frac{\sinh\left(\sqrt{\frac{\alpha}{4}}\,(t - t_0)\right)}{\cosh^3\left(\sqrt{\frac{\alpha}{4}}\,(t - t_0)\right)},$$

which has a fish–shaped form (see Fig. 4.2).
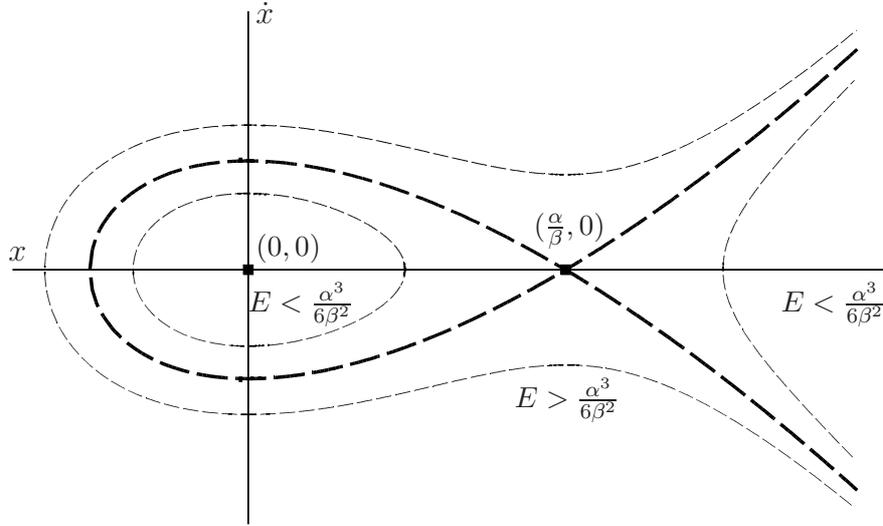
Figure 4.2. Phase space of the Helmholtz oscillator. The separatrix, in thick dashed line, is the stable manifold of an unstable periodic orbit. Therefore, bounded orbits correspond to the close curves around $(0,0)$, that is, the orbits inside the separatrix, and the unbounded orbits are the curves outside.

Actually, it is easy to check that $y_{sx}(t)$ and $x_{sx}(t)$ are related this way

$$y_{sx}^2 = \frac{2}{3}\beta\left(x_{sx} - \frac{\alpha}{\beta}\right)^2\left(x_{sx} + \frac{\alpha}{2\beta}\right).$$

The bounded motions lie in the interior of the separatrix, while the unbounded motions lie outside. In this case the separatrix corresponds to a *homoclinic orbit*, since the orbit connects the hyperbolic fixed point $(\frac{\alpha}{\beta}, 0)$ to itself.

4.2.5   Stochastic layer

Once the Helmholtz oscillator has been analyzed, it is interesting the study on how the orbits behave in the proximity of the separatrix when a periodic force is applied.

The time–dependent Hamiltonian in Eq. 4.4 can be used, as was explained in the introduction of this section, to study the Helmholtz oscillator with a periodic force. This time–dependent Hamiltonian can be seen as the sum of a time–independent Hamiltonian

$$H_0(x, p) = \frac{1}{2}p^2 + \frac{\alpha}{2}x^2 - \frac{\beta}{3}x^3$$

and a time–dependent Hamiltonian

$$H_1(x, t) = -\gamma x \cos \omega t,$$

that is, the Hamiltonian $H(p, x, t)$ can be written this way

$$H(p, x, t) = H_0(x, p) + H_1(x, t).$$

The former Hamiltonian allows analyzing the effect of the forcing by means of an area preserving map, which is called the *whisker map* or the *separatrix map*. This map measures the energy and phase change of a trajectory close to the separatrix for each period of the motion [17].

In order to construct this map it is needed to evaluate the change of the Hamiltonian H_0. The total derivative of H_0 is the following

$$\frac{dH_0}{dt} = \{H_0, H\} = \{H_0, H_1\} = -\frac{\partial H_0}{\partial \dot{x}}\frac{\partial H_1}{\partial x} = \gamma \dot{x} \cos \omega t, \qquad (4.11)$$

where $\{\ \}$ is the Poisson bracket.

Since our main interest is discussing the motion of the particle when its energy is close to the separatrix, it is assumed that γ is small enough to consider that H_1 is a small perturbation. Then, it is close to the separatrix where big effects in the dynamics of the particle may be expected. The effect of a small perturbation on the orbits of small energy is negligible.

The method to obtain the separatrix map, when H_1 is consider to be a small perturbation, is a standard one [17]. The first step is the computation of the energy ΔE. This energy accounts for the amount of the energy that an orbit close to the separatrix needs to accomplish a complete cycle, and is given through the integration of Eq. 4.11

$$\Delta E = \gamma \int_{\Delta t} \dot{x} \cos \omega t \, dt,$$

where $\Delta t = T/2 = \pi/\omega$. Notice that this integral signals the border of the stochastic layer.

This energy is usually written in the following way to be evaluated around the separatrix

$$\Delta E_n = \gamma \int_{t_n - \frac{T}{2}}^{t_n + \frac{T}{2}} \dot{x} \cos \omega t \, dt \approx \gamma \int_{-\infty}^{+\infty} \frac{dx_{sx}}{dt} \cos(\omega t + \omega t_n) \, dt.$$

From the third equality in Eq. 4.5 and Eqs. 4.6 a relationship between the energy E and the parameter m is found. Expanding around $m = 1$ up to second order, it is obtained the following expression $8E \approx (1 - m)^2$. This approximation is used later to determine the separatrix map and its corresponding stochastic layer.

The change of the phase is given by $\Delta\phi = \omega T$. The expression for the energy relationship found before in terms of m, when m is close to 1, suggests that the period of the orbits close to the separatrix behaves like

$$T(m) \approx \frac{1}{\sqrt{\alpha}} \ln\left(\frac{32}{E}\right).$$

In this manner the change of energy E and phase ϕ from the period n to the period $n + 1$ is given by the separatrix mapping [12]

$$E_{n+1} = E_n + \Delta E_n, \quad \phi_{n+1} = \phi_n + \omega T_{n+1},$$

where the variables (E, ϕ) are to be understood as a canonical pair. This map contains in principle the essential dynamics in the region close to the separatrix. Thus, the separatrix map is given by

$$E_{n+1} = E_n + \frac{6\pi\omega^2}{\beta} \frac{\gamma \sin\phi_n}{\sinh\left(\frac{\pi\omega}{\sqrt{\alpha}}\right)}, \quad \phi_{n+1} = \phi_n + \frac{\omega}{\sqrt{\alpha}} \ln\left(\frac{32}{E_{n+1}}\right).$$

Another way of measuring the instability is through the calculation of the following parameter K defined as [12]

$$K = \left| \frac{\delta\phi_{n+1}}{\delta\phi_n} - 1 \right|,$$

from which the stochastic layer width is achieved as a by–product. It supplies the information about how a small phase interval is stretched. The measure of the local instability is given by $K \geq 1$, because close to the separatrix a small change in frequency may cause a large effect in phase. The stochastic layer width is given by the value

$$E \approx \frac{6\pi\gamma\omega^3}{\sqrt{\alpha}\beta \sinh\left(\frac{\pi\omega}{\sqrt{\alpha}}\right)},$$

which corresponds to the width of the region close to the separatrix where it is likely to expect chaotic motions.

4.3 Dynamics of the Helmholtz Oscillator with Friction

In this section the Helmholtz oscillator in Eq. 4.2 is analyzed in the absence of the periodic forcing, i.e., when $\gamma = 0$. Then, the equation of motion of a particle of unit mass reads

$$\ddot{x} + \delta\dot{x} + \alpha x - \beta x^2 = 0.$$

To investigate the integrability of this equation the *Lie theory of differential equations* will be used [18, 19]. However, it should be noticed that the integrability of a differential equation can be also analyzed by means of the Kowalewski's asymptotic method (also called the Painlevé singularity structure analysis) and the same result is achieved.

For example, in [20, 21] the Duffing oscillator is analyzed in this manner. Nevertheless, the Lie theory is used in this work because this approach, in addition to give information about when the equation is integrable, allows reducing the problem to canonical variables which eases integrating the equation in a more general and natural way.

It can be seen in [18, 19] that in order to find the symmetry group G admitted by a differential equation with infinitesimal operator

$$X = \eta(t, x)\frac{\partial}{\partial x} + \xi(t, x)\frac{\partial}{\partial t}, \tag{4.12}$$

it is needed to find an infinitesimal operator X_{+2} such that

$$X_{+2}(\ddot{x} + \delta\dot{x} + \alpha x - \beta x^2) = 0. \tag{4.13}$$

The operator X_{+2} is

$$X_{+2} = \xi(t, x)\frac{\partial}{\partial t} + \eta(t, x)\frac{\partial}{\partial x} + A(t, x, \dot{x})\frac{\partial}{\partial \dot{x}} + B(t, x, \dot{x}, \ddot{x})\frac{\partial}{\partial \ddot{x}},$$

where $A(t, x, \dot{x})$ and $B(t, x, \dot{x}, \ddot{x})$ are defined as follows

$$A(t, x, \dot{x}) = \eta_t + \dot{x}(\eta_x - \xi_t) - \dot{x}^2\xi_x, \tag{4.14}$$
$$B(t, x, \dot{x}, \ddot{x}) = \eta_{tt} + \dot{x}(2\eta_{xt} - \xi_{tt}) + \dot{x}^2(\eta_{xx} - 2\xi_{tx}) - \dot{x}^3\xi_{xx} + \ddot{x}(\eta_x - 2\xi_t - 3\dot{x}\xi_x),$$

with the usual notation $\omega_z \equiv \frac{\partial\omega}{\partial z}$.

All $\xi(t, x)$ and $\eta(t, x)$ such that verify Eq. 4.13 generate infinitesimal operators X as in Eq. 4.12 which comprise the symmetries of the differential equation. Also, it is known that one symmetry can be used to reduce by one the order of a differential equation.

Thus, to integrate a second order differential equation two symmetries are needed. Hence, the Helmholtz oscillator will be integrated only if $\xi(t, x)$ and $\eta(t, x)$ are such that they generate two linearly independent infinitesimal operators.

4.3.1   Condition of integrability

Following the procedure to determine the symmetries of a differential equation mentioned in the former section, Eq. 4.13 reads

$$X_{+2}(\ddot{x} + \delta\dot{x} + \alpha x - \beta x^2) = \eta(\alpha - 2\beta x) + \delta\left(\eta_t + \dot{x}(\eta_x - \xi_t) - \dot{x}^2\xi_x\right) + \eta_{tt}$$
$$+\dot{x}(2\eta_{xt} - \xi_{tt}) + \dot{x}^2(\eta_{xx} - 2\xi_{xt}) - \dot{x}^3\xi_{xx} - (\delta\dot{x} + \alpha x - \beta x^2)(\eta_x - 2\xi_t - 3\dot{x}\xi_x).$$

This is a polynomial of third degree in $[\dot{x}]$ which is zero if and only if the coefficients of every monomial is zero

$$[\dot{x}^3] : \xi_{xx} = 0, \tag{4.15}$$

$$[\dot{x}^2] : \eta_{xx} - 2\xi_{xt} + 2\delta\xi_x = 0, \tag{4.16}$$

$$[\dot{x}] : 2\eta_{xt} - \xi_{tt} + 3\xi_x(\alpha x - \beta x^2) + \delta\xi_t = 0, \tag{4.17}$$

$$[1] : \eta(\alpha - 2\beta x) + \delta\eta_t + \eta_{tt} - (\eta_x - 2\xi_t)(\alpha x - \beta x^2) = 0. \tag{4.18}$$

From the condition in Eq. 4.15 it is plain that $\xi(x,t) = f(t) + k(t)x$, and this result in Eq. 4.16 implies that $\eta(x,t) = (k'(t) - \delta k(t))x^2 + xg(t) + h(t)$. If both results are used in Eq. 4.17 it is deduced that

$$4\left(k'' - \delta k'\right)x + 2g' - (f'' + k''x) + 3k\left(\alpha x - \beta x^2\right) + \delta\left(f' + k'x\right) = 0.$$

This is a polynomial of second degree in $[x]$ which is zero if and only if the three following equations are verified

$$[x^2] : 3\beta k = 0,$$

$$[x] : k'' + 3\delta k' - 3\alpha k = 0,$$

$$[1] : 4k'' - f'' + \delta f' + 2g' = 0.$$

These three equations imply that $k = 0$, hence $\xi(x,t) = f(t)$ and $\eta(x,t) = xg(t) + h(t)$, with the following relation between $f(t)$ and $g(t)$

$$\delta f' + 2g' - f'' = 0. \tag{4.19}$$

According to these results the condition in Eq. 4.18 is reduced to

$$(gx + h)(\alpha - 2\beta x) + \delta(xg' + h') + xg'' + h'' + \left(\alpha x - \beta x^2\right)(-g + 2f') = 0.$$

This is a polynomial of second degree in $[x]$ which is zero if and only if the following three equations are verified

$$[x^2] : g + 2f' = 0, \tag{4.20}$$

$$[x] : 2\alpha f' + \delta g' + g'' - 2\beta h = 0, \tag{4.21}$$

$$[1] : \alpha h + \delta h' + h'' = 0. \tag{4.22}$$

The conditions in Eq. 4.19 and Eq. 4.20 imply that $g = Ae^{\frac{1}{5}\delta t}$ with A a constant. When this result is used in Eq. 4.21 it is obtained that $h = \frac{1}{2\beta}\left(\frac{6}{25}\delta^2 - \alpha\right)g$. And finally, this result in Eq. 4.22 means that $\frac{1}{2\beta}\left(\frac{6}{25}\delta^2 + \alpha\right)\left(\frac{6}{25}\delta^2 - \alpha\right)g = 0$. But, since it is supposed that $\alpha > 0$ and so $\frac{6}{25}\delta^2 + \alpha > 0$, there are only two options to verify all conditions.

The first one is when $g = 0$. In this case $h = 0$ and $f = constant$ and this means that $\eta = 0$ and $\xi = constant$. Hence, only one infinitesimal operator is obtained, namely $X = \partial_t$, and as a consequence, the differential equation is partially integrable.

The second option in order to get two symmetries is when

$$\alpha = \frac{6}{25}\delta^2.$$

In this case $h = 0$ and $g = Ae^{\frac{1}{5}\delta t}$, which implies that $f = B - \frac{5}{2\delta}Ae^{\frac{1}{5}\delta t}$ and consequently $\xi = B - \frac{5}{2\delta}Ae^{\frac{1}{5}\delta t}$ and $\eta = Axe^{\frac{\delta}{5}t}$. Therefore, two infinitesimal generators are found, namely

$$X_1 = \frac{\partial}{\partial t} \qquad X_2 = -\frac{5}{2\delta}e^{\frac{1}{5}\delta t}\frac{\partial}{\partial t} + xe^{\frac{1}{5}\delta t}\frac{\partial}{\partial x}. \tag{4.23}$$

In conclusion, only when it is verified that $\alpha = \frac{6}{25}\delta^2$ the Helmholtz oscillator with friction is completely integrable. Therefore, there is a lot of information about the oscillator in this particular case, but there should be noticed that the information applies just for a two–dimensional (2D) manifold in the parameter space $\{\delta, \alpha, \beta, \gamma\}$. When $\alpha \neq \frac{6}{25}\delta^2$ the oscillator is only partially integrable and there is no way to write down the solution in terms of known functions.

4.3.2   Reduction to canonical variables

The infinitesimal generators X_1 and X_2 defined in Eqs. 4.23 are a two–dimensional algebra L_2 since $[X_1, X_2] = \frac{\delta}{5}X_2$, where $[\,,\,]$ is a *commutator*, called Lie bracket, defined in the following manner $[X_1, X_2] = X_1X_2 - X_2X_1$.

This *Lie algebra* can be classified according to its structural properties [18] as type III because $[X_1, X_2] = \frac{\delta}{5}X_2 \neq 0$ and $X_1 \vee X_2 = xe^{\frac{1}{5}\delta t} \neq 0$, where $\vee$ is a *pseudoscalar product* defined this way $X_1 \vee X_2 = \xi_1\eta_2 - \xi_2\eta_1$, if $X_i = \xi_i\partial_1 + \eta_i\partial_2$ for $i = 1, 2$. Actually, L_2 is the algebra of the homothety transformations of the real line $\mathbb{R}$, where X_1 is a homothety operator and X_2 is a translation operator.

Then, it is known that there exists a pair of variables w and z, called *canonical variables*, which linearizes the action of the group G on $\mathbb{R}$ and reduce the algebra L_2 to $X_1 = w\partial_w + z\partial_z$ and $X_2 = \partial_z$.

Let w and z be

$$w \equiv Axe^{\frac{2}{5}\delta t} \qquad z \equiv Be^{-\frac{1}{5}\delta t}, \tag{4.24}$$

where A and B are constants, then

$$X_1 = \frac{2\delta}{5}\omega\frac{\partial}{\partial\omega} - \frac{\delta}{5}z\frac{\partial}{\partial z} \qquad X_2 = \frac{B}{2}\frac{\partial}{\partial z}.$$

Although it is not the canonical form, there is no need to introduce more changes because it is simple enough to reduce the Helmholtz oscillator to an easily integrable equation.

From the definitions stated in Eqs. 4.24 the following result is obtained

$$w'' = \frac{d}{dz}\left(\frac{dw}{dz}\right) = \frac{25A}{B^2\delta^2}e^{\frac{1}{5}\delta t}\frac{d}{dt}\left(\left(\dot{x} + \frac{2}{5}\delta x\right)e^{\frac{3}{5}\delta t}\right)$$

$$= \frac{25A}{B^2\delta^2}e^{\frac{4}{5}\delta t}\left(\ddot{x} + \delta\dot{x} + \frac{6\delta^2}{25}x\right) = \frac{25\beta}{\delta^2 AB^2}w^2.$$

Therefore, if A and B are chosen such that

$$AB^2 = \frac{25\beta}{6\delta^2}, \tag{4.25}$$

then $w'' = 6w^2$, which is easily integrated yielding

$$(w')^2 = 4w^3 - g_3, \tag{4.26}$$

where g_3 is a constant.

The solution of this differential equation is the *Weierstrass function* $\wp(z|0, g_3)$, since $\wp(z|g_2, g_3)$ verifies that $(\wp')^2 = 4\wp^3 - g_2\wp - g_3$ (see Fig. 4.3). Hence, the solution of the Helmholtz oscillator with friction is $w = \wp(z|0, g_3)$, which is called the *equianharmonic case of the Weierstrass function* because $g_2 = 0$ [16].
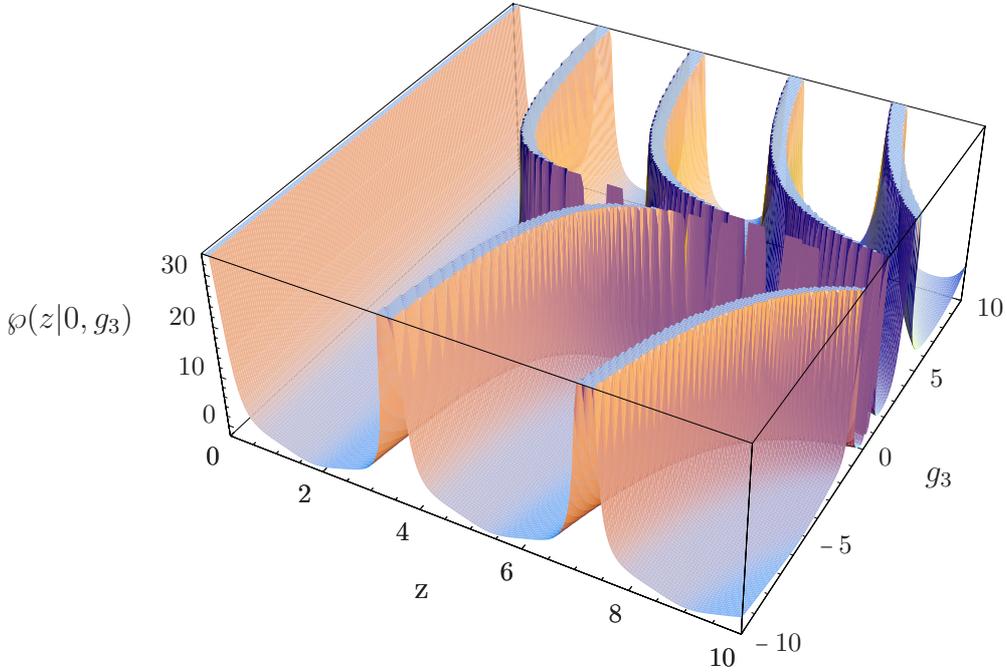

Figure 4.3. The equianharmonic case of the Weierstrass function, $\wp(z|0, g_3)$, is shown. This is the solution corresponding to the equation $(w')^2 = 4w^3 - g_3$, where g_3 is a first integral of motion. Notice that, once g_3 is fixed, the solution is periodic.

It should be noticed that $g_3 = 4w^3 - (w')^2$ is a first integral of motion and when a change of variables from (w, z) to (x, t) is carried out in Eq. 4.26, the first integral g_3 becomes $I(t, x, \dot{x})$ in this manner

$$\left[\left(\dot{x} + \frac{2}{5}\delta x\right)^2 - \frac{2}{3}\beta x^3\right] e^{\frac{6}{5}\delta t} = \Lambda g_3 = I(t, x, \dot{x}),$$

where $\Lambda = \left(\frac{6B^3\delta^3}{125\beta}\right)^2$, and consequently is always a positive constant.

The former result is an explicitly time–dependent first integral which is analogous to the first integral of the Duffing oscillator obtained in [21]. Also, it can be related to the Hamiltonian function of the Helmholtz oscillator with friction in the following way. Define two variables p and q as follows

$$p = \sqrt{2} \left(\dot{x} + \frac{2}{5}\delta x \right) e^{\frac{3}{5}\delta t}, \tag{4.27}$$

$$q = \sqrt{2}xe^{\frac{2}{5}\delta t},$$

so the first integral $I(t, x, \dot{x})$ can be written as

$$I(p, q) = \frac{1}{2}p^2 - \frac{\beta}{3\sqrt{2}}q^3.$$

Define a function $H(p, q, t)$ related to the first integral $I(p, q)$ as

$$H(p, q, t) = I(p, q)e^{-\frac{1}{5}\delta t} = \left(\frac{1}{2}p^2 - \frac{\beta}{3\sqrt{2}}q^3 \right) e^{-\frac{1}{5}\delta t}.$$

This function verifies the Hamilton equations, namely

$$\frac{\partial H}{\partial p} = pe^{-\frac{1}{5}\delta t} = \sqrt{2} \left(\dot{x} + \frac{2}{5}\delta x \right) e^{\frac{2}{5}\delta t} = \dot{q}, \tag{4.28}$$

$$\frac{\partial H}{\partial q} = -\frac{\beta}{\sqrt{2}}q^2 e^{-\frac{1}{5}\delta t} = -\sqrt{2}\beta x^2 e^{\frac{3}{5}\delta t} = -\dot{p},$$

and hence $H(p, q, t)$ is a Hamiltonian function. Moreover, by means of Eqs. 4.28 it is obtained that

$$\ddot{q} = \left(\dot{p} - \frac{1}{5}\delta p \right) e^{-\frac{1}{5}\delta t} = \frac{\beta}{\sqrt{2}}qe^{-\frac{2}{5}\delta t} - \frac{1}{5}\delta pe^{-\frac{1}{5}\delta t},$$

which can be written in terms of (x, t) by using Eqs. 4.27 as

$$\sqrt{2}e^{\frac{2}{5}\delta t} \left(\ddot{x} + \delta\dot{x} + \frac{6\delta^2}{25}x - \beta x^2 \right) = 0.$$

Therefore, $H(p, q, t)$ is the Hamiltonian function of the Helmholtz oscillator with friction for the integrable case since the solutions to $\ddot{x} + \delta\dot{x} + \frac{6\delta^2}{25}x - \beta x^2 = 0$ and the solutions to the Hamilton equations of $H(p, q, t)$ are the same.

Then, two remarks can be made. First, the explicitly time–dependent Hamiltonian is not a first integral of motion, which is reasonable since the energy is not constant in this system because of the friction. Second, the first integral $I(p, q)$ can be seen as the energy of a particle in a potential $V(q) = -\frac{\beta}{3\sqrt{2}}q^3$ and, thus, the Helmholtz oscillator can be regarded as a system with energy $I(p, q)$ at $t = 0$, which vanishes exponentially with time.

4.3.3 Solutions of the integrable case

Case $g_3 = 0$

The equation to solve is $(w')^2 = 4w^3$ whose solution is $w = (z - c')^{-2}$ with c' an arbitrary constant. The definitions of w and z and the relation in Eq. 4.25 implies that

$$x(t) = \frac{6\delta^2}{25\beta} \left(1 + c_2 e^{\frac{1}{5}\delta t} \right)^{-2},\tag{4.29}$$

where c_2 is an arbitrary constant because c' is arbitrary.

Case $g_3 > 0$

The Weierstrass function $\wp(z|g_2, g_3)$ for $g_2 = 0$ and $g_3 > 0$ can be written in terms of the Jacobian Elliptic cosine [16] as

$$w(z) = r + H \frac{1 + \mathrm{cn}\left(2\sqrt{H}z + c_2 | m \right)}{1 - \mathrm{cn}\left(2\sqrt{H}z + c_2 | m \right)},\tag{4.30}$$

with c_2 an arbitrary constant and where $m = \frac{2-\sqrt{3}}{4} \simeq 0.067$ and $H = \sqrt{3}r$ with $r = \sqrt[3]{\frac{g_3}{4}}$. Notice that, as it was explained in section 4.2.2, it is being used the elliptic parameter m instead of the elliptic modulus k, which are related in this way $k^2 = m$.

By using the definitions of w and z and the relation in Eq. 4.25 the following result in terms of t is obtained

$$x(t) = \frac{6\delta^2}{100\beta} c_1^2 \left[\frac{1}{\sqrt{3}} + \frac{1 + \mathrm{cn}\left(c_1 e^{-\frac{1}{5}\delta t} + c_2 | m \right)}{1 - \mathrm{cn}\left(c_1 e^{-\frac{1}{5}\delta t} + c_2 | m \right)} \right] e^{-\frac{2}{5}\delta t},$$

where $c_1 = 2\sqrt{H}B$ and hence c_1 is arbitrary because B is arbitrary.

Case $g_3 < 0$

It is known [16] that $\wp(z|g_2, g_3) = -\wp(iz|g_2, -g_3)$. This relation lets apply the result in Eq. 4.30 for $g_3 < 0$ this way

$$w(z) = -r' - H' \frac{1 + \mathrm{cn}\left(2\sqrt{H'}iz + ic_2 | m \right)}{1 - \mathrm{cn}\left(2\sqrt{H'}iz + ic_2 | m \right)},\tag{4.31}$$

where $m = \frac{2-\sqrt{3}}{4}$ and $H' = \sqrt{3}r'$ with $r' = \sqrt[3]{\frac{|g_3|}{4}}$. By means of the relation $\mathrm{cn}(iu|m)\mathrm{cn}(u|m') = 1$ where $m + m' = 1$, it is possible to write Eq. 4.31 as follows

$$w(z) = -r' + H' \frac{1 + \mathrm{cn}\left(2\sqrt{H'}z + c_2 | m' \right)}{1 - \mathrm{cn}\left(2\sqrt{H'}z + c_2 | m' \right)},$$

Hence, the solution may be written in terms of t by changing variables and using Eq. 4.25

$$x(t) = \frac{6\delta^2}{100\beta}c_1^2 \left[-\frac{1}{\sqrt{3}} + \frac{1 + \mathrm{cn}\left(c_1 e^{-\frac{1}{5}\delta t} + c_2|m'\right)}{1 - \mathrm{cn}\left(c_1 e^{-\frac{1}{5}\delta t} + c_2|m'\right)} \right] e^{-\frac{2}{5}\delta t},$$

where $m' = \frac{2+\sqrt{3}}{4} \simeq 0.933$ and $c_1 = 2\sqrt{H'}B$ and hence c_1 is arbitrary because B is arbitrary.

Discussion

In Fig. 4.4 the two basins of attraction of the Helmholtz oscillator are depicted in the phase space. The green region represents the set of initial conditions that end up in the attractor $(0,0)$. They correspond to bounded orbits in the phase space that asymptotically spiral inside the potential well. The white region is the set of initial conditions that correspond to unbounded orbits, i.e., tending to infinity.
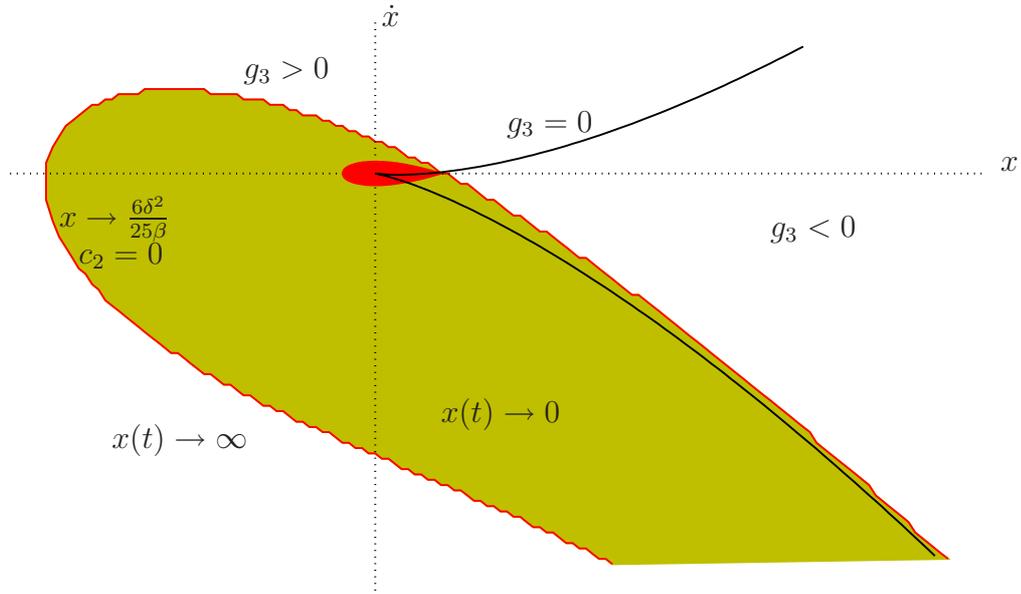

Figure 4.4. Relation between the geometry of the basins of attraction and the analytical features of the exact solutions when the Helmholtz oscillator is integrable. The green region is made of the initial conditions that tend to $(0,0)$ and the white region is made of the ones tending to infinity. The boundary between both basins corresponds to the set of initial conditions tending to the local maximum and whose solutions have $c_2 = 0$. Also the curve $g_3 = 0$ is depicted and represents the initial conditions whose solutions have the first integral of motion $I(t, x, \dot{x}) = 0$. Finally, the region where there are bounded orbits in absence of friction is shown in red. It is comparatively smaller than the region $x \to 0$ because the integrable case implies a large friction, since $\alpha = \frac{6}{25}\delta^2$ and, hence, dissipation makes more initial conditions end up inside the potential well.

The boundary between both sets is formed by the stable manifold of an unstable periodic orbit. Actually, this orbit is the one that stays forever on the local maximum $(\frac{6\delta^2}{25\beta}, 0)$ of the potential, which means that all points in the boundary tend asymptotically to this point.

The basins of attraction are related to the analytical solutions via c_2 and to check this, it is necessary to study the asymptotical behavior of the solutions. To calculate the limit $t \to \infty$ when $g_3 > 0$ the following change of variable $z \equiv c_1 e^{-\frac{1}{5}\delta t}$ is carried out, so the former limit becomes $z \to 0$. This implies in Eq. 4.30 that

$$\lim_{t \to \infty} x(t) = \lim_{z \to 0} \frac{6\delta^2}{100\beta} \left(\frac{1}{\sqrt{3}} + \frac{1 + \mathrm{cn}(z + c_2|m)}{1 - \mathrm{cn}(z + c_2|m)} \right) z^2.$$

The Jacobian Elliptic function $\mathrm{cn}(z|m)$ is a periodic function since $\mathrm{cn}(z+2K|m) = -\mathrm{cn}(z|m)$, i.e., $2K$ plays a role similar to π in a circular function. In fact, cn is periodic with period $4K$ being $2K \simeq 3.197$ because $m = \frac{2-\sqrt{3}}{4}$, and thus c_2 is comprised within $(-2K, 2K)$. Consequently, if $c_2 = 4NK$ with $N \in \mathbb{Z}$ then

$$\lim_{t \to \infty} x(t) = \lim_{z \to 0} \frac{6\delta^2}{100\beta} \left(\frac{1}{\sqrt{3}} + \frac{1 + \mathrm{cn}(z|m)}{1 - \mathrm{cn}(z|m)} \right) z^2$$
$$= \lim_{z \to 0} \frac{6\delta^2}{100\beta} \left(\frac{z^2}{\sqrt{3}} + 4 - z^2 \right) = \frac{6\delta^2}{25\beta},$$

in which it has been used the following result $\mathrm{cn}(z|m) = 1 - \frac{1}{2}z^2 + o(z^4)$ [16]. Therefore, the boundary when $g_3 > 0$ can be defined to as the points in the phase space whose analytical solutions have $c_2 = 0$.

When $g_3 < 0$ the result $x(t \to \infty) = \frac{6\delta^2}{25\beta}$ when $c_2 = 0$ is equally achieved. However, $\mathrm{cn}(z|m')$ is now a periodic function with $2K' \simeq 5.535$ since $m' = \frac{2+\sqrt{3}}{4}$, and thus c_2 is comprised within $(-2K', 2K')$. Nevertheless, also in this case the boundary can be defined to as the points in the phase space whose analytical solutions have $c_2 = 0$. Also, it is easy to verify from Eq. 4.29 that in the case $g_3 = 0$ the solution tends to $\frac{6\delta^2}{25\beta}$ when $c_2 = 0$.

In summary, the condition $c_2 = 0$ on the exact solutions yields the boundary between the two basins of attraction, which links the geometry of these two regions in the phase space with an analytical feature in the exact solutions.

Inside the green region in Fig. 4.4, it can be seen in red the region where there are bounded orbits in absence of friction. It is a small region as compared with the integrable case because $\alpha = \frac{6\delta^2}{25}$ and then, dissipation is more important than its potential energy. In other words, many initial conditions, which were unbounded orbits without friction, dissipate energy quickly in this case and, as they go by the potential well, are trapped in it.

The existence of a strong dissipation in the integrable case also explains why there is no oscillatory behavior in Fig. 4.5. When the orbit tends to the minimum inside the well the particle is so damped that it goes straight to that minimum.
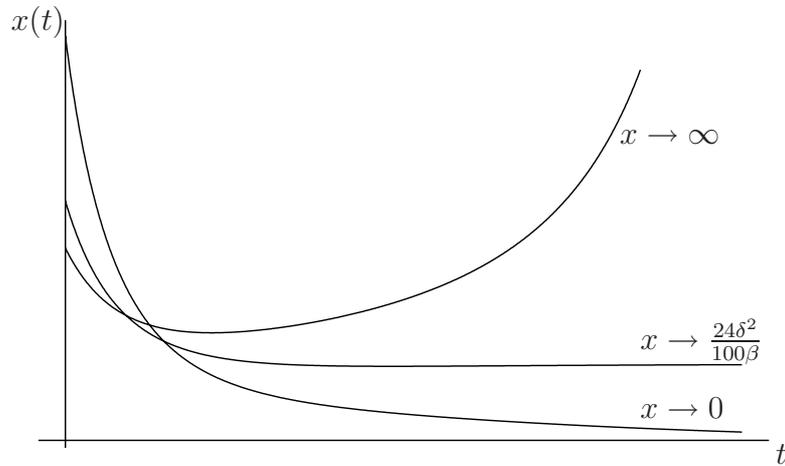
Figure 4.5. The phase space of the Helmholtz oscillator with friction has two basins of attraction and hence there are three kinds of orbits. Orbits spiralling inside the potential well tending to the minimum $x \to 0$, orbits tending to infinity $x \to \infty$ and orbits tending to the local maximum $x \to \frac{24\delta^2}{100\beta}$ which correspond to initial conditions upon the boundary of both basins. Notice that particles are so damped in the integrable case that inside the potential well they go straight to zero instead of spiralling and so there are no oscillations in the curve $x \to 0$.

4.4   Conclusions

The Helmholtz oscillator is a simple model for studying phenomena that under certain conditions present a stable behavior of oscillatory kind, but for other conditions the behavior is unstable (i.e., this oscillator presents an escape). Then, a question of interest is what happens close to the separatrix when a forcing term is introduced. The effect of forcing is not relevant for an orbit with little energy (i.e., close to the minimum in the potential well), because essentially its stable behavior is not altered by the forcing. The width of the stochastic layer by using the separatrix map has been computed here. This gives the width of the energy band around the separatrix, where it is likely that an orbit presents transient chaos.

Another important aspect considered in this chapter is the inclusion of friction. To solve the equation of the Helmholtz oscillator with friction and without forcing the Lie theory for differential equations is used. We show that the Helmholtz oscillator is completely integrable only when certain relation between the parameters is satisfied. When this relation is not satisfied, the equation is partially integrable. Also, we calculate that the symmetries for the completely integrable case are a translation and a homothopy. Moreover, this two symmetries are the two dimensional algebra of the homothety transformations of the real line, and the symmetry for the partially integrable case is a translation.

A first integral of motion is obtained when the equation is integrated by using one symmetry. We prove that this time–dependent integral of motion is related to

a Hamiltonian function. The second symmetry allows integrating the first integral of motion to obtain, as a solution, the Weierstrass function. Finally, we write this solution in terms of Jacobian Elliptic functions to show that there exists a relation with the basins of attraction of the oscillator.

However, the condition required to completely integrate the equation is just a two–dimensional (2D) manifold in the parameter space. Then, in most of cases, we cannot write down the function that solves the equation. No matter the effort we make.

Then, as Poincaré advocated after his discovery of chaotic behavior in the three–body problem [22], we should analyze this type of problems from a global viewpoint since it is nonsensical to study individual trajectories. To understand the motions that surround us, mainly due to non–linear laws and interactions, requires the development of new techniques.

Bibliography

[1] D.J. WATTS. *Six degrees: The science of a connected age*, W.W. Norton & Company, Inc., New York, 2003.

[2] M. TABOR. *Modern dynamics and classical analysis*. Nature 310, 277–282 (1984).

[3] H. GIACOMINI AND S. NEUKIRCH. *Integrals of motion and the shape of the attractor for the Lorenz model*. Physics Letters A 227, 309–318 (1997).

[4] Y.T. CHANG, M. TABOR AND J. WEISS. *Analytic structure of the Henon-Heiles Hamiltonian in integrable and nonintegrable regimes*. Journal of Mathematical Physics 23, 531–538 (1982).

[5] S.N. RASBAND. *Marginal stability boundaries for some driven, damped, non–linear oscillators*. International Journal of Non–Linear Mechanics 22(6), 477–495 (1987).

[6] J.M.T. THOMPSON. *Chaotic phenomena triggering the escape from a potential well*. Proceedings Royal Society London A 421, 195–225 (1989).

[7] I.S. KANG AND L.G. LEAL. *Bubble dynamics in time–periodic straining flows*. Journal Fluid Mechanics 218, 41–69 (1990).

[8] I.S. KANG. *Dynamics of a conducting drop in a time–periodic electric field.* Journal Fluid Mechanics 257, 229–264 (1993).

[9] E.V. BOGDANOVA–RYZHOVA AND O.S. RYZHOV. *Solitary–like waves in boundary–layer flows and their randomization.* Phil. Trans. R. Soc. Lond. A 352, 389–404 (1995).

[10] A.D.D. CRAIK. *Wave interactions and fluid flows.* Cambridge University Press, Cambridge, 1985.

[11] B.V. CHIRIKOV. *A universal instability of many–dimensional oscillator systems* Physics Reports 52, 263–379 (1979).

[12] G.M. ZASLAVSKY, R.Z. SAGDEEV, D.A. USIKOV AND A.A. CHERNIKOV. *Weak chaos and quasi–regular patterns.* Cambridge University Press, Cambridge, 1991.

[13] Y. YAMAGUCHI. *Structure of the stochastic layer of a perturbed double–well potential system.* Physics Letters A 109, 191–195 (1985).

[14] H.E. NUSSE, E. OTT AND J.A. YORKE. *Saddle–node bifurcations on fractal basin boundaries.* Physical Review Letters 75, 2482–2485 (1995).

[15] M.A.F. SANJUÁN. *Comments on the hamiltonian formulation for linear and nonlinear oscillators including dissipation.* Journal of Sound and Vibrations 185, 734–736 (1995).

[16] M. ABRAMOWITZ AND I.A. STEGUN. *Handbook of mathematical functions.* Dover, New York, 1970.

[17] G.M. ZASLAVSKY. *The physics of chaos in Hamiltonian dynamics.* Imperial College Press, London, 1998.

[18] N.H. IBRAGIMOV. *Lie group analysis of differential equations Vol. 1.* CRC Press, Boca Raton, 1994.

[19] P.J. OLVER. *Applications of Lie groups to differential equations.* Springer–Verlag, New York, 2000.

[20] S. PARTHASARATHY AND M. LAKSHMANAN. *On the exact solutions of the Duffing oscillator.* Journal of Sound and Vibrations 137, 523–526 (1990).

[21] N. EULER, W.H. STEEB AND K. CYRUS. *On exact solutions for damped anharmonic oscillators.* Journal of Physics A: Mathematical and General 22, 195–199 (1989).

[22] H. POINCARÉ. *Science and method,* Dover Publications, New York, 2003.

Chapter 5

Dynamics in complex networks

5.1 Introduction

After the seminal papers by Watts and Strogatz [1] and by Barabási and Albert [2], complex systems started to be described within the framework of complex networks. First, attention was focused on their structural and functional properties, being the most studied the small–world [3] and scale–free [4, 5] networks since many natural (neural, genetic, chemical) and man–made (power grids, Internet, social networks) systems have been characterized with a similar underlying connectivity structure.

The interest was then shifted to the implications on the global dynamical behavior of ensembles of non–linear active units when they are coupled through a non–trivial scheme [6] instead of being organized in a lattice. Among the dynamical processes that can take place on a network [7], such as pattern formation [8, 9], spreading processes or synchronization, the latter is the one capturing more pages in the bibliography.

Synchronous behavior is considered one of the mechanisms to transmit and code information in complex systems, ranging from neuronal assemblies [10], to networks of chemical oscillators of the Belousov–Zhabotinsky reaction [11, 12], or social communities [13]. The interplay between the network structure and the local dynamics of the interacting subsystems can provide stronger synchronizability or faster propagation of information [6]. This enhancement is mainly due to a smaller average distance between the dynamical units.

Theoretically, the network propensity for synchronization has been first tackled in [14]. Since then, several strategies have been developed with the aim of finding the best way to achieve synchronization in complex networks. These approaches have mainly focused on the role that weighted links play in networks with a heterogeneous degree distribution [15, 16, 17], the importance of the shortest paths and clustering between nodes in small–world networks [10], and the effect of the input degree received by each node regardless of the global structure [18]. Another recent approach, a kind of reverse engineering, consists in defining a recursive algorithm to build up a network with N nodes and a mean degree k that minimizes some synchronizability parameter [19].

Most of this research has been devoted to attractively coupled dynamical elements. However, it is known that biological networks combine different types of connections to improve synchronization and transmission performance, as in the case of the coexistence of excitatory and inhibitory synapses in the brain [20].

In [21] it is studied pattern formation in a two–dimensional array of oscillators with phase–shifted coupling, in particular for phase shift π which corresponds to a repulsive coupling, while in [22] a chain of negatively coupled chaotic oscillators is compared to an experimental laser system with negative feedback and delay. Obviously, two attractively coupled oscillators tend to oscillate in phase whereas they do it in anti–phase if they are repulsively coupled.

Nevertheless, little attention has been paid to the effect of repulsive coupling or to the interaction between different types of coupling in complex networks. The scarce literature addressing synchronization in repulsively coupled oscillators refers mainly to phase oscillators and considers either a lattice [23] or a fully connected topology [24], but the influence of the network structure is still an open question.

In addition, almost all the published work on synchronization in complex networks basically deals with arrays of identical dynamical units. However, heterogeneity is an inherent feature that natural systems exhibit, which can be especially relevant in the dynamics of biological networks.

In this chapter, we explore the influence of the network topology on the dynamics of non–identical coupled units, when a small fraction of the links is phase–repulsive. We first consider a chain of excitable and oscillatory units and show that sparse repulsive links in a small–world structure can induce a coherent oscillatory state when the equivalent small–world composed of only attractive connections is unable to synchronize or even to activate the heterogeneous ensemble. In Sec. 5.4, the effect of sparse repulsive couplings is also shown for a much simpler network of spin–like dynamical units. Then, just by means of an analysis focused on the eigenvalues of the connectivity matrix (i.e., its spectra), we link the emerging dynamical behavior to the structural properties of the sparsely coupled repulsive network in Sec. 5.5.

5.2   A network of excitable and oscillatory elements

In our study, we consider that the dynamical elements to be placed on each of the N nodes of our network are non–identical Hodgkin–Huxley (HH) units [25]. Then, our model is described by the following equations,

$$C\dot{V}_i = I_i - I_i^{ion}(V_i, x_i) + \frac{d}{k_i} \sum_j c_{ij}(V_j - V_i), \qquad (5.1)$$

$$I_i^{ion} = g_{Na}m_i^3 h_i(V_i - V_{Na}) + g_K n_i^4(V_i - V_K) + g_l(V_i - V_l),$$

$$\dot{m}_i = \frac{0.1(V_i + 40)}{1 - \exp(-\frac{V_i+40}{10})}(1 - m_i) - \frac{4}{\exp(\frac{V_i+65}{18})}m_i,$$

$$\dot{n}_i = \frac{0.01(V_i + 55)}{1 - \exp(-\frac{V_i+55}{10})}(1 - n_i) - \frac{0.125}{\exp(\frac{V_i+65}{80})}n_i,$$

$$\dot{h}_i = \frac{0.07}{\exp(\frac{V_i+65}{20})}(1 - h_i) - \frac{1}{1 + \exp(-\frac{V_i+35}{10})}h_i,$$

where

- V_i is the voltage across the membrane of neuron i of capacitance C.

- I_i^{ion} is the ionic current of neuron i, mainly carried by Na$^+$ and K$^+$ ions and other ionic currents (known as *leakage current*) through voltage–dependent channels. These currents are driven by the voltage difference with respect to the equilibrium potentials V_{Na}, V_K and V_l and the maximal ionic conductances g_{Na}, g_K and g_l.

- $\dot{m}$, $\dot{n}$ and $\dot{h}$ describe the gating of the ion channels.

- Parameter values and functions are the standards in the literature [25].

  - C=1 μF/cm^2,
  - $g_{Na} = 120$ mS/cm^2, $g_K = 36$ mS/cm^2, $g_l = 0.3$ mS/cm^2,
  - $V_{Na} = 50$ mV, $V_K = -77$ mV, $V_l = -54.4$ mV.

- I_i controls the dynamics of an isolated unit and it is chosen as the control parameter to introduce heterogeneity in the population. We set I_i uniformly distributed within the interval $I_0 \pm \Delta I$ to obtain an ensemble of excitable and oscillatory units. The value $I_0 = 9$ μA/cm^2 is fixed close to the point where an inverse Hopf bifurcation occurs. This way, for the chosen $\Delta I = 0.2$ μA/cm^2, we observe that about 90% of the elements stay around the silent state, while the rest oscillate.

- The coupling structure in Eq. 5.1 is given by the connectivity matrix $\mathbf{C} = (c_{ij})$, defined by $c_{ii} = 0$, $c_{ij} = \pm 1$ if nodes i and j are connected, and $c_{ij}=0$ otherwise. k_i normalizes the connection strength by the number of incoming links to node i, and the coefficient d stands for the global coupling strength. The positive sign in $\mathbf{C}$ stands for an attractive coupling whereas the negative sign does for a repulsive one. The coupling term in Eq. 5.1 can be written as $d\sum_j \ell_{ij}V_j$, being $\mathbf{L} = (\ell_{ij})$ the Laplacian of the graph [7],

$$\ell_{ii} = -\frac{1}{k_i}\sum_{j=1}^{N} c_{ij} \quad , \qquad \ell_{ij} = \frac{c_{ij}}{k_i}. \tag{5.2}$$

5.3   Numerical results

5.3.1   Local coupling

Initially we consider the dynamics of an ensemble of N elements locally linked on a one–dimensional array, being all couplings either phase–attractive or phase–repulsive. The resulting connectivity matrix becomes $c_{i,i\pm1} = +1$ for the locally

attractive coupling scheme, $c_{i,i\pm1} = -1$ in case of purely repulsive coupling, and $c_{ij} = 0$ otherwise. The system given by Eq. 5.1 is numerically integrated using a fourth order Runge–Kutta method with time step $\Delta t = 0.05$ ms and open boundaries.

Figure 5.1 shows the global mean frequency of oscillation (MF) and the standard deviation σ_{MF} as a function of the coupling strength d ranging from negative to positive values. The negative sign of d corresponds to the phase–repulsive case. It can be seen that while the system is frequency entrained to a phase synchronization state for a $d > 0$ large enough, the system reaches an anti–phase synchronization state for a sufficient $d < 0$.

Precisely, a small σ_{MF} means that all elements are oscillating at the same rate, which is about 70 Hz (see Fig. 5.1A), and a large standard deviation reflects that many elements are silent, resulting in a MF much lower than the 70 Hz that the oscillating elements have.

It can be noted from Fig. 5.1 that the entrainment with negative couplings is achieved for smaller absolute values of d compared to the case with positive ones. This indicates that a phase–repulsive coupling is more effective to activate and entrain the whole network.
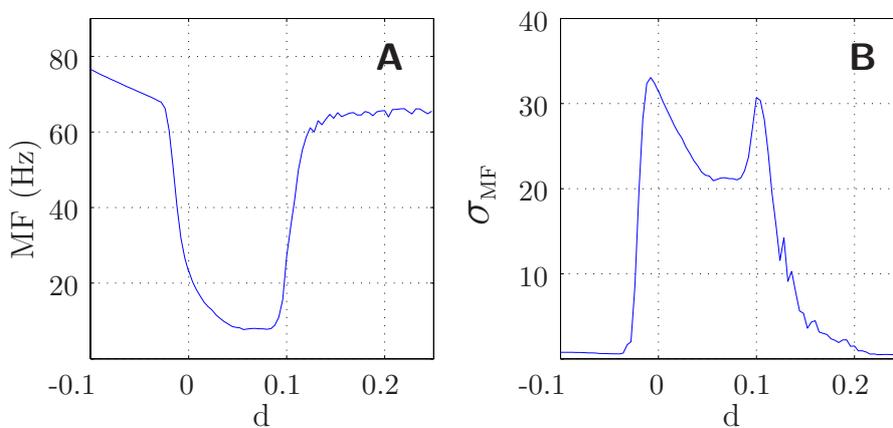

Figure 5.1. The effect of local couplings. (A) Mean frequency of oscillation (MF) and (B) its standard deviation σ_{MF} for an array of $N = 400$ locally coupled HH units as a function of the coupling strength d. Each point is the average of 100 realizations. Notice that the negative sign of d corresponds to the phase–repulsive case.

Many biological systems exhibit this kind of repulsive coupling when their dynamical units are in competition with each other. Known examples are the inhibitory coupling present in neuronal circuits associated to a synchronized behavior in central pattern generators [26] or calcium oscillations in epileptic human astrocyte cultures [27].

5.3.2 Non–local random coupling

Now, our main interest is to explore the influence of a small–world connection topology in the activation and synchronization of the network as the repulsive couplings are varied. From the results obtained in the previous section, we know that a small positive coupling strength is less efficient than a negative one to activate and synchronize the whole array when the units are locally coupled.

Taking this into account, we consider now the possibility of both attractive and repulsive non–local links. The global coupling strength is fixed to $d = 0.1$, i.e., within the unsynchronized regime for local positive coupling as shown in Fig. 5.1.

The coupling matrix $\mathbf{C}$ is modelled now by keeping the local connections positive, $c_{i,i\pm1} = +1$, and by randomly adding (rather than rewiring) a fraction p of the $(N-1)(N-2)/2$ possible long–range links, being negative with probability q. That is, the probability of having a long–range connection, $c_{ij} \neq 0$ with $j \neq i \pm 1$, is given by $p \in [0,1]$. Then, we have $c_{ij} = -1$ with probability pq, and $c_{ij} = +1$ with probability $p(1-q)$.

Figure 5.2 shows space–time plots of the voltage variable through the whole array for different values of p and q. As expected, in the absence of long–range connections ($p = 0$), few more than the initial 10% of the units is oscillating for the chosen coupling strength d, i.e., the array is not even activated (see Fig. 5.2A).
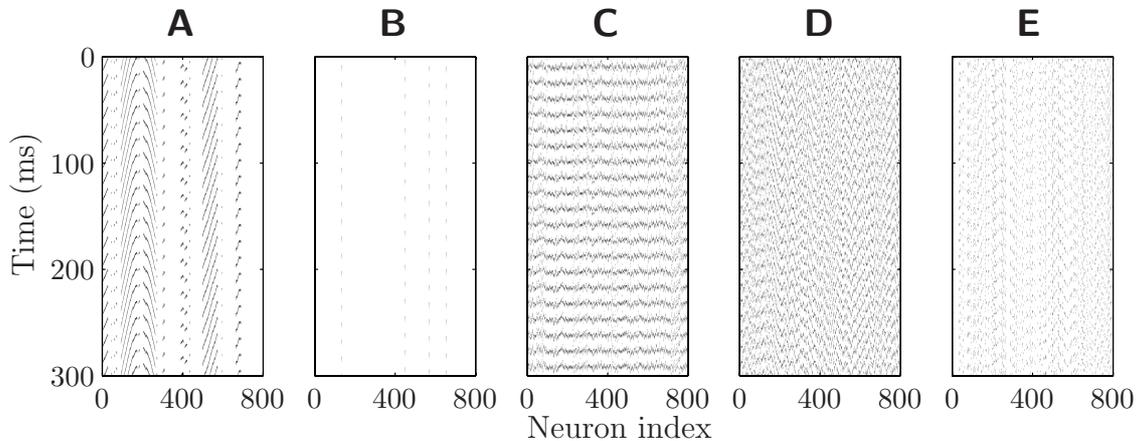

Figure 5.2. Raster plots. Space–time plots of the voltage variable for a $N = 800$ HH units network with $d = 0.1$ (i.e., within the unsynchronized regime for local positive coupling) and different coupling connectivities. (A) Attractive local coupling, $p = 0$. (B)-(E) Network with long–range couplings: (B) fully attractive $p = 0.0055$ and $q = 0$, (C)-(E) partially repulsive: (C) $p = 0.0055$ and $q = 0.3$, (D) $p = 0.0055$ and $q = 0.45$, (E) $p = 0.015$ and $q = 0.3$.

When long–range links are included, the first observation is that for any p, a minimum fraction of the new added links needs to be repulsive ($q \neq 0$) in order to increase the activity of the network. This becomes evident when comparing Fig. 5.2B with Figs. 5.2C-D-E.

In Fig. 5.2B the activity generated by the 10% of initially active units is re-
duced, or even annihilated, when all long–range connections are attractive ($q = 0$).
However, the scenario completely changes when some of the shortcuts are repulsive
($q > 0$) as Figs. 5.2C-D-E depict, where self–sustained electrical activity emerges
for nonzero q.

In addition, we observe the existence of optimal probabilities p and q for which
the collective oscillation becomes maximally phase–coherent. This fact can be ob-
served by comparing Fig. 5.2C, where p and q are optimal, with Fig. 5.2D, in which
p is the same but q is higher, and with Fig. 5.2E, in which q is the same but p is
slightly different.

To study quantitatively how the dynamics is affected by p and q, we measure
the MF of the network and the standard deviation of the global electrical voltage,

$$V(t) = \sum_{i=1}^{N} V_i(t),$$

obtained as

$$\sigma_V = \sqrt{\overline{V^2} - \overline{V}^2}, \tag{5.3}$$

being $\overline{V} = \langle V(t) \rangle_t$ and $\overline{V^2} = \langle V^2(t) \rangle_t$ where $\langle \ldots \rangle_t$ denotes temporal average.

While the MF gives us an estimation of how much the network is activated, the
σ_V defines how coherent is the activity of the entire network. If the network is fully
activated, the MF approaches to a rate of around 70 Hz, whereas σ_V is maximal if
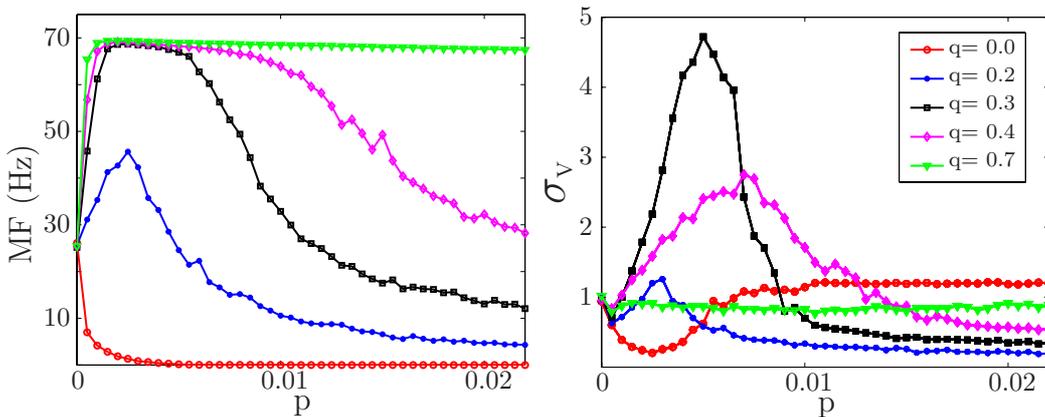this activity is synchronized.

Figure 5.3. The effect of non–local couplings. MF (left) and network coherence σ_V
(right) as a function of p for several q in a $N = 800$ network. Each point is averaged over
100 simulations, 1 s long (transients avoided), for different network and initial conditions
realizations. Note that the legend applies to both figures.

We have plotted in Fig. 5.3 both the MF and the σ_V as a function of the proba-
bility p for different values of q. The signature of a network resonance both in p and
q is clear in this figure since the frequency entrainment increases and the phase syn-
chronization is maximally enhanced for the optimal values $p = p_c = 0.0055$ (value

of p at which the maximum of σ_V occurs) and $q \approx 0.3$ (see also Fig. 5.2C). Note that the probability p_c depends slightly on q, shifting to higher p as q increases, but remaining very small.

The interplay between topology and dynamics becomes evident when we observe that the optimal link probability depends on the size ensemble as $p_c \propto \ln(N)/N$ (see Fig. 5.4). This means that the probability at which the global dynamics is more coherent coincides with the birth of the giant connected component (GCC) of a Poisson random graph with N elements, which is precisely the network we have when only the randomly added long–range connections are considered (i.e., when we neglect the local couplings).
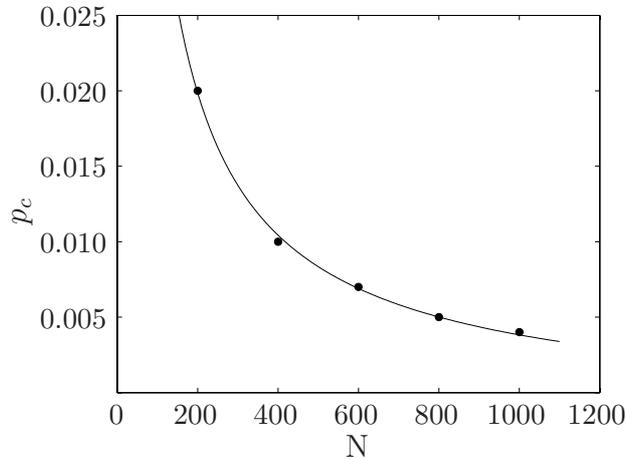

Figure 5.4. Dependence of p_c on N. This figure shows that the emergence of coherent oscillations coincides with the birth of the GCC of a random network, i.e., $p_c \propto \ln N/N$. Here, we fix $q = 0.25$.

5.4 Ising network

To analyze if the previous small–world connectivity structure with long–range sparse repulsive links affects other dynamics imposed on it, we consider a discrete spin–like dynamics in which each node i has only two possible states $s_i = \pm 1$. This could model a social system with N agents choosing from two different opinions or in a biological context it could represent the firing state of a neuron.

We prepare the system by setting rN of the spins at the state -1 and the rest at the opposite, being r the initial probability of finding a spin at -1. Consequently, with the same Laplacian matrix $\mathbf{L}$ defined in Eq. 5.2, node i receives an input

$$h_i = \sum_j \ell_{ij} s_j \in [-2, 2].$$

Hence, as other authors have pointed out [3, 28], these spin–like networks can be regarded as a pattern of the internal states and their evolution represent the global dynamics.

Notice that the neighbor vertices linked repulsively contribute to the input with the opposite state. Then, in this model it is implicit that nodes linked with an attractive connection tend to follow the same evolution, whereas repulsive connection leads them to evolve differently.

We can prove analytically that the distribution of h_i presents two peaks (see Fig. 5.5):

$$\mu_1 = -2r\sqrt{1 - 4q(1 - q)}$$
$$\mu_2 = 2(1 - r)\sqrt{1 - 4q(1 - q)}.$$

Note that the position of these two peaks does not depend on the node degree k, thus neither does on the link probability p.
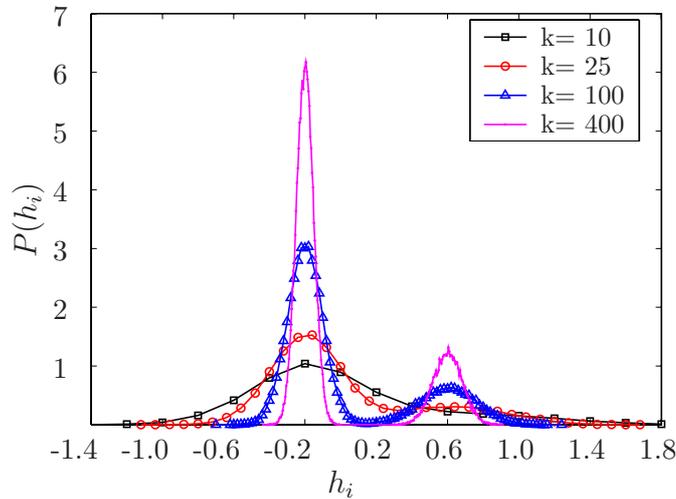

Figure 5.5. Probability distribution (in percentage) of the input h_i received by a node for several node degrees k when $q = 0.3$, $r = 0.25$. Notice the presence of two peaks in the distribution whose positions do not depend on the degree of the node, thus neither does on the link probability p.

Then, we choose to evolve the network according to a local majority rule in which the new state of node i is updated to $s_i(n + 1)$ as follows

$$s_i(n + 1) = \begin{cases} +1 & \text{if } h_i(n) > \mu_2 \\ s_i(n) & \text{if } h_i(n) \in [\mu_1, \mu_2] \\ -1 & \text{if } h_i(n) < \mu_1 \end{cases}$$

Using the quantity σ_m defined as in Eq. (5.3) to estimate the coherence of the output, we find that the system changes its behavior at $p \approx p_c$. Now, σ_m measures the deviation of the global average state of the spin network after a transient.

It can be seen in Fig. 5.6 that the maximum of σ_m is reached again when the GCC associated to the long–range links spans the whole network with a minimal number of links. Interestingly, a similar resonant trend with q is observed. This shows how p and q contribute to improve the synchronization even for this discrete dynamics.
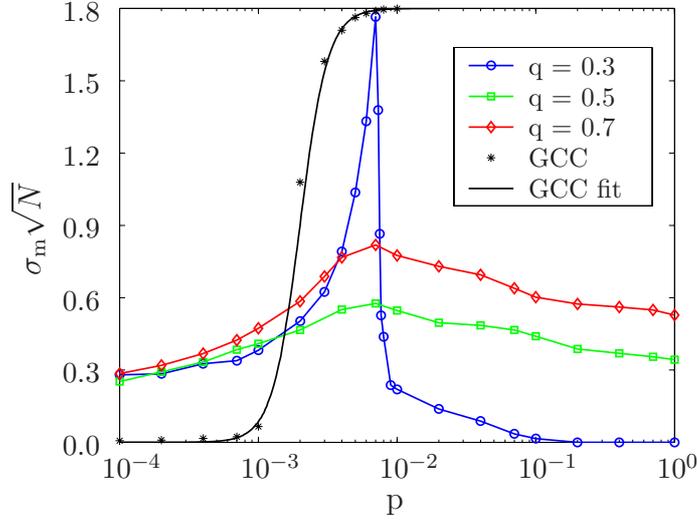
Figure 5.6. Deviation $\sigma_m \sqrt{N}$ of the mean state *vs.* p for different q values in a log–linear scale, with $N = 800$. Each point averages 1000 runs after a transient of 100 iterations and fixed $r = 0.1$.

5.5 Spectral analysis

Recently [17, 29], the method of the *master stability function* [30] has been successfully used to analyze whether the network structure has some bearing on the dynamics evolving on it. However, this approach requires the dynamical units to be identical (which is not our case) and the results are model–dependent since the master stability function is calculated for a given model.

Hence, in order to understand the influence of a complex connectivity, we use a purely structural analysis based on the properties of **L**. This is done by ignoring the intrinsic dynamics of the units in Eq. (5.1), that is, we just consider

$$\dot{\mathbf{V}} = d\,\mathbf{LV},$$

where $\mathbf{V} = (V_1, \ldots, V_N)$.

Then, there is a basis in which

$$V_i \approx \exp(d\lambda_i t),$$

where λ_i are the eigenvalues of **L**.

It is well known that all the eigenvalues of the Laplacian associated to a network with only attractive couplings are negative. However, when we add some repulsive connections, **L** has positive and negative eigenvalues. We find that any set of initial states rapidly evolves into the subspace S^+ associated to the positive eigenvalues within a time smaller than the characteristic temporal scale of the system dynamics ($\tau \approx 15$ ms).

To quantify the effect of S^+, we note that, for a given positive λ_i, $e^{d\lambda_i}$ is a measure of how much the system spreads into the subspace defined by the corresponding

eigenvector. Then, the ratio

$$\frac{\mathrm{e}^{d\lambda_i t}}{\mathrm{e}^{d\lambda_{\max} t}} = \mathrm{e}^{d(\lambda_i - \lambda_{\max})t}$$

measures how different is the evolution in that subspace with respect to the one where the system develops faster. By defining the geometric average

$$g(t) = \sqrt[N]{\prod_{i=1}^{N} \mathrm{e}^{d(\lambda_i - \lambda_{\max})t}} = \mathrm{e}^{\sum_{i=1}^{N} d(\lambda_i - \lambda_{\max})t/N} = \mathrm{e}^{d(\langle\lambda\rangle - \lambda_{\max})t},$$

we can estimate the homogeneity of the evolution in S^+ with a number in $(0, 1]$. A value close to 1 means the system evolves similarly in all dimensions of S^+, whereas a low g implies that its behavior is determined by those vectors with the largest associated eigenvalues.

We are interested in the behavior of $g(t)$ as a function of p and q. As the shape of $g(t)$ with p is not very sensitive to time, we fix $t = d^{-1} \sim \tau$ to focus our study within the time scale of our dynamical unit. In Fig. 5.7 we observe that $g \equiv g(\tau)$ presents a minimum at p_c which is lower for higher values of q, and whose position shifts to higher p as q increases, as observed both in the numerical simulations of the network with excitable and oscillatory elements (see the right panel on Fig. 5.3) and in the Ising network (see Fig. 5.6).

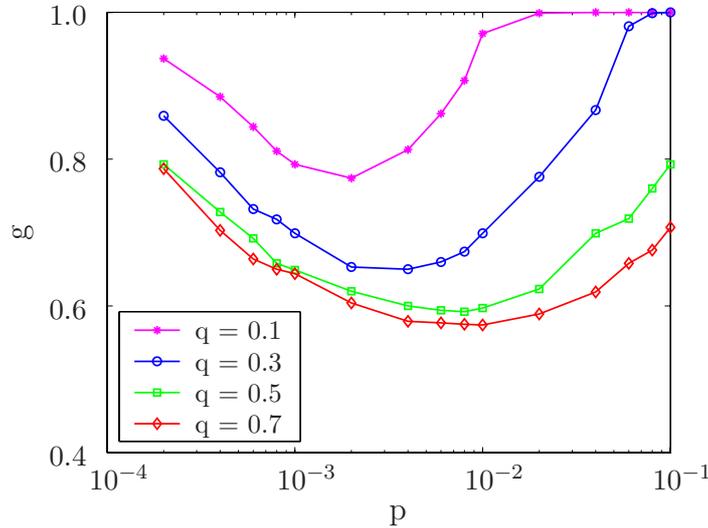**Figure 5.7.** Dependence of g with the adding probability p, in a log–linear scale, for different probabilities q. Each point is an average over 100 different realizations of a $N = 800$ network.

This means that, for values of p far from p_c, i.e. where $g \approx 1$, the global dynamics is basically determined by only one positive eigenvalue,

$$\mathbf{V}(t) = \mathbf{V}_0 \exp(\lambda t).$$

On the contrary, for values of p close to p_c, we need to consider not just one but several eigenvalues (the largest ones) to account for the global dynamics. Therefore, the intrinsic dynamics of the system is minimally constrained by the structure that arises around p_c due to the repulsive shortcuts.

5.6 Conclusions

In summary, we have shown how a small fraction of phase–repulsive links can enhance synchronization in a complex network of dynamical units. A structural analysis allows us to obtain information about how the topology influences the dynamics. Surprisingly, around a probability p_c, the versatility arising from the network structure due to q drives the system to a more ordered state, while far from p_c the stiffness of the structure freezes the initial disorder.

Precisely, we find that the effect of topology can be seen through two quantities: the number of eigenvalues $\lambda_i > 0$ (i.e., those in S^+) and their dispersion σ_V. We relate the number of positive eigenvalues with the activity and the dispersion with synchronization. While the activation is enhanced as the number of λ_i increases, the synchronization improves with the dispersion.

If we have few positive eigenvalues (i.e., when $p \approx 0$, which essentially corresponds to a lattice), the initial oscillating units are unable to spread the activity throughout. However, when there are many λ_i, the problem is not the activation of the system but its coherence.

Namely, if the dispersion in the positive eigenvalues is small (i.e., when $p \approx 1$, which is a fully connected network), there are many λ_i contributing to activate the whole system but, since all dimensions in S^+ contribute similarly to the dynamics, nodes are indistinguishable from the viewpoint of the topology and the dynamical units are constrained to evolve alike when they have different intrinsic dynamics. Consequently, they remain unsynchronized.

On the contrary, if the dispersion is large, there is a balance between the intrinsic dynamics and the structure of the network. The topology close to p_c, due to the presence of phase–repulsive links is such that, not only the activity is enhanced, but also the connectivity of the network is compatible with the heterogeneity of the system.

Bibliography

[1] D.J. Watts and S.H. Strogatz. *Collective dynamics of "small–world" networks.* Nature 393, p440–442 (1998).

[2] A.-L. Barabási and R. Albert. *Emergence of scaling in random networks.* Science 286, 509–512 (1999).

[3] D.J. Watts. *Small worlds: The dynamics of networks between order and randomness,* Princeton University Press, Princeton, New Jersey, 1999.

[4] R. Albert and A.-L. Barabási. *Statistical mechanics of complex networks.* Review of Modern Physics 74, 47–97 (2002).

[5] S.N. Dorogovtsev and J.F.F. Mendes. *Evolution of networks.* Adv. Phys. 51, 1079–1145 (2002).

[6] S.H. Strogatz. *Exploring complex networks.* Nature 410, 268–276 (2001).

[7] S. Boccaletti, V. Latora, Y. Moreno, M. Chavez and D.-U. Hwang. *Complex networks: Structure and dynamics.* Physics Reports 424, 175–308 (2006).

[8] D. He, G. Hu, M. Zhan, W. Ren and Z. Gao. *Pattern formation of spiral waves in an inhomogeneous medium with small–world connections.* Physical Review E 65, 055204 (2002).

[9] X. Wang, Y. Lu, M. Jiang and Q. Ouyang. *Attraction of spiral waves by localized inhomogeneities with small–world connections in excitable media.* Physical Review E 69, 056223 (2004).

[10] L.F. Lago–Fernández, R. Huerta, F. Corbacho and J.A. Sigüenza. *Fast response and temporal coherent oscillations in small–world networks.* Physical Review Letters 84, 2758 (2000).

[11] M. Tinsley, J. Cui, F.V. Chirila, A. Taylor, S. Zhong and K. Showalter. *Spatiotemporal Networks in Addressable Excitable Media.* Physical Review Letters 95, 038306 (2005).

[12] A.J. Steele, M. Tinsley and K. Showalter. *Spatiotemporal dynamics of networks of excitable nodes.* Chaos 16, 015110 (2006).

[13] M. Kuperman and G. Abramson. *Small World Effect in an Epidemiological Model.* Physical Review Letters 86, 2909 (2001).

[14] M. Barahona and L.M. Pecora. *Synchronization in Small–World Systems.* Physical Review Letters 89, 054101 (2002).

[15] T. Nishikawa, A.E. Motter, Y.-C. Lai and F. Hoppensteadt. *Heterogeneity in oscillator networks: Are smaller worlds easier to synchronize?*. Physical Review Letters 91, 014101 (2003).

[16] A.E. Motter, C. Zhou and J. Kurths. *Network synchronization, diffusion, and the paradox of heterogeneity*. Physical Review E 71, 016116 (2005).

[17] M. Chavez, C.-U. Hwang, A. Aman, H.G.E. Hentschel and S. Boccaletti. *Synchronization is enhanced in weighted complex networks*. Physical Review Letters 94, 218701 (2005).

[18] I. Belykh, E. de Lange and M. Hasler. *Synchronization of bursting neurons: What matters in the network topology*. Physical Review Letters 94, 188101 (2005).

[19] L. Donetti, P.I. Hurtado and M.A. Muñoz. *Entangled Networks, Synchronization, and Optimal Network Topology*. Physical Review Letters 95, 188701 (2005).

[20] M. I. Rabinovich, P. Varona, A.I. Selverston and H.D.I. Abarbanel. *Dynamical principles in Neuroscience*. Review of Modern Physics, in press.

[21] P.-J. Kim, T.-W. Ko, H. Jeong and H.-T. Moon. *Pattern formation in a two–dimensional array of oscillators with phase–shifted coupling*. Physical Review E 70, 065201 (2004).

[22] I. Leyva, E. Allaria, S. Boccaletti and F.T. Arecchi. *In phase and antiphase synchronization of coupled homoclinic chaotic oscillators*. Chaos 14(1), 118–122 (2004).

[23] G. Balázsi, A. Cornell–Bell, A.B. Neinman and F. Moss. *Synchronization of hyperexcitable systems with phase–repulsive coupling*. Physical Review E 64, 041912 (2001).

[24] L.S. Tsimring, N.F. Rulkov, M.L. Larsen and M. Gabbay. *Repulsive synchronization in an array of phase oscillators*. Physical Review Letters 95, 014101 (2005).

[25] A.L. Hodgkin and A.F. Huxley. *A quantitative description of membrane current and its application to conduction and excitation in nerve*. Journal of Physiology 117, 500–544 (1952).

[26] G.B. Ermentrout and N. Kopell. *Inhibition–produced patterning in chains of coupled nonlinear oscillators*. SIAM Journal of Applied Mathematics 54, 478–507 (1994).

[27] G. Balázsi, A.H. Cornell–Bell and F. Moss. *Increased phase synchronization of spontaneous calcium oscillations in epileptic human versus normal rat astrocyte cultures.* Chaos 13, 515–518 (2003).

[28] H. Zhou and R. Lipowsky. *Dynamic pattern evolution on scale–free networks.* PNAS USA 102, 10052–10057 (2005).

[29] G. Tanaka, B. Ibarz, M.A.F. Sanjuán and K. Aihara. *Synchronization and propagation of bursts in a ring of coupled map neurons.* CHAOS 16, 013113 (2006).

[30] L.M. Pecora and T.L. Carroll. *Master Stability Functions for Synchronized Coupled Systems.* Physical Review Letters 80, 2109-2112 (1998)

Chapter 6
Conclusions

In this work, we have studied in detail the topology and the dynamics in complex networks. A summary of the main results are the following:

Empirical approach to complex networks

We have thoroughly analyzed the complex network constituted by the scientific collaborations of the fifth Framework Programme to study the interplay between research and industry. This study uses the methods coming from the field of complex networks to derive several measures that allow us to quantify the features of this relationship and assess their potential improvements.

The FP5 network is scale–free with an accelerated growth, meaning that new collaborations are created at a faster rate than usual. We have also concluded that some sort of synergy among the participants exists since new collaborations appear.

However, the fact that only Universities use the different programmes to create new collaborations shows that this is not enough to assure the transfer of knowledge. While the network of Universities is well integrated and established in accordance to what is observed for other social networks, the same does not seem to be true for the Companies network, mainly due to its relatively small largest connected component. Competition is probably the origin of this effect, which is moderated by the presence of Universities.

We find that the transmission of information is more efficient between Universities than among Companies. Furthermore, when Universities are excluded from the projects, Companies tend to form clusters, turning difficult (if not impossible) the communication between them. These results point to the central function played by Universities in the FP5 network to reduce the distance between research and applications.

We also show that Companies and Universities are organized differently. Large corporations are reluctant to choose as partners small companies, whereas size is not important between Universities. But if we analyze how Universities and Companies cooperate; the result is that large Universities prefer working with large Companies, while Companies select their partners between Universities regardless of their sizes.

Therefore, while Companies exhibit a hierarchical structure, Universities do not. Then, although Universities contribute to approach Companies which would be separated otherwise, small Companies are not well integrated yet. Therefore, we believe that the industry–industry and industry–research interactions should be particularly encouraged, while maintaining the investment in the research–research interplay.

Spreading processes in complex networks

We have found that hierarchical networks are so spread because this structure arises when each actor only looks for maximizing his information. The result is a structure that mainly benefits the higher levels, by providing them a higher information centrality and improving their dominance of information.

When edges, between vertices with the same upper neighbor, are added to a hierarchical tree, we show that the information each actor manages decreases. This means that a hierarchical tree is a stable network against relationships between members of the same group.

This stability can be seen as another reason that explains why hierarchical trees are so spread in companies all over the world. A hierarchical tree backs the leader's superiority of information despite the strength of the relationship that links the members of a group.

Nevertheless, it should be noticed that in our model edges between vertices in the same level with different upper neighbor are not included, or between vertices in different levels. This study may yield a different result.

When we assume that the transmission of information is perfect, without degradation, but the access to this information is somehow restricted, the problem is how to fairly share it, if some users act in a selfish manner.

We have shown that, if the policy used to manage the common resource is oblivious (that is, if it does not differentiate between requests belonging to different users) then any efficient Nash equilibrium will highly depend on the number of users, in the sense that they must adapt their request rate in a significant manner.

Taking into account that, in many realistic situations, the number of users changes rapidly and that the time needed to adapt from one equilibrium to another one can be significant, this means that the system will be most of time out of equilibrium. Actually, as illustrative examples, we point out a pair of congestion schemes in which the above mentioned effect may have a real impact.

Dynamics in networks

We have first analyzed the Helmholtz oscillator to justify why a new methodology is required to analyze complex systems. This oscillator is a simple model for studying phenomena that under certain conditions present a stable behavior of oscillatory kind, but for other conditions the behavior is unstable.

We find that the width of the stochastic layer by using the separatrix map. This gives the width of the energy band around the separatrix, where it is likely that an orbit presents transient chaos.

Next, we have considered the effect of friction. To solve the equation of the Helmholtz oscillator with friction and without forcing the Lie theory for differential equations is used. We show that the Helmholtz oscillator is completely integrable only when certain relation between the parameters is satisfied. When this relation is not satisfied, the equation is partially integrable. Also, we calculate that the symmetries for the completely integrable case are a translation and a homothopy.

A first integral of motion is obtained when the equation is integrated by using one symmetry. We prove that this time–dependent integral of motion is related to a Hamiltonian function. The second symmetry allows integrating the first integral of motion to obtain the Weierstrass function as a solution. Finally, we write this solution in terms of Jacobian Elliptic functions to show that there exists a relation with the basins of attraction of the oscillator.

Since the condition required to completely integrate the equation is just a two–dimensional manifold in the parameter space, we cannot write down the function that solves the equation in general. Then, we should analyze this type of problems from a global viewpoint since it is nonsensical to study individual trajectories. To understand the motions that surround us, mainly due to non–linear laws and interactions, requires the development of new techniques.

As an example of the utility of complex network in this issue, we have shown how a small fraction of phase–repulsive links can enhance synchronization in an ensemble of dynamical units. A structural analysis allows us to obtain information about how the topology influences the dynamics. Surprisingly, around a probability p_c, the versatility arising from the network structure due to q drives the system to a more ordered state, while far from p_c the stiffness of the structure freezes the initial disorder.

Precisely, we find that the effect of topology can be seen through two quantities: the number of eigenvalues $\lambda_i > 0$ (i.e., those in S^+) and their dispersion σ_V. We relate the number of positive eigenvalues with the activity and the dispersion with synchronization. While the activation is enhanced as the number of λ_i increases, the synchronization improves with the dispersion.

If we have few positive eigenvalues (i.e., when $p \approx 0$, which essentially corresponds to a lattice), the initial oscillating units are unable to spread the activity throughout. However, when there are many λ_i, the problem is not the activation of the system but its coherence.

Namely, if the dispersion in the positive eigenvalues is small (i.e., when $p \approx 1$, which is a fully connected network), there are many λ_i contributing to activate the whole system but, since all dimensions in S^+ contribute similarly to the dynamics, nodes are indistinguishable from the viewpoint of the topology and the dynamical units are constrained to evolve alike when they have different intrinsic dynamics. Consequently, they remain unsynchronized.

On the contrary, if the dispersion is large, there is a balance between the intrinsic dynamics and the structure of the network. The topology close to p_c, due to the presence of phase–repulsive links is such that, not only the activity is enhanced, but also the connectivity is compatible with the heterogeneity of the system.

Publications

ARTICLES

1. Juan A. Almendral, Miguel A. F. Sanjuán
   Integrability and Symmetries for the Helmholtz oscillator with friction
   Journal of Physics A: Mathematics and General **36**, 695–710 (2003).

2. Luis López, Juan A. Almendral, Miguel A. F. Sanjuán
   Complex networks and the WWW market
   Physica A **324**, 754–758 (2003).

3. Juan A. Almendral, Luis López, Miguel A. F. Sanjuán
   Information flow in generalized hierarchical networks
   Physica A **324**, 424–429 (2003).

4. Juan A. Almendral, Jesús Seoane, Miguel A. F. Sanjuán
   The nonlinear dynamics of the Helmholtz oscillator
   Recent Res. Devel. Sound and Vibration Vol. 2, 115–150 (2004)
   Transworld Research Network, Kerala, India.

5. Juan A. Almendral, Luis López, Vicent Cholvi, Miguel A. F. Sanjuán
   Oblivious Router Policies and Nash equilibrium
   ISCC Proceedings, New Jersey, 736–741 (2004).

6. Juan A. Almendral, Luis López, Vicent Cholvi, Miguel A. F. Sanjuán
   Congestion schemes and Nash equilibrium in complex networks
   Physica A **355**, 602-618 (2005).

7. Juan A. Almendral, João G. Oliveira, Luis López, Jose F. F. Mendes, Miguel A. F. Sanjuán
   Structure and Information Flow in a Complex Network
   Submitted to Physica A (2006).

8. Juan A. Almendral, João G. Oliveira, Luis López, Jose F. F. Mendes, Miguel A. F. Sanjuán

   Dynamics of research and industry interplay network

   Submitted to Chaos (2006).

9. Inmaculada Leyva, Irene Sendiña–Nadal, Juan A. Almendral, Miguel A. F. Sanjuán

   Sparse repulsive coupling enhances synchronization in complex networks

   Submitted to PRE (2006).

CONTRIBUTIONS TO CONFERENCES

1. Juan A. Almendral, Miguel A. F. Sanjuán

   Simetrías e integrabilidad en el oscilador de Helmholtz con fricción

   No Lineal 2002. Cuenca. 2002.

2. Juan A. Almendral, Luis López, Jose F. F. Mendes, Miguel A. F. Sanjuán

   Complex Networks and Socioeconomic Applications

   7th Granada Seminar 2002. Granada. 2002.

3. Juan A. Almendral, Luis López, Vicent Cholvi, Miguel A. F. Sanjuán

   Oblivious Router Policies and Nash equilibrium

   9th IEEE International Symposium on Computers and Communications. Alejandra (Egipto). 2004.

4. Juan A. Almendral, Miguel A. F. Sanjuán

   La red de colaboraciones europea en el contexto del Programa Marco

   No Lineal 2004. Toledo. 2004.

5. Jesús Seoane Sepúlveda, Juan A. Almendral, Miguel A. F. Sanjuán

   Estudio analítico y computacional del oscilador de Helmholtz

   No Lineal 2004. Toledo. 2004.

6. Juan A. Almendral, Irene Sendiña Nadal, Jose F. F. Mendes, Miguel A. F. Sanjuán

   How non–local couplings affect the synchronization of a food-web model network

   International Conference Science of Complex Networks. Aveiro (Portugal). 2004.

7. Juan A. Almendral, João G. Oliveira, Luis López, Jose F. F. Mendes, Miguel A. F. Sanjuán

   The complex network of scientific collaborations in the 5th European Framework Programme

   SIAM Conference on Applications of Dynamical Systems. Snowbird, Utah (USA). 2005.

8. Juan A. Almendral, Irene Sendiña Nadal, Inmaculada Leyva , Miguel A. F. Sanjuán

   Effects of long range couplings in a predator–prey model network

   Dynamics Days Europe 2005. Berlin (Alemania). 2005.

9. Inmaculada Leyva, Irene Sendiña Nadal, Juan A. Almendral, Miguel A. F. Sanjuán

   Entrainment of small–world Hodking–Huxley neuron networks

   Dynamics Days Europe 2005. Berlin (Alemania). 2005.